# MASTER THESIS - DIPLOMARBEIT

# TOPOLOGY OPTIMIZED DESIGN OF A CYLINDER HEAD USING ADDITIVE LAYER MANUFACTURING

## TOPOLOGIEOPTIMIERTE KONSTRUKTION EINES ZYLINDERKOPFES FÜR ADDITIVE FERTIGUNG

Author:
Benjamin Meier, BSc

Supervisors:

University of Technology Graz: Professor DI. Dr. Hannes Hick

Institut für Maschinenelemente und Entwicklungsmethodik

AVL Graz: DI. Bernhard Kaltenegger

Graz, 2016

Deutsche Fassung:
Beschluss der Curricula-Kommission für Bachelor-, Master- und Diplomstudien vom 10.11.2008
Genehmigung des Senates am 1.12.2008

## EIDESSTATTLICHE ERKLÄRUNG

Ich erkläre an Eides statt, dass ich die vorliegende Arbeit selbstständig verfasst, andere als die angegebenen Quellen/Hilfsmittel nicht benutzt, und die den benutzten Quellen wörtlich und inhaltlich entnommenen Stellen als solche kenntlich gemacht habe.

Graz, am 31. 12. 2016 ..
(Unterschrift)

Englische Fassung:

## STATUTORY DECLARATION

I declare that I have authored this thesis independently, that I have not used other than the declared sources / resources, and that I have explicitly marked all material which has been quoted either literally or by content from the used sources.

date 31. 12. 2016 ..
(signature)

# Table of Contents

# 1 Abstract

Main goal of this thesis is topology optimization of a cylinder head to minimize weight using the capabilities of additive layer manufacturing (AM) while still meeting all functional and mechanical requirements. Due to this new production processes it is possible to overcome structural as well as material constraints given by the currently used casting technologies.

The following topics will be covered:

- Additive Manufacturing: Introduction and comparison of AM Processes
- Constrains of todays production technologies compared to the possibilities of additive layer manufacturing
- Functional requirements of a cylinder head
- Mechanical and thermal loads working on the component
- Designing of a flow optimized water jacket
- FEM Simulation
- Topology optimization
- Conclusions and future work

## 1.1 Introduction

Additive Manufacturing (AM), commonly known as 3D printing, has grown exponentially in recent years. Component size, material selection and process control rise steadily while prices are becoming more affordable. Aside from prototypes and medical implants first repetition parts are already used even under load conditions. Especially aerospace industries lead the way since near net shape construction ease the path to system integration and therefore weight savings, which play a crucial role. However, the technology is still in its infancy and much has to be learned as well as new possibilities discovered.

Within the scope of this master thesis, prospects of additive manufacturing an engine cylinder head, commonly produced by cast technology, are evaluated. As a first step, current technologies and their limits are explained as well as material selection and properties are summarized. Current cylinder head features and loads are covered which must be achieved by the new design. Since AM allows nearly any geometry, a new cylinder head is created by numerical topology optimization offering ideas for an optimal design for the given purpose.

Finally, the feasibility of this design has to be checked. It is therefore the goal of this paper to show the weight saving and functional optimization potential of an additive manufactured cylinder head as a base for further optimization and a new design which might lead to a working prototype in near future.

# 2 Additive Layer Manufacturing

Additional layer manufacturing or colloquially 3D printing, is a form of rapid prototyping. To produce a certain component, it is fractionized to a finite number of planes, which are applied one atop another. There are different methods to achieve the final goal of a 3D component following this process, depending on material, intended use, component size and prize. Only processes which can handle metals are covered since they are of main interest for technical applications. The main advantage of this technology is the freedom of structure and form. Conversely its drawbacks are production costs and times for larger production numbers, today's maximal printer sizes, and a sometimes limited selection of materials as well as a number of unknowns on properties of printed material. Thus, application nowadays is limited to low number and/or high performance parts such as prototypes, medical implants, turbine plates, rocket parts etc. But in the foreseeable future, as realizable component size increase and cost go down, the number of applications will definitely rise.

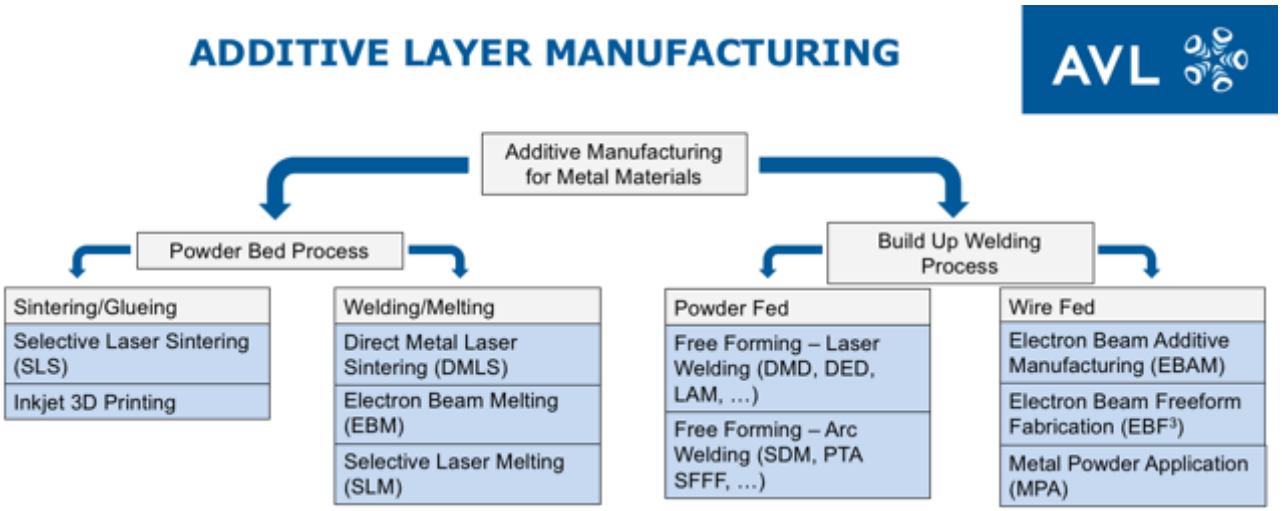


Figure 1: Overview Additive Manufacturing Processes for Metals

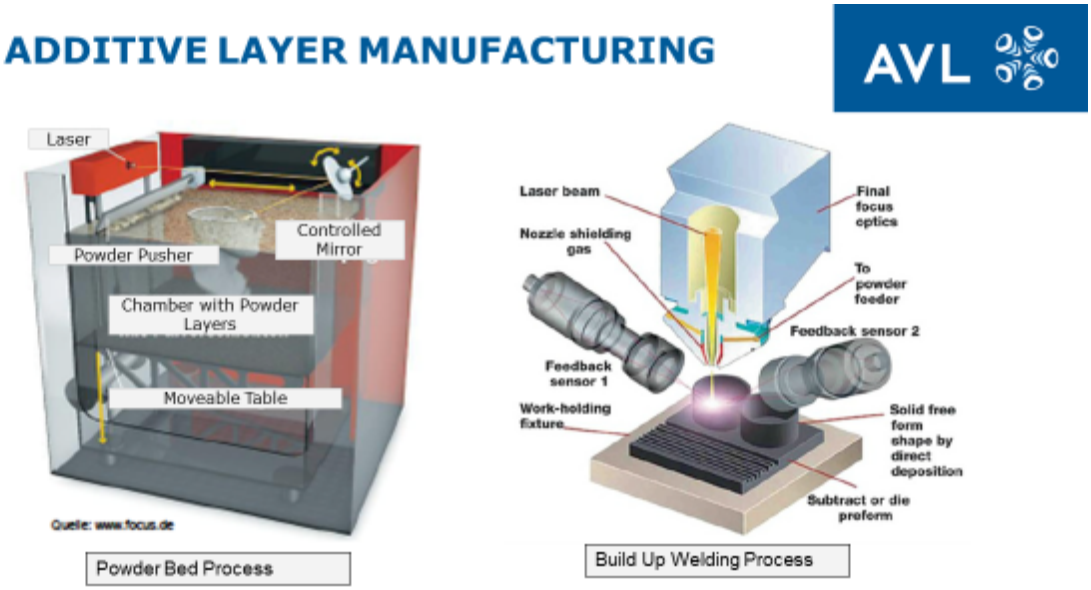


Figure 2: Additive Manufacturing – Powder-Bed am Build-Up Welding Process [56][37]

## 2.1 Powder Bed Processes

Most of the additive layer manufacturing processes for metals are based on a powder bed procedure, for which the material has to be provided in powder form. Commonly a pusher or roller applies this powder in fine layers on a working table. The thickness of this powder layers determines the grading in z-axis of the final part. Following powder particles, which form the component in this cross section are either sintered or welded (or in exceptional cases clued) together. In order to do so, an energy source both powerful and position accurate is obligatory. As for high precision welding, a laser or electron beam is utilized in most cases. After connecting all the structure particles in one cross section, the working table moves downwards and a new layer of powder is applied and the operating sequence described above repeated until the component is finished. In a nutshell the energy source traverses in the x-y direction while the table movement provides build up along the z-axis.

Due to the small zone of affected burden of the energy sources and the highly precise optics, the build structure is only limit by the workspace size, and in the case of larger box sections, by the load-bearing capacity of the powder underneath. Therefore, supportive structures have to be built for box sections below an angle of 45° and wider than approximately 8mm to achieve high accuracy and minimize errors. These structures must be removed afterwards. An exception is the 3D inkjet metal printing which is described later. Excessive powder can be collected afterwards and recycled respectively reused, but standards for recycle powder quality and properties are still an issue today and universal standards have to be developed.

### 2.1.1 Selective Metal Sintering (SLS)

#### 2.1.1.1 Excurse Sintering [3]

**Sintering** is the process of compacting and forming a solid mass of material by heat and/or pressure without melting it to the point of liquefaction. It is used as a master forming process in powder metallurgy. Basically as the metal powder grains get heated up and/or are pressed together, their surfaces touch. To reduce the free surface energy, grains try to minimize their surface, therefore connecting to the neighbor grains, forming so called sinter bridges. Since the metal is still in a solid state, this occurs via a diffusion process. Keeping the energy input up, this process continues until the former grains form one solid part. Following the sintering, steps are demonstrated by a model of two spherical particles.

As already mentioned, to minimize their surface particles connect to each other. This connection is called Sinter Bridge. First, material transport takes place on the particles surface, the distance between the particle centers stays the same. As the neck of the sinter bridge begins to grow, material diffusion from the core particle starts. Due to this bulk transport, the particles change their original form which lead to shrinkage.

With just two particles that eventually ends up in one larger spherical particle with the same volume but smaller overall surface. Considering there are a bunch more of them around, this leads to one solid component. Depending on the process used, its density can reach 100 percent, known as full sintering. Further information on porosity and grain growth can be found in relevant literature.

A differentiation is made between 1-phase and 2-phase sintering - the former applies on powders which stay in solid state during the whole procedure.

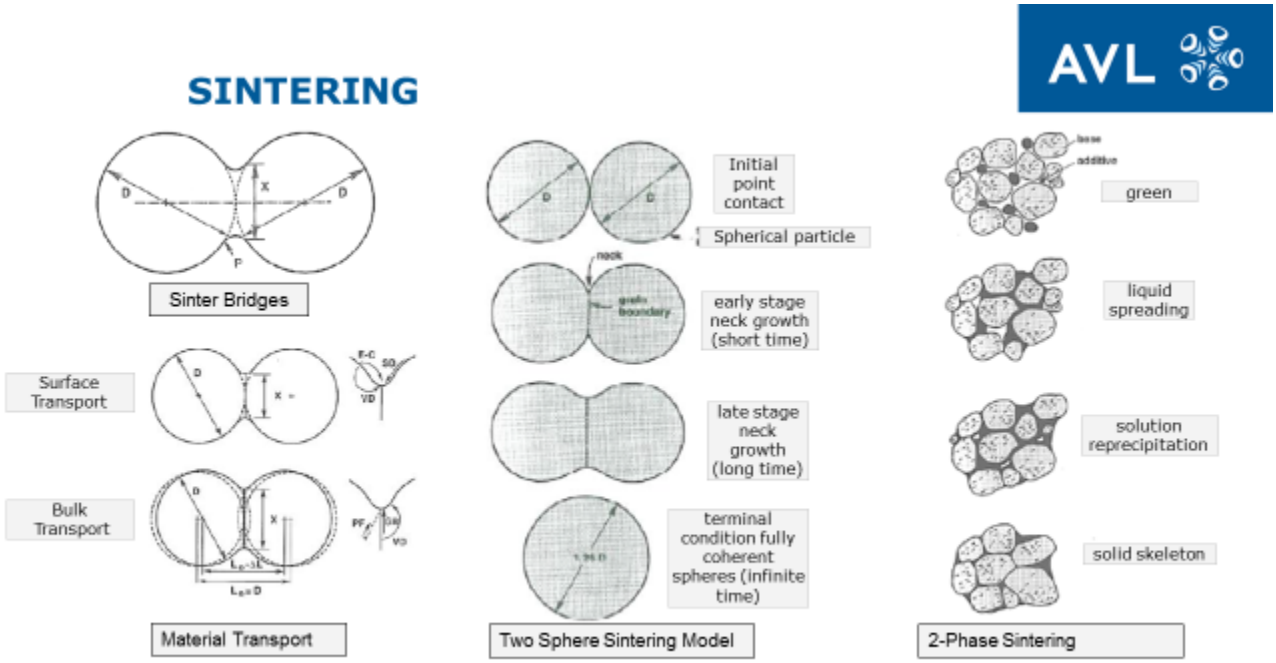


Figure 3: Sintering Process [3]

2-phase sintering or liquid state sintering applies to powders consisting of more than one material with different melting points. Thus, one material transfers to liquid state while the other stays in solid state. The 2 phases may be both metal but also polymers can be used. Therefore, it is possible to form parts from nearly any material.

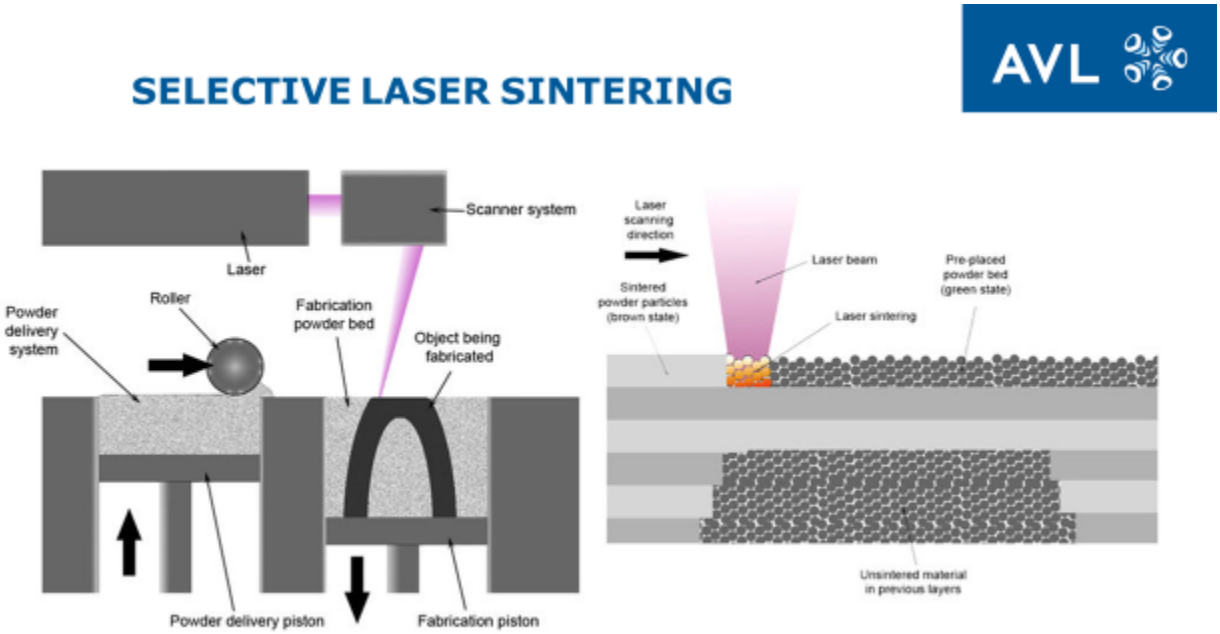


Figure 4: Selective Laser Sintering – Process Overview

SLS was the first additive layer manufacturing process able to create useable metal components. It was developed in the mid 80s at the University of Texas, Austin and is based on liquid phase sintering using a polymeric binder and metallic matrix. The metal powder always remains in solid state while a laser beam liquefies the polymeric binder that connects the metal powder grains together. Due to this power of the energy source can be kept low. The product of this process is a so-called green part, representing the final form but lacking mechanical strength. Therefore further production steps are necessary, known from standard sintering processes. To achieve high mechanical load capacity, the binder has to be extruded and hereupon the part resintered in a common sinter oven. Porosity then can be reduced by either filling the porosity capillary by a highly wetting lower melting metal or other apply post processing treatments like high isostatic pressing (HIP). Parts produced by SLS undergo noticeable shrinkage during sintering, which has to be considered in advance.

Today SLS is rarely used for metal applications but still common for plastics. Advantages are the low heat and energy input needed due to the low melting polymer binder and a great selection of possible materials, since the final sintering is done afterwards. A similar process is inkjet 3D printing, which will be covered in chapter 2.1.5.

### 2.1.2 Direct Metal Laser Sintering (DMLS) and Micro Laser Sintering (MLS)

Although carrying the term sintering in its name, DMLS is not a sintering but a melting process, since powder particles are transferred at least partially to liquid state. This means the main master forming mechanism is through building a melt pool as sintering might occur as a side effect. It is actually a trade name from German company EOS for a Selective Laser Melting process. However, a lot of ambiguous information on that topic can be found on the internet as well as in scientific papers and it seems that copyright and patent issues as well as process development led to this delusive name.

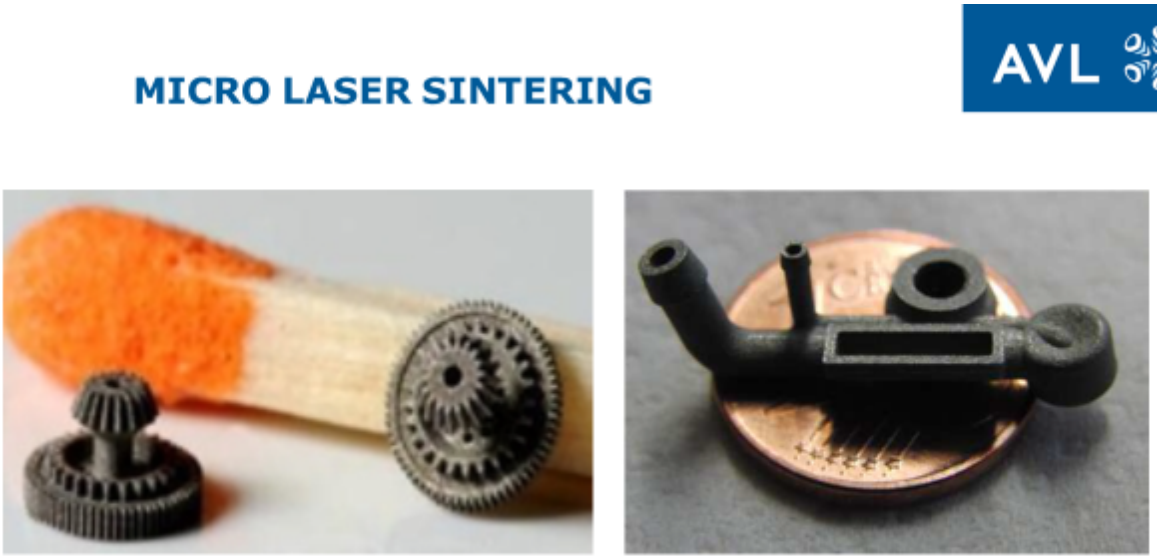


Figure 5: Micro Laser Sintering – Examples [52]

A variant of DMLS is Micro Laser Sintering for, as the name implies, miniaturized parts. The Process works with a powder grain size of just 5 micrometers and is capable to build layers as thin as these

particles. Minimum wall thickness is around the LASER beam size of just 30 micrometers. However, this leads to a small build size of just around 50mm in diameter. [42][52][53]

### 2.1.3 Selective Laser Melting (SLM), LaserCusing

SLM was developed by the Frauenhofer Institute. LaserCusing is a trade name by the company Laser Concept, but the process is more or less the same as is DMLS from EOS. However, Laser Concept emphasizes on their stochastically distributed heat input to reduce temperature gradients and thereby residual stresses and production errors.

In contrast to SLS, the powder grains are not sintered together but are heated over melting temperature and transferred into the liquid state. The process is therefore comparable to build-up welding, due to that fact a more powerful energy source is necessary. However, by melting material properties are quite different to those of sintered materials. The higher heat input leads to crystal growth across the layers. Therefore, SLM delivers lower porosity, therefore higher density and a better isotropy even without heat treatment.

The variety of material is a little smaller compared to SLS because they have to meet certain flow criteria in liquid state and be weldable. However, it has to be said that most technical metals are weldable using a LASER beam as energy source and under an inert gas atmosphere. Today the selection of materials is mainly limited by their availability as powder and if the process parameters for the powder selected are determined yet. A number of titanium, aluminum, nickel alloys, cobalt-chrome and steels are offered by most providers, while magnesium, tantalum, tungsten and some others are mostly in development or available from specialized companies.

With a growing number of users of additive manufacturing both, the number of available powders as well as public process parameters will rise. Also alloys especially developed for additive manufacturing will show up, since todays alloy powders are actually not designed for this processes but were developed for other production technologies.

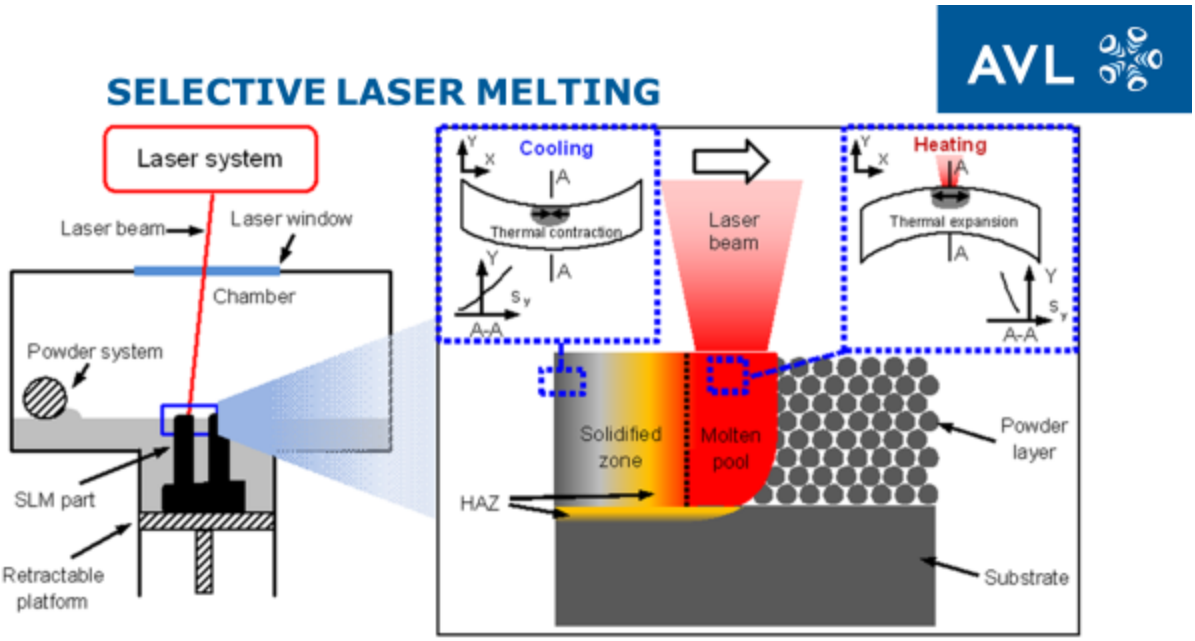


Figure 6: Selective Laser Melting – Process Overview [58]

### 2.1.4 Electron Beam Melting (EBM)

This technology was developed by the Swedish ARCAM Company. As the name implies EBM utilizes the energy of an electron beam to melt the powder particles. Hence, the process has to take place in a vacuum chamber. Working under high vacuum delivers excellent material properties and allows for a huge variety of working materials, especially supersensitive ones like the intermetallic Titanium-Aluminide and all kinds of titanium and its alloys. Also tolerances are better than with SLM and multiple melting points can be realized. However surface quality is a little rougher. The vacuum chamber is preheated to a point below melting temperature, reducing temperature gradient in the build part as well as needed energy input by the electron beam. On the other hand, it is more expensive and the component size is limited, mostly due to the vacuum chamber. Also controlled preheating a bigger chamber and a component surrounded by an always varying amount of powder is challenging.

As for available materials the process seems especially suitable for titanium and nickel alloys, but information on aluminum alloys is rare. Reason might be either a lack in development or limitations for low melting materials due to the vacuum. Other available materials today are cobalt-chrome and copper. Since General Electrics acquired ARCAM lately a specialization on materials useable for aerospace and turbine components is expectable.

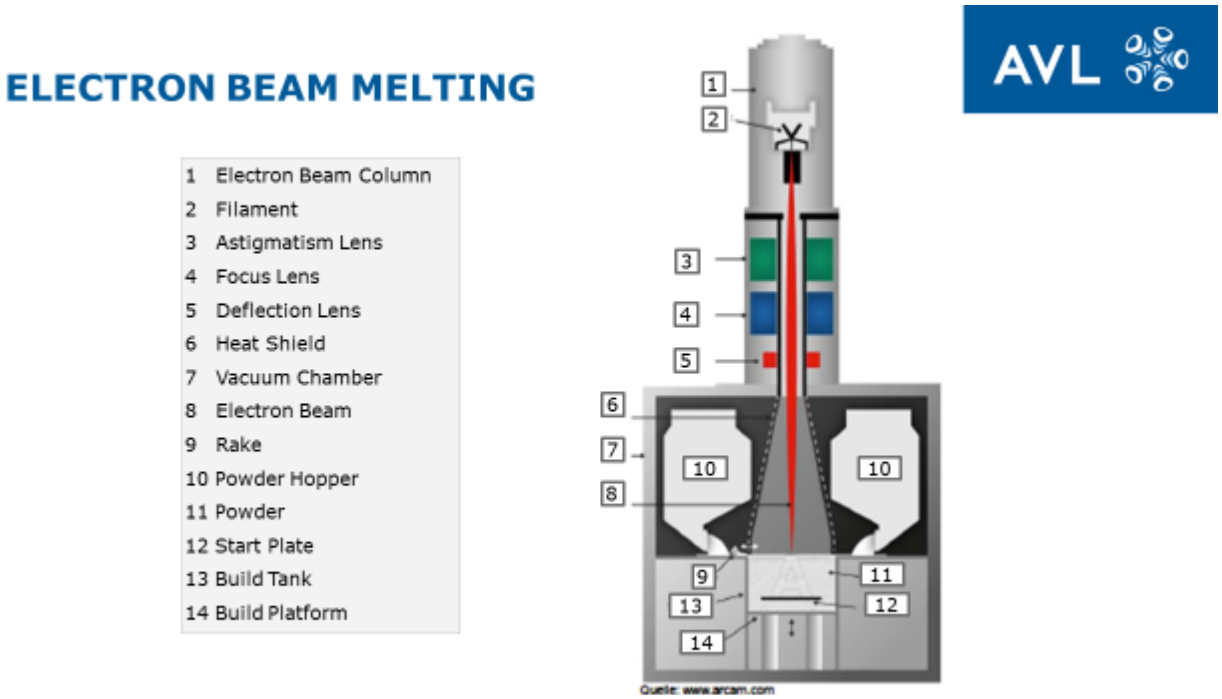


Figure 7: Electron Beam Melting – Process Overview [5]

### 2.1.5 Inkjet 3D-Metal Printing

This process is similar to a common inkjet printer. Instead of melting or sintering the building spots a clue is deposited layer by layer. The resulting product is a green part, which then is continued processing with common sinter technology. The biggest advantage of this technology is the absence of any heat input. Due to the fact that there are no residual stresses and highly reactive materials like titanium are well under the reactive temperature, use of a protective gas is obsolete. Also structural limitations of other powder bed processes, like large box section, can be built without support structures. Drawbacks are the shrinkage from green part to final component, higher porosity, and the

somehow worse mechanical properties. To obtain better material properties, shell printing is an option. Printing only the solid outlines with the binder and filling volumes between just with metal powder leads to higher green density and therefore reduces shrinking as well as porosity drastically. [14] Still, this method is more favorable with plastics and composites, as it also facilitates colored parts and layer wise restricted combinations of material.

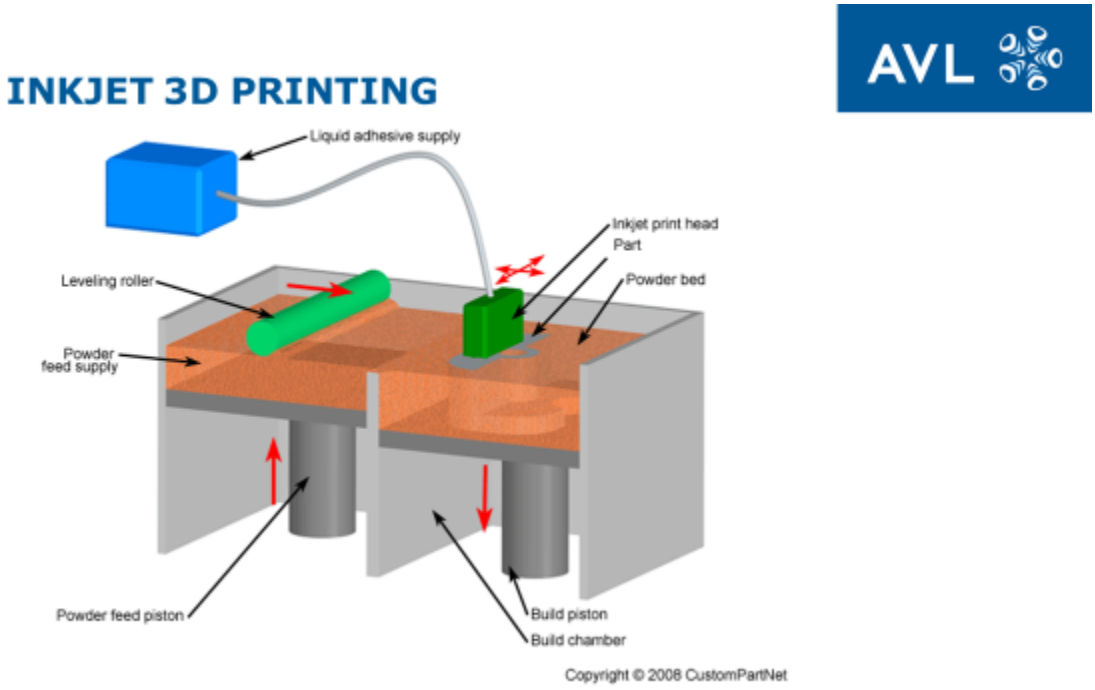


Figure 8: Inkjet 3D Printing – Process Overview [57]

## 2.2 Build Up Welding Processes

Irrespective of what has previously been discussed, there are alternative non-powder bed processes to create near net-shape structures. Most of these are based on some form of highly accurate build up welding, combining energy and material source in one machine head. Hence, limitations in building size are minimal compared to powder bed processes but accuracy and material selection seems to be constrained so far. This processes are also known as solid free forming (SFF). [14][29]

### 2.2.1 Laser Based Build-Up Welding based Processes: 3D Laser Cladding, Direct Metal Deposition (DMD), Direct Energy Deposition (DED), Free Form Laser Melting (FLM), Laser Engineered Net Shaping (LENS™), Laser Additive Manufacturing (LAM)

All of these processes are highly accurate forms of laser build-up welding developed and licensed by different companies, hence the variety of names. Metal powder is added directly on the heated spot from the heat source, which can move along and around all axis. It is like a welding apparatus on either a robotic arm or multiple axis jig. By getting rid of the powder bed limitations in component size are diminished. Furthermore, it allows to work on existing components, repairing or expanding them, and even opens the possibility to combine different materials. Also the powder handling is less complicated since only powder needed for the structure gets applied. If shroud gas is needed, it is either applied directly out of the weld head or the whole process takes place in a chamber.

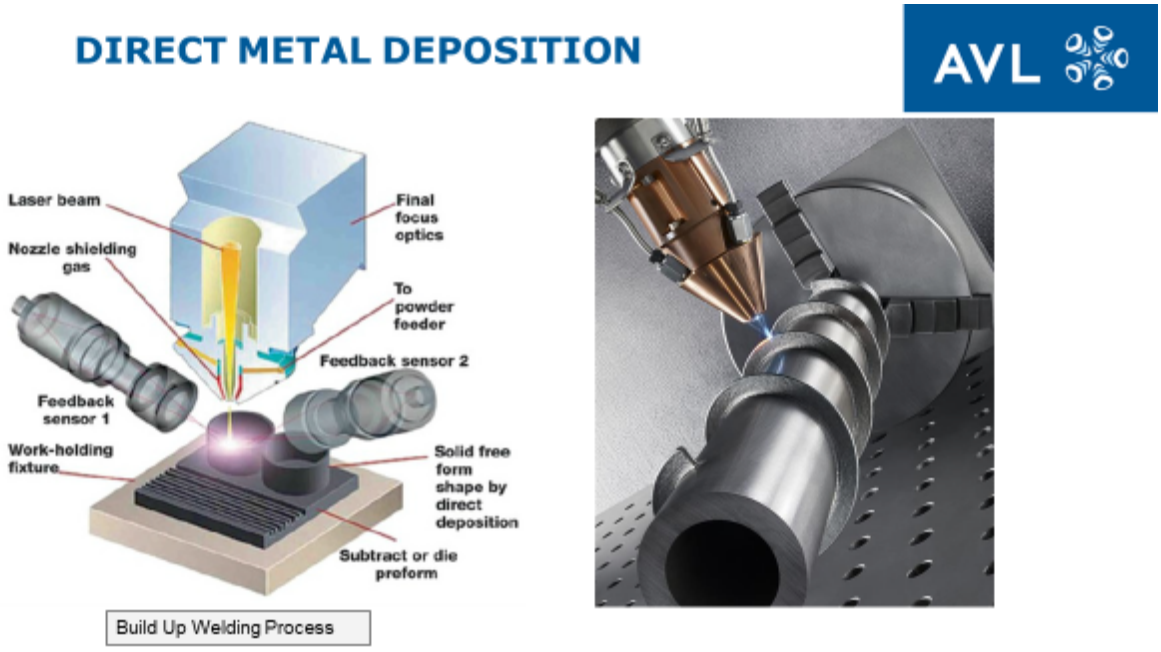


Figure 9: Direct Metal Deposition – Process Overview and Example [59]

### 2.2.2 Arc Welding Based Build-Up Welding based Processes: Plasma Transferred Arc Solid Free Form Fabrication (PTA SFFF), Shaped Metal Deposition (SDM)

Principally the same as LASER based build up welding processes, but using some kind of arc welding, may it be plasma, Metal Inert Gas (MIG) or Tungsten Inert Gas (TIG) welding. As with this processes everyone has advantages and disadvantages on certain materials, tolerances and properties, generally the same as the welding processes they are based on.

### 2.2.3 Wire Based Build up welding

In this process, material supply is provided by wire instead of metal powder. This leads to high productivity and build rate as well as lower material costs because metal wires are much cheaper than metal powders. Porosity is also low due to the full density of the wire. However, minimum wall sizes and layer thickness are limited by the wire size. There are some different wire fed processes around nowadays, using either electron beam or arc welding. Following two promising ones are described more closely

#### 2.2.3.1 Electron Beam Freeform Fabrication (EBF³)

EBF was developed by American space agency NASA as a portable additive manufacturing process useable in zero gravity surroundings. Similar to EBM, an electron beam is used as an energy source. However, the powder bed is replaced by wire as a material source and a 4 or 6-axis positioning table (x,y,z-axis longitudinal as well as Rotation in x,y-plane), which allows for an fixed position electron beam. Since room on a space ship/station is limited, size and simplicity is a main feature of this system. The fixed position electron beam allows for less voltage and therefore x-ray radiation is little, which allows for a thinner shielding and smaller department and less overall weight. Also the wire feed reduces material waste and allows for a smaller material support system. Furthermore, porosity is close to zero because of the massive wire. Material properties of build components should be close

to the classically build ones they are replacing. Material wise high duty aluminum alloys like 2219 Al and titanium alloys (Ti-6Al-4V) are available, but also other materials are possible, as long as they are weldable by an electron beam. By using two wire feeders, it is also possible to either use two different size wires (a fine one for details, a thicker one for higher build speed) or two different alloys to produce parts with compositional gradient. [47] [48] [49]

.

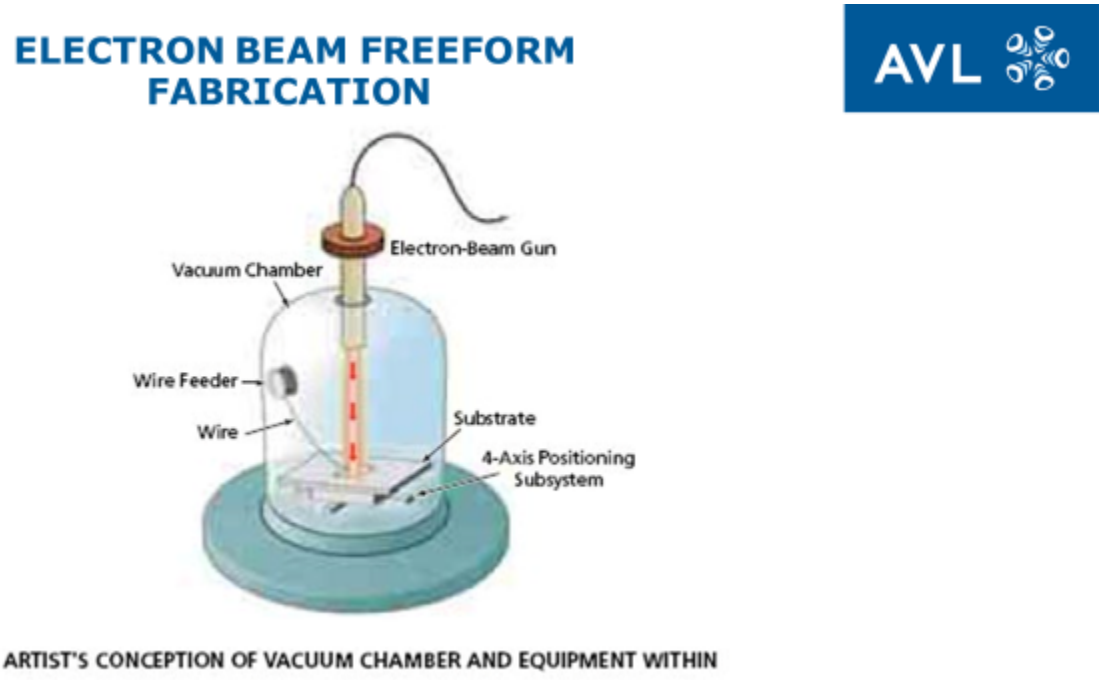


Figure 10: Electron Beam Freeform Fabrication – Process Overview [47]

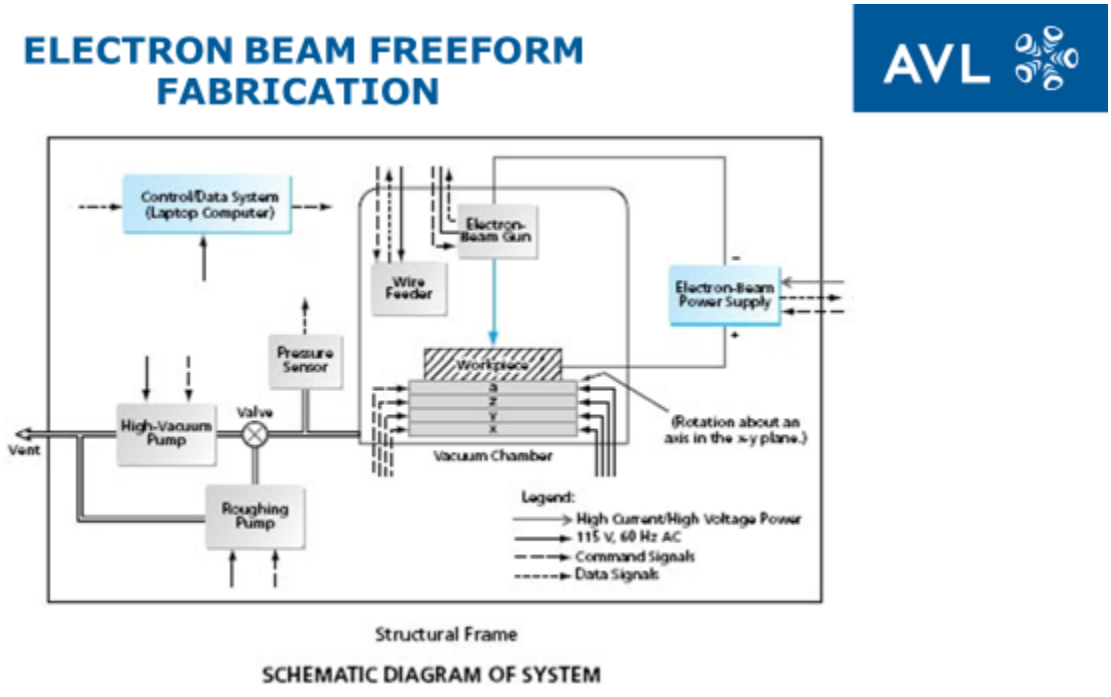


Figure 11 Electron Beam Freeform Fabrication – Process [47]

### 2.2.3.2 Electron Beam Additive Manufacturing (EBAM)

Similar to EBF³, EBAM uses an electron beam as an energy source and material is supplied in wire form. However, the electron beam gun is not fixed but also moveable, which allows for more freedom in structure and very high build rates. Like in EBF³, different wires (diameter as well as material) can be used in one build. The process was developed by the US company Sciaky. All in all, it offers high build rates to low prices because wire is cheaper than powder. Furthermore, the build size goes up meters, limited by the vacuum chamber the process requires. On the other hand, variation in wall thickness and therefore the whole structure relies on wire thickness which leads to less structural freedom than powder processes and wider tolerances. [50][51]

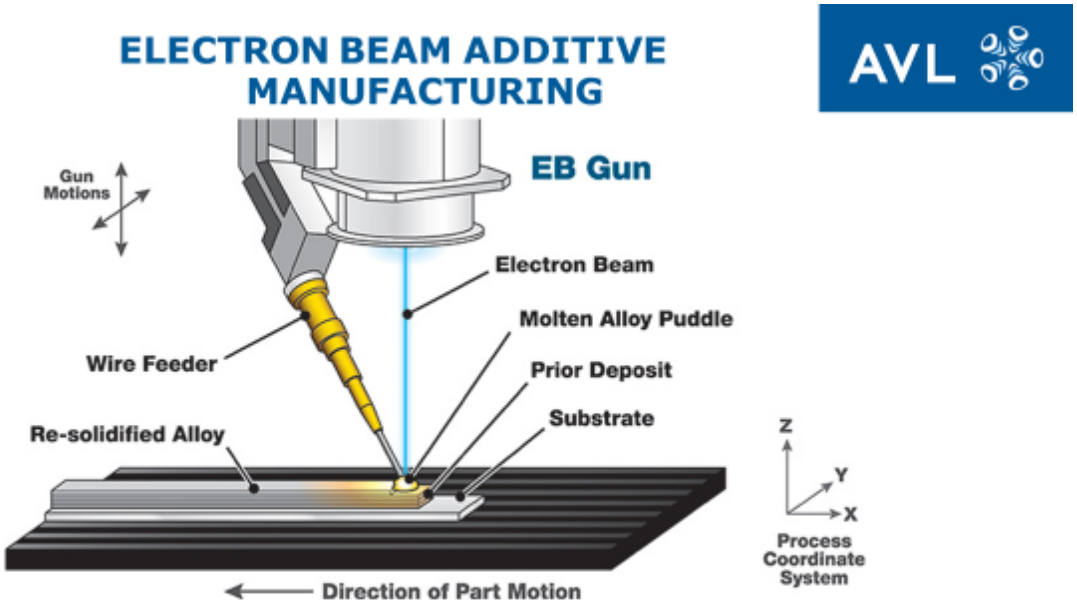


Figure 12 Electron Beam Additive Manufacturing – Process Overview [50]

## 2.2.4 HERMLE Metal Powder Application (MPA)

The MPA process developed by the German HERMLE® AG uses a combination of build-up welding and CNC machining, but in this case the build-up is done by accelerating the powder grains through a Laval nozzle using a carrier gas and shooting the particles on the substrate. Therefore, MPA is actually based on force welding. This leads to high build rates and opens the possibility of building large volume components as well as building on precast blanks. Also material combinations are possible. However, the process seems more adequate for massive rather than fine detailed components.

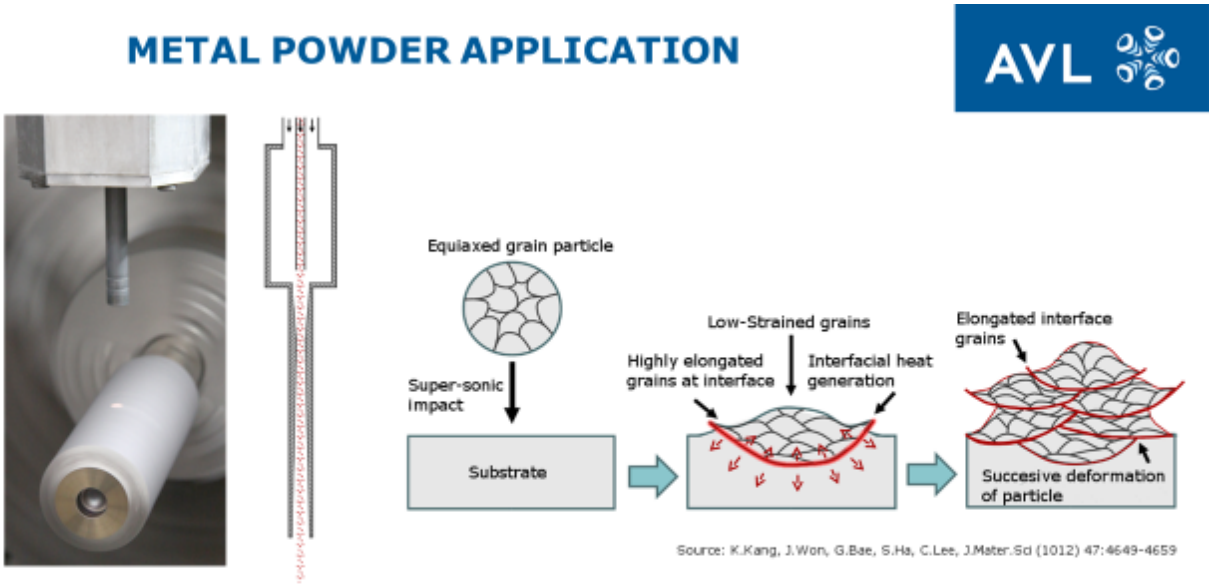


Figure 13: Metal Powder Application – Process Overview

To create hollow parts and add further structural freedom, a milling machine is needed. Both, the milling and MPA are integrated in on 5 axis machining center. Hollow parts like cooling channels are milled into the prepared blank, filled by MPA with a water-soluble filling which can be dissolved after it is covered and closed with further metallic layers. But as of today selection of materials is limited.

## 2.3 Useable Materials and corresponding Properties

Since additive layer manufacturing is basically a powder metallurgy process a wide selection of metals powders is available as well as process able and therefore outperforms casting processes by numbers. However, each metal powder requires the determination of the adequate process parameters (laser energy, temperature, layer thickness etc.). Considering that additive layer technology is still in its infancy and finding those parameters is also a cost issue most manufactures provide a limited number of common alloys for day-to-day applications but offering personal support for particular requests. Standard materials offered by most providers are steel, aluminum, titanium and nickel alloys as well as chrome cobalt alloys.

Mechanical properties of printed materials surpass those of casted ones and are close to forged or wrought products. Inherent structural anisotropies along z-axis, if present due to the layer wise application, can be diminished by heat treatment.

### 2.3.1 Material Selection

Due to the different processes (sintering, welding etc.) material selection varies depending on the manufacturing process. While sintering processes allow for a wider selection of materials, namely most metals and ceramics, melting (and therefore welding) procedures call for weldable materials. It has to be mentioned that for laser and electron beam welding in an inert gas or even vacuum surrounding many metals meet this criterion.

The main issue with any material which meets the criteria is finding the right process parameters. Energy input (scan speed and beam energy), layer thickness, powder form, size, and even component form and size are crucial and vary for any metallurgical powder composition. Their evaluation is critical in order to reach the best result possible. Much research and development nowadays goes into process control and simulation to predict those parameters for certain powders and regulate them even during the built process.

Also the limitation of available powders has to be taken into account. Although nearly any metal can be transformed into powder form economic reasons oppose that. However, with a growing market this might change in the future.

However, today's materials for additive manufacturing are mainly just taken from other processes. Hence, the process is adapted to the available materials. [15] Most likely the future will bring a wider selection of materials specially developed or adapted for additive manufacturing processes with superior properties.

### 2.3.2 Material Properties

In order to achieve satisfying mechanical properties, finding the right process parameters is crucial. Under ideal conditions, material properties are somewhere in between cast and forged, comparable to wrought parts. Following some properties and frequently asked questions that are of interest and maybe need some clarification.

Anisotropy: Depending on material and process additive, manufactured parts can show some anisotropy in the z-axis compared to the x- and y-axes. This is due to the directional build-up process and consequential heat input. However, this mostly occurs with sintering processes and can be overcome by heat treatment.

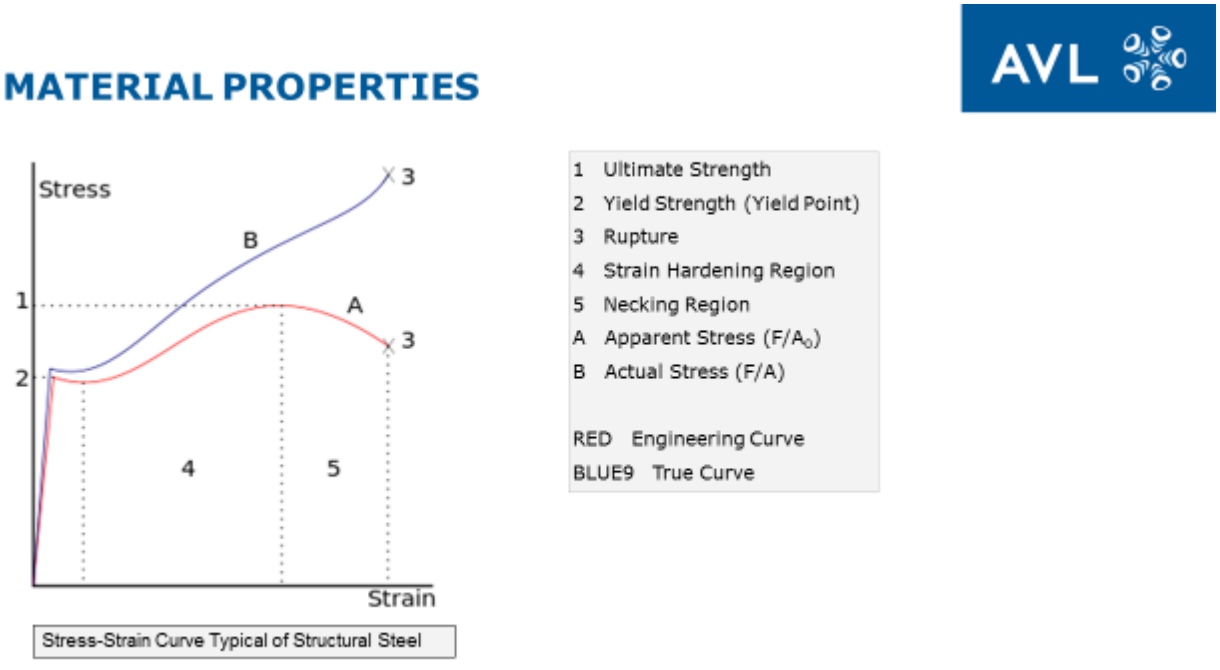


Figure 14: Stress-Strain Curve [44]

Yield strength: The amount of stress at which a material begins to deform plastically. This should be avoided in order to be reached for most design applications. Usually additive manufactured parts show similar results as wrought probes and are superior to cast ones.

Porosity: A problem also known to result from sintering and therefore an issue with AM processes using sintering, especially SLS and 3D Inkjet printing. Porosity depends principally on the system parameters and their proper choice results in densities well above 99% can be reached especially using SLM or EBM. Otherwise technologies known from sintering, like high isostatic pressing (HIP), help to deal with porosity. [15]

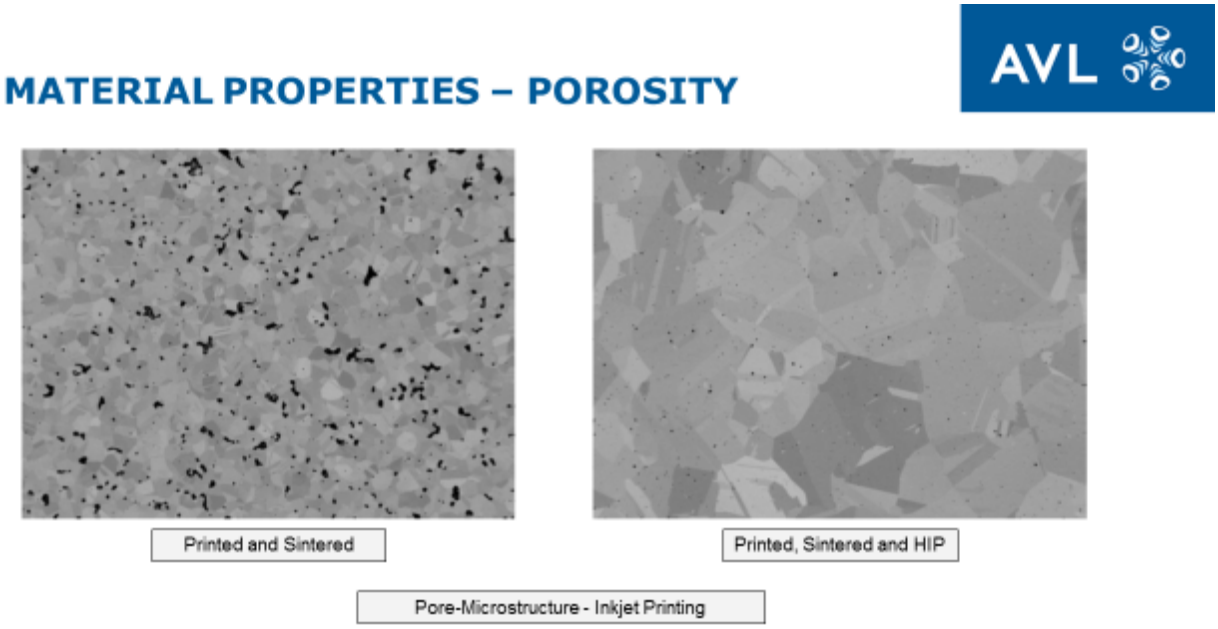


Figure 15: Material Properties – Porosity [29]

Heat Treatment: Principally possible and recommended to reach certain properties. It must be pointed out that parameters known from heat treatments on parts created with another master forming process may not directly apply or end in the same results with ones formed by AM. Therefore, finding the right parameters is crucial again, but a lot of papers are already published on this topic [12][13][15] [18].

Crystal Growth: Crystal growth also depends largely on the system parameters, although it can be generally said that crystals grow through the different layers, due to reheating. However, orientation and size vary however but can also be influenced in post processing.

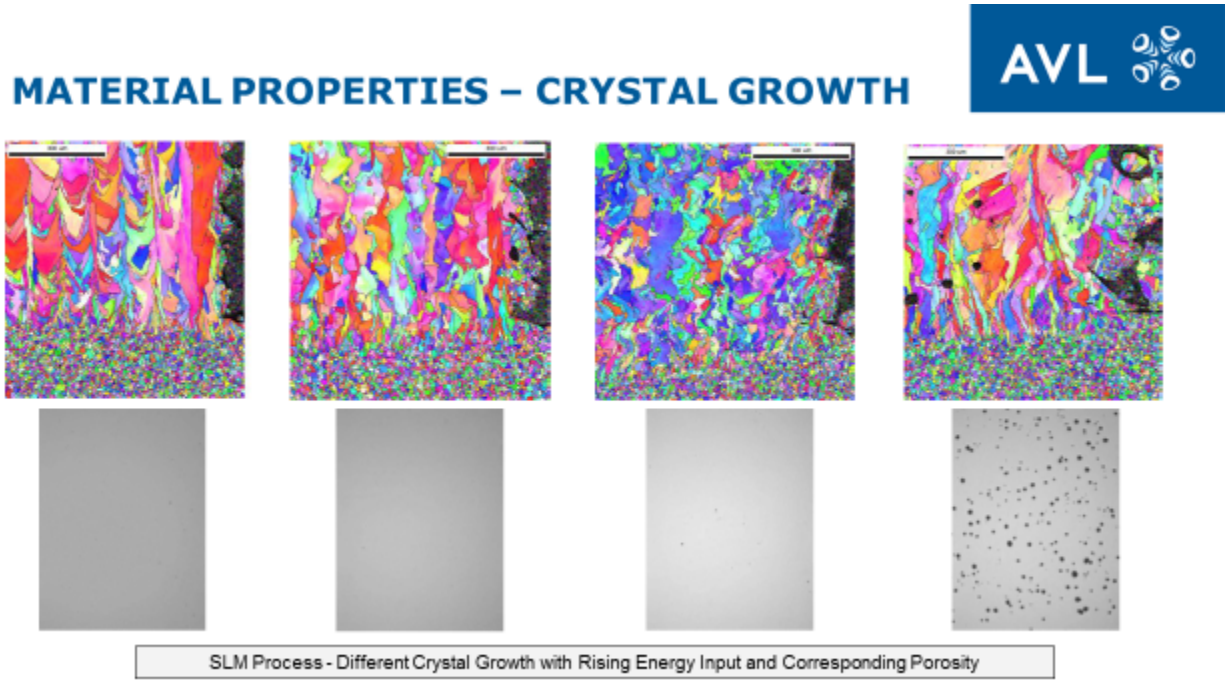


Figure 16: Material Properties – Crystal Growth of Inconel 625 [12]

As-Built: AM Component out of the "printer", without any post processing (e.g. heat treatment)

To obtain the best possible material properties in AM processes finding the right process parameters is key, and as such will be the focus of next chapter. Furthermore, a list of AM materials and their properties can be found in the appendix.

### 2.3.3 System Parameters

#### 2.3.3.1 Energy Input

Of course the main parameter for any sintering or welding process is the amount of energy that's put into a certain spot or area. It is proportional to the LASER/electron beam power, number of beams and scan speed. Preheating changing temperature of the chamber must always be considered. [15]

#### 2.3.3.2 Scan Speed

The velocity of the LASER beam over the powder layer, normally given in mm/s. [15]

#### 2.3.3.3 LASER/electron beam power

Power of the LASER/electron beam in watts. [15]

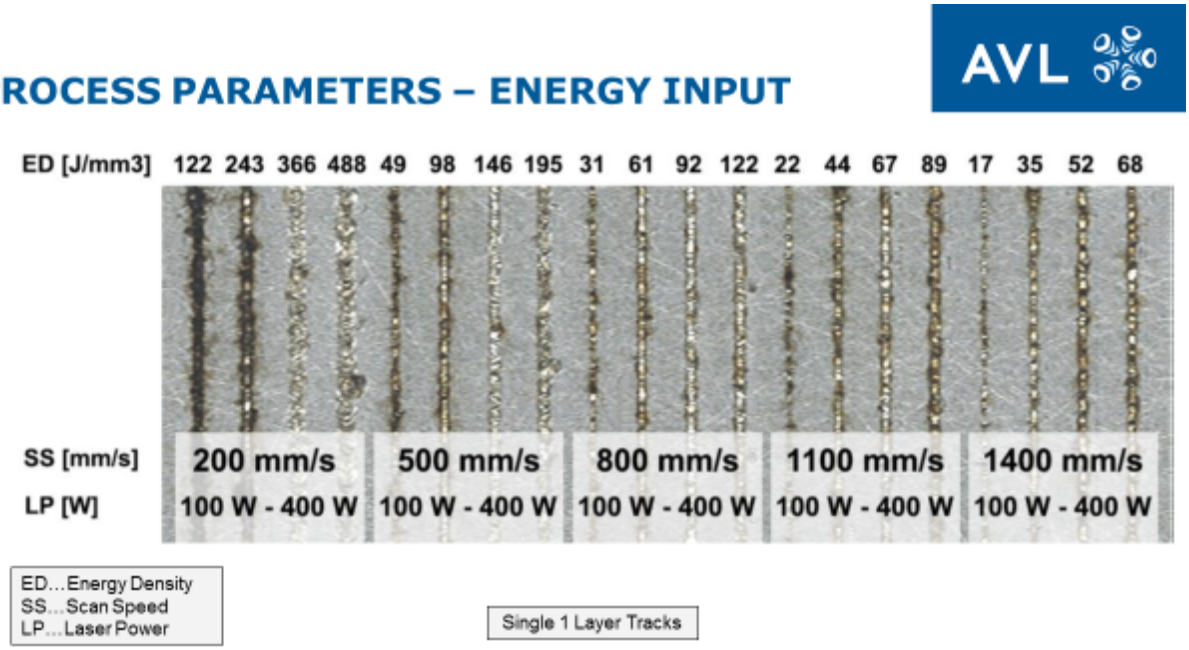


Figure 17: Process Parameters – Energy Input (high strength aluminum alloy EN AW 2618) [15]

#### 2.3.3.4 Layer Thickness

The minimum layer thickness varies between processes as well as materials, powder sizes and machines. Finer layers principally lead to better mechanical properties and structures, but also to lower build rates and require fine powder and appropriate energy input. Different layer thickness in one build can be realized to reach higher build rates by thicker layers while keeping structural accuracy where it is needed and accordingly thinner layers. For wire fed processes layer thickness dements on the wire diameter.

#### 2.3.3.5 Powder Size and Form

Power size and form influences porosity as well as surface quality, layer thickness etc. An issue about powders nowadays are missing standards, see also 2.4.3.6. [16] [17]

#### 2.3.3.6 Build Rate

The build rate is a result of layer thickness and scan speed. Basically build rate gives an idea how fast components can be built and therefore their costs. However, different build rates can be realized with every process but higher built rates normally lead to either less accuracy or worse material properties. The unit is either kg/h or $cm^3/h$.

#### 2.3.3.7 Powder Pollution and Age – Recycling

Principal idea of powder bed processes is to reuse unused loose powder after the component is taken out. However, there are a few points that have to be considered and are topic of today's studies. The main issue is an international standard to qualify and test used powder. On one hand powder size and form can vary from the original powder. Powder particles close to the melting or sintering zone may also increase in size or change their form. On the other hand reactive materials, like titan, aluminum etc. may react if they are exposed to gases like oxygen. [16]

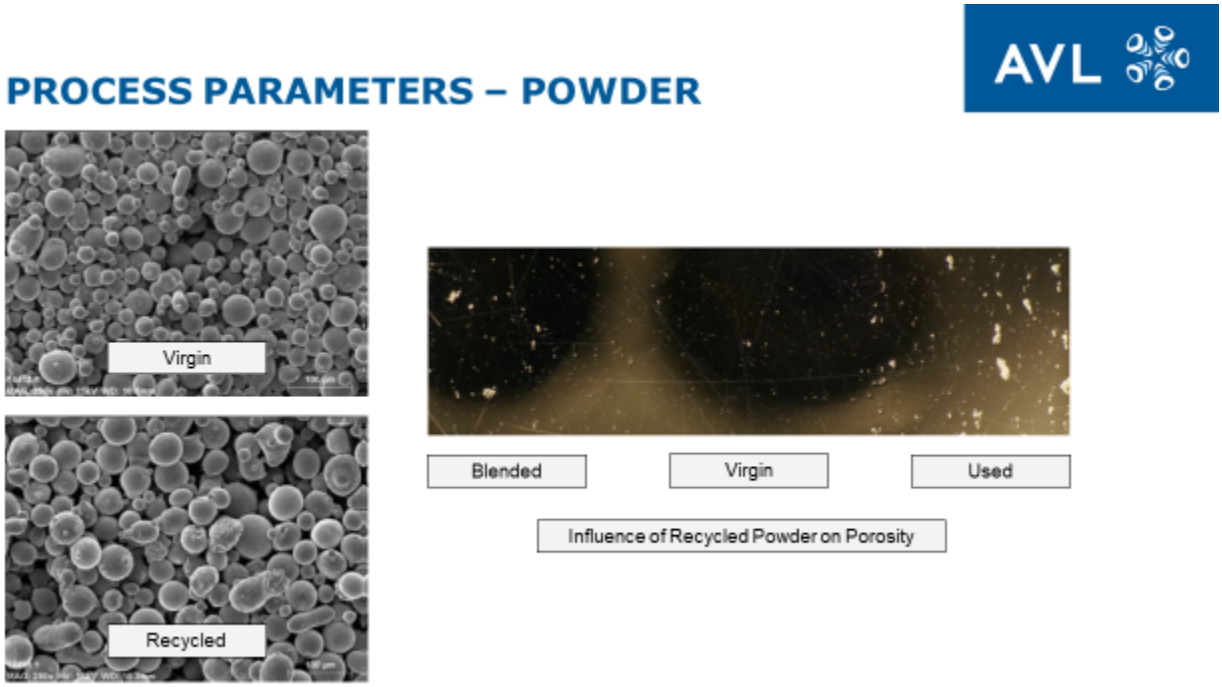


Figure 18: Process Parameters – Powder Properties [16]

As a result, critical parts nowadays are produced from virgin powder, although, more knowledge about process parameter, international quality standards and used powder post processing methods may soon change that.

#### 2.3.3.8 Inert Gas - Chamber Atmosphere

Some metals are more reactive than others, especially if they exceed certain temperatures. In the case of titanium, for example, oxygen must be avoided in welding processes. Therefore, the powder bed chamber has to be filled with inert gas to prohibit embrittlement. Also for non-powder-bed processes like DMD an inert gas coverage is obligatory for those materials.

Another way to keep hazardous atmosphere away is a vacuum chamber used in the EBM process. High vacuum leads to the least pollution of the build component but are subject to the highest costs and time constraints which result from evacuating a larger chamber. Furthermore, low overall pressure is proportional to the material's vapor pressure which can lead to sublimation during the welding process.

## 2.4 Comparison AM processes

### 2.4.1 Processes

First a short summary of the AM processes and the corresponding materials.

Table 1: Short Forms

| Legend | |
|---|---|
| SLS | Selective Laser Sintering |
| DMLS | Direct Metal Laser Sintering |
| SLM | Selective Laser Melting |
| EBM | Electron Beam Melting |
| Inkjet | Inkjet 3D Printing |
| DMD | Direct Metal Dispositioning |
| MPA | Metal Powder Application |
| EBF³ | Electron Beam Freeforming |
| EBAM | Electron Beam additive Manufacturing |

Table 2: Process Comparison 1

| Process | SLS | DMLS | SLM | EBM | Inkjet |
|---|---|---|---|---|---|
| Build Up Process | Powder Bed | Powder Bed | Powder Bed | Powder Bed | Powder Bed |
| Build Up Process | Sinter | Melting/Welding | Melting/Welding | Melting/Welding | Glueing (Sinter) |
| Material Source | Powder | Powder | Powder | Powder | Powder |
| Required Material Property | Sinterable | Weldable | Weldable | Weldable | Glueable/ Sinterable |
| Energy source | LASER | LASER | LASER | Electron Beam | none |
| Max Build Size (today) | | 400 x 400 x 400 mm (EOS) | 800 x 400 x 500 mm (Laser Concept) | Ø350×380 mm (ACRAM) | 508 x 381 x 229 mm (z Cooperation) |
| Form Tolerance | | 20 -50 µm or 0.2% | | | |
| Surface Tolerances Ra | | 4-20 | | | |
| Layer Thickness | | 20 µm | | | |
| Min Wall Thickness | | 0.3 mm | 0.3 mm | | |
| Max Build Rate | 0,2 kg/h [51] | 100 cm³/h [7] | 100 cm³/h [4] | 0,2 kg/h [51] | 0,2 kg/h ([51] |

Table 3: Process Comparison 2

| Process | DMD | MPA | EBF³ | EBAM |
|---|---|---|---|---|
| **Build Up Process** | Build Up Welding | Build up welding/Milling | Freeforming | Freeforming |
| **Connecting Process** | Welding | Force Welding | Welding | Welding |
| **Material Source** | Powder | Powder | Wire | Wire |
| **Required Material Property** | Weldable | Weldable (cold) | Weldable | Weldable |
| **Energy source** | LASER | Gas Pressure | Electron Beam | Electron Beam |
| **Max Build Size (today)** | Limitless | depents on milling maschine | 2500*2000*2700mm (NASA) | 5790 x 1220 x 1220mm (Sciaky)<br>2440 mm Diameter (Sciaky) |
| **Form Tolerance** | | | | |
| **Surface Tolerances** | | | | |
| **Layer Thickness** | | | | |
| **Min Wall Thickness** | | | ca 0,9mm (depends on wire thickness) | ca 0,9mm (depends min wire thickness) |
| **Max Build Rate** | 2,3 kg/h [51] | | 3 kg/h [51] | 9 kg/h [51] |

Table 4: Process Comparison - Materials

| Process | SLS | DMLS | SLM | EBM | Inkjet | DMD | MPA | EBF³ | EBAM |
|---|---|---|---|---|---|---|---|---|---|
| **Steel** | yes | yes | yes | yes | yes | yes | yes | yes | yes |
| **Aluminum Alloys** | yes | yes | yes | yes | yes | yes | yes | yes | yes |
| **Titanium** | yes | yes | yes | yes | yes | yes | | yes | yes |
| **Titanium Alloys** | yes | yes | yes | yes | yes | yes | | yes | yes |
| **Nickel Alloys** | yes | yes | yes | yes | yes | yes | | yes | yes |
| **Cobalt Chrome** | | yes | yes | yes | | | | | |
| **Magnesium Alloys** | | yes | yes | | | yes | | | |
| **Copper** | | | | yes | | yes | yes | yes | yes |
| **Ceramics** | yes | yes | yes | | yes | yes | | | |
| **Plastics** | yes | no | no | no | yes | no | no | no | no |
| **Titanium-Aluminde (Inter-metallic)** | no | | | yes | no | | | | |

| | | | | | | | | | |
|---|---|---|---|---|---|---|---|---|---|
| **Ti-Ni-Al (Inter-metallic)** | no | | | | no | yes | | | |
| **Cu-Ni-Al (Inter-metallic)** | no | yes | yes | | no | | | | |
| **Posttreat-ment materialwise necessary** | yes | no | no | no | yes | no | yes | no | no |
| **Different Material Layers** | lim. | limite d | limited | limited | limited | yes | yes | yes | yes |
| **Material Gradients** | | yes | yes | | | yes | limited | limited | limited |
| **Build on premanu-factured surfaces** | no | just planar | just planar | just planar | no | any accessible | most | any accessibly | any accessibly |

Empty fields: no source available but technically not impossible

As to be expected, every process has its advantages and drawbacks. While powder bed processes offer great tolerances and accuracy, build up welding has theoretically no restriction size wise. Powder bed processes however, also vary widely in that department. While DMLS and SLM and even Inkjet printing offer build chambers around 500mm EBM stays with around 350mm. The main reason seems to be the obligatory vacuum chamber for EBM, and while a raise in maximal build sizes can be expected, EBM will probably always be a step behind SLM/DMLS. Another advantage of build-up welding processes is the possibility to work on nearly any surface. This makes it also applicable to combining half built components and repairs.

In regards to material selection, all processes seem to offer the main candidates in form of steels, super-alloys, aluminum alloys, titan alloys and titanium. It has to be said that Information on EBM processed Aluminum Alloys is rare. Also materials like magnesium, molybdenum and most of the intermetallic phases are possible but are mainly experimental and in need of further development. Also further metals like tungsten, tantalum and niobium are not listed but processable with e.g. EBAM.

However, every process seems to offer some specialties. While Sintering processes allow the processing of ceramics and plastics, EBM can handle intermetallic phases like titanium aluminide. Furthermore, it seems to be especially suitable for nickel and titanium alloys which explains the focus of aerospace industries on this process.

Laser cladding seems to deliver promising results with the same materials as SLM, probably because they principal welding process is the same. Steels, aluminum alloys as well as titanium alloys can be processed delivering excellent results.

Wire based processes offer higher build rates and easier material handling. Additionally, build size is closer to laser cladding then powder bed processes. On the other hand, tolerances and minimal wall thickness are inferior.

### 2.4.2 Material Properties

Material property charts are presented here to provide an overview. First a comparison of EBM manufactured, casted and wrought TiAl6V4, which is a high purpose titanium alloy. Source of the data is ARCAM. [5]. The EBM probe shows better results than the cast end even the wrought one. However, there is no information on probe size and form as well as number of tests.

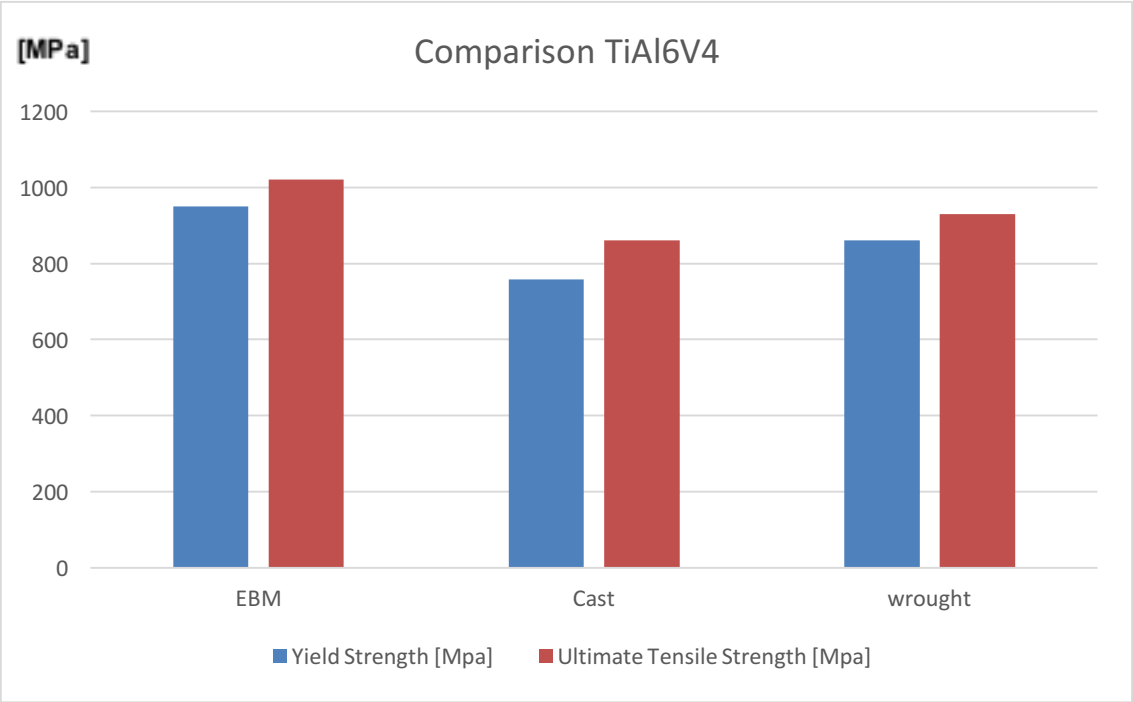


Diagram 1: Process Comparison – Material Properties for TiAl6V4 [5]

Secondly a comparison between DMLS and SLM manufactured 17-4PH Stainless Steel. Source [17]. The SLM process shows better results than DMLS in hardness and ultimate tensile strength, however, yield strength is a little lower, and the variance in SLM probes is higher. Both processes are at least on a level with wrought probes.

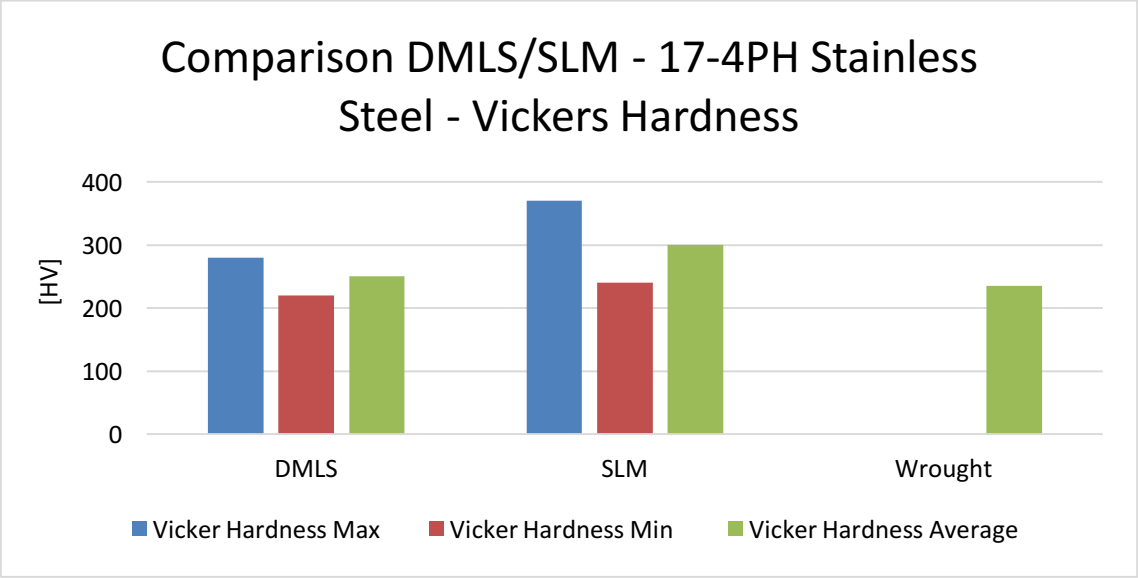


Diagram 2: Process Comparison – Material Properties - Stainless Steel – Hardness [17]

Also hardness tests show very satisfactory results. As for any other primary shaping process the can be influenced by post process treatment. It has to be mentioned that some of this treatment have to be adapted to the surfaces crystal structure which can be different for varying form processes.

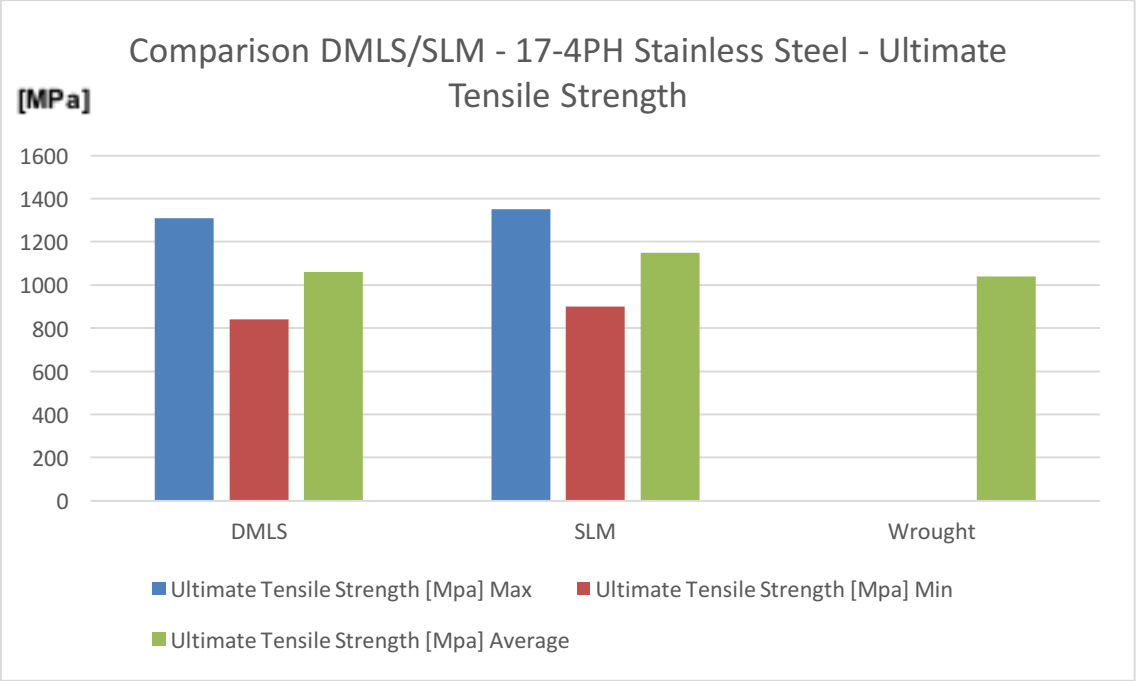


Diagram 3: Process Comparison – Material Properties - Stainless Steel [17]

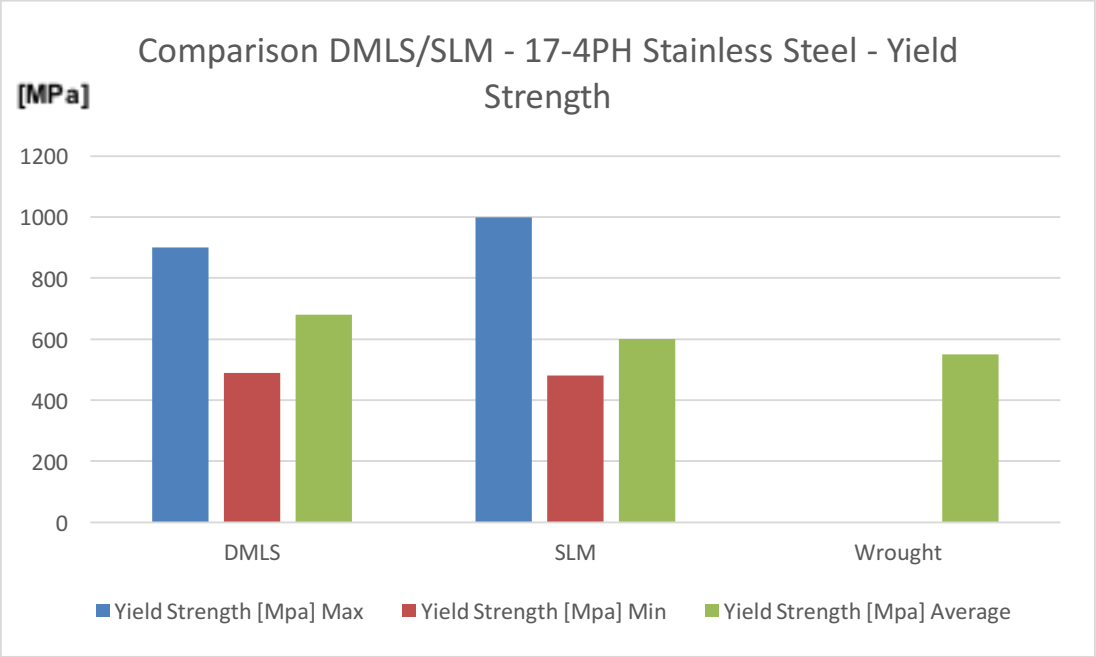


Diagram 4: Process Comparison – Yield Strength – Stainless Steel [17]

It has to be mentioned that public data on high cycle fatigue is rare. It seems like companies doing these time and cost excessive tests prefer to keep the results to themselves. Data available for Titanium alloys show good results but a high dependency on heat treatment.

#### 2.4.2.1 Materials with Potential for Cylinder Head Application

As standard cylinder heads for gasoline engines of passenger cars are usually made from cast aluminum it is obvious to take a look at material properties of aluminum alloys produced additive manufacturing. However, also some other materials that cannot be processed properly or economically by classically production processes should be taken into account, especially titanium alloys.

##### 2.4.2.1.1 Aluminum Alloys

As mentioned cast aluminum alloy is the usual material of choice for todays gasoline cylinder heads. It offers great heat transport and sufficient strength under temperature while allowing lightweight design. However, the standard cast aluminum alloys offer relatively low strength compared to available machined and forged high strength alloys. As for additive manufacturing the available aluminum alloys are mostly limited to the low strength cast alloys like AlSiMg and AlSiCu combinations. However, the reason for this is not that other alloys are not processable but that powders of those cast alloys are easily available. As weldability is the main limitation for materials for additive manufacturing a lot of known high strength aluminum alloys could be handled and there is potential to develop new ones optimized for this production process. But for all of those the right process parameters have to be found. As of today some of the available high strength alloys are Scalmalloy, AlSiC and AlCu7

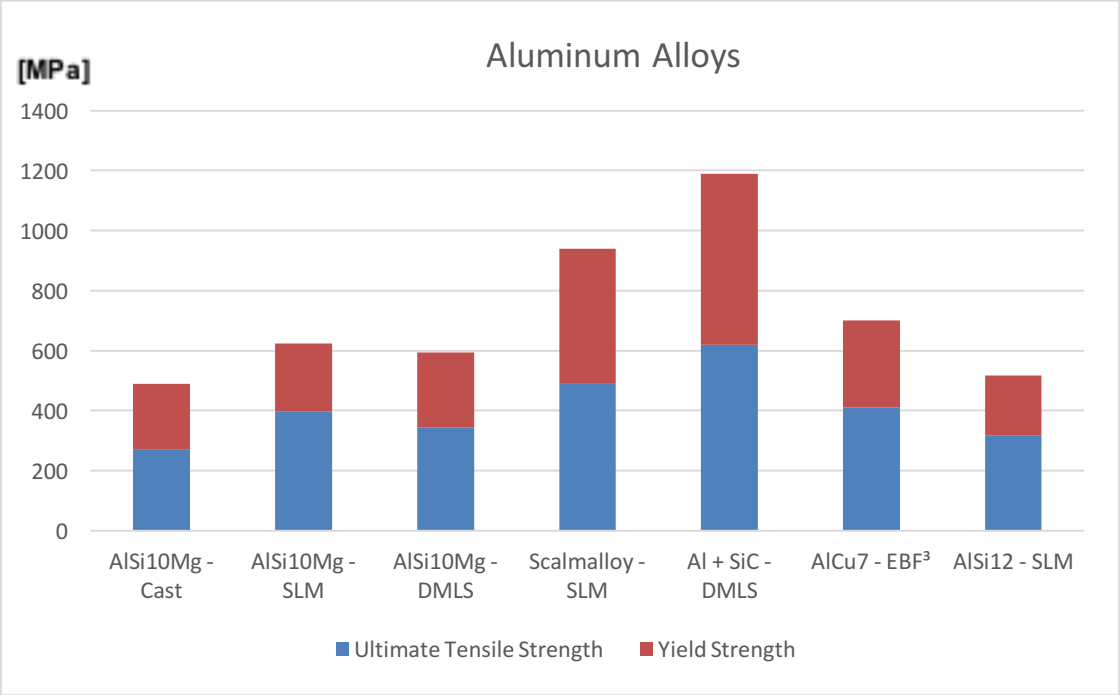


Diagram 5: Selection of Available Aluminum Alloys

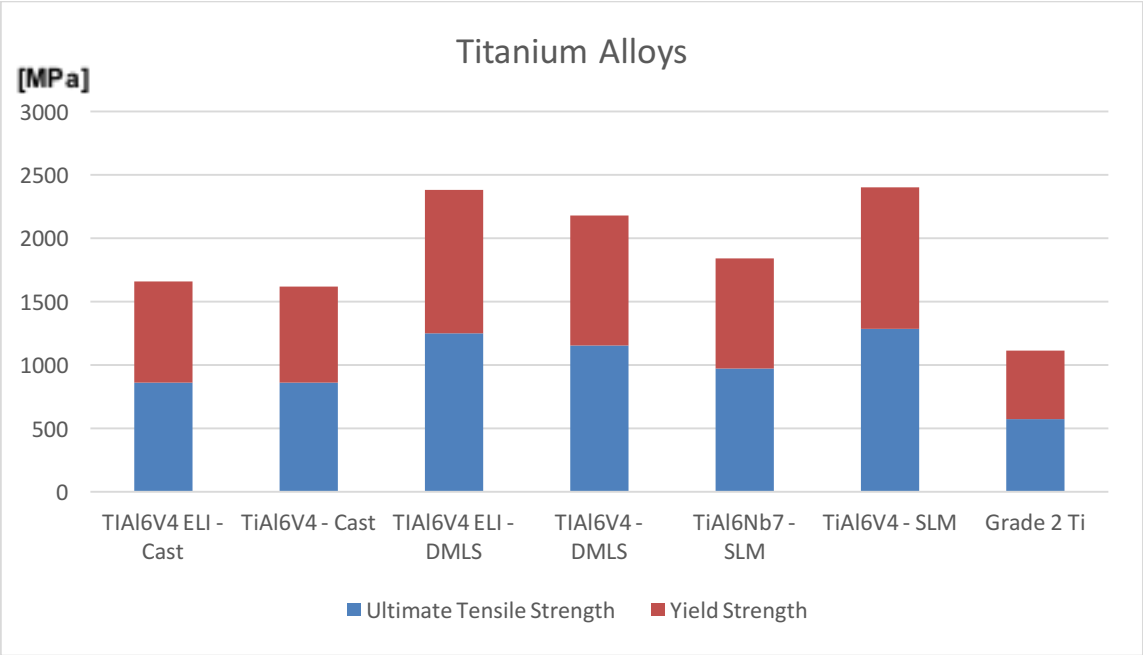


Diagram 6: Selection of Available Titanium Alloys

#### 2.4.2.1.2 Titanium Alloys

Titanium alloys offer high strength and sufficient heat resistance at a reasonable weight. However, they are hard to process and it is nearly impossible to achieve complex structures with classical production technologies. Main reason is the high affinity to oxygen when heated, extremely hindering welding, milling and casting. For many alloys later forming processes are severely limited. Since

additive manufacturing processes work with either shield gas or vacuum welding is not an obstacle and due to the near net shape structures produced post treatment processes are mainly limited to surfaces and heat treatment. With aerospace industry pushing the development titanium alloys like TiAl6V4 are available from most providers. If heat loads can be mastered titanium alloys would offer up to 3 times the tensile strength of classical cast aluminum alloys at just 2 times the density.

#### 2.4.2.1.3 Others

Other materials processable with additive manufacturing that might be interesting for cylinder head application are magnesium alloys, offering strength at minimal density but is inflammable, and titanium aluminide, an intermetallic combination of titanium and aluminum. It offers extreme high strength, heat and creep resistance at a low weight, but both, brittleness and and processability are still an issue. However, useable results can be achieved with EBM.

# 3 Cylinder Head

## 3.1 Functions and Resulting Loads and Stresses [1]

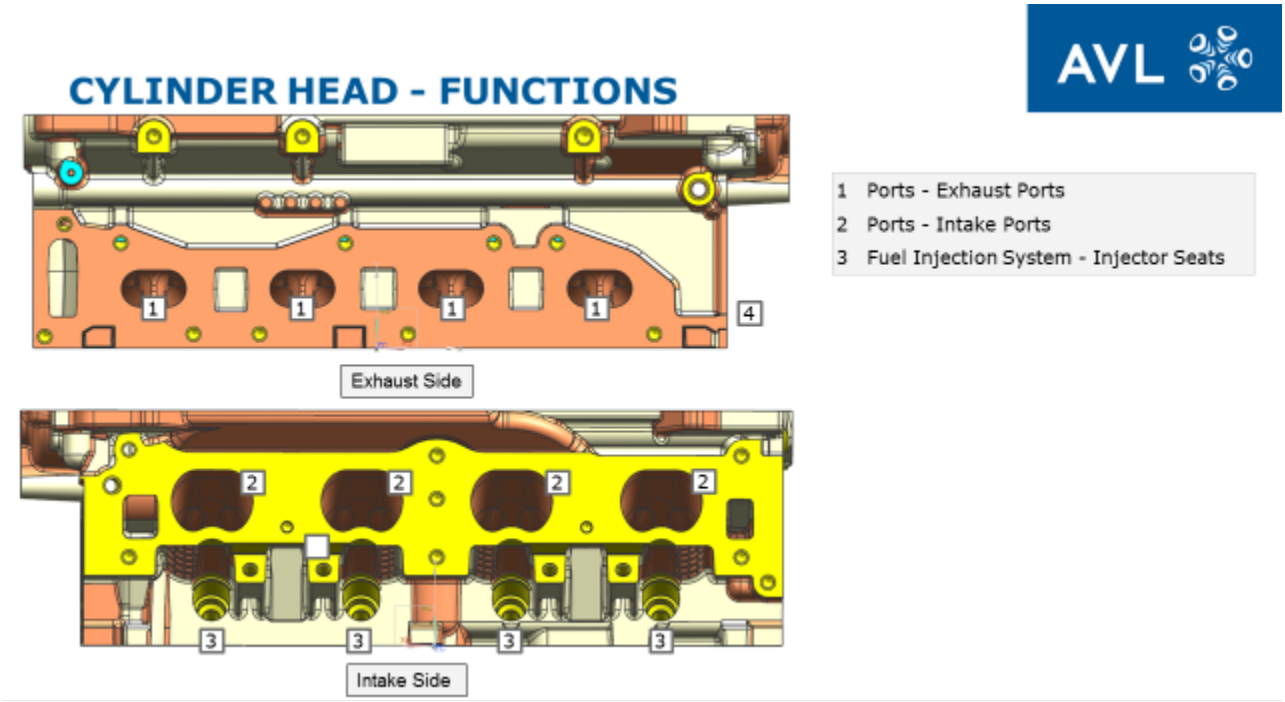


Figure 19: Cylinder Head Functions

### 3.1.1 Ports

Inlet and exhaust ports are integrated in the cylinder head. While the inlet port brings cooling with relative cold air, the exhaust port transports exhaust gas from the combustion chamber. Therefore, cooling of the exhaust port is necessary.
Locking the ports from the combustion chamber is taken care of by the valves, which leads to high loads at the valve seats. Hence these are made from a different material, usually steel which is pressed into the aluminum cast head.

### 3.1.2 Valve Train

The cylinder head is the housing for the valve train. Due to this bearing seats and room for the camshaft are needed as well as valve guidance. This leads to mechanical loads as well as requirements in tolerances. Furthermore, lubrication and further cooling can be necessary.

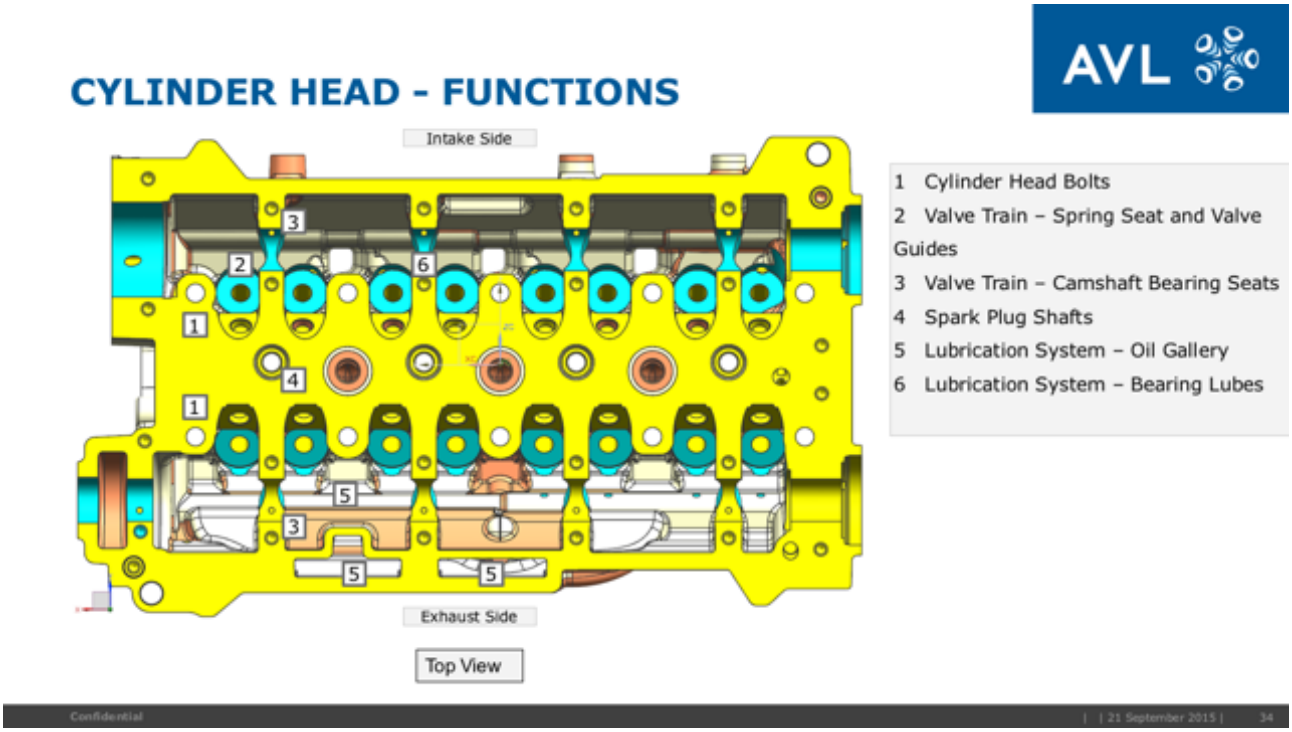


Figure 20: Cylinder Head Functions 2

### 3.1.3 Fuel Injection System

The fuel injectors of direct injection fuel systems and the injectors and combustion chamber of indirect injection Diesel engines are located in the cylinder head.

### 3.1.4 Ignition System

The spark plugs of gasoline engines and injectors of Diesel engines are located in the cylinder head. Additionally, the glow plugs of Diesel engines are placed there.

### 3.1.5 Cooling System

The cylinder head has to guide the coolant flow to keep the metal temperatures below critical levels. Usually the temperature limit in gasoline engines is not just set by material properties in form of thermal induced cracks but knock resistance of the gasoline. For standard gasoline maximal wall temperatures should be kept below 300°C to prohibit self-ignition. Weak points are on the exhaust side, therefore called the hot side, mainly the bridge between the ports and the vent seats.

### 3.1.6 Combustion Chamber

While sidewalls of the combustion chamber are part of the motor block, fire deck is part of the cylinder head. Its form has immense influence on flow characteristics and combustion leads to the main thermal and mechanical (pressure) loads.

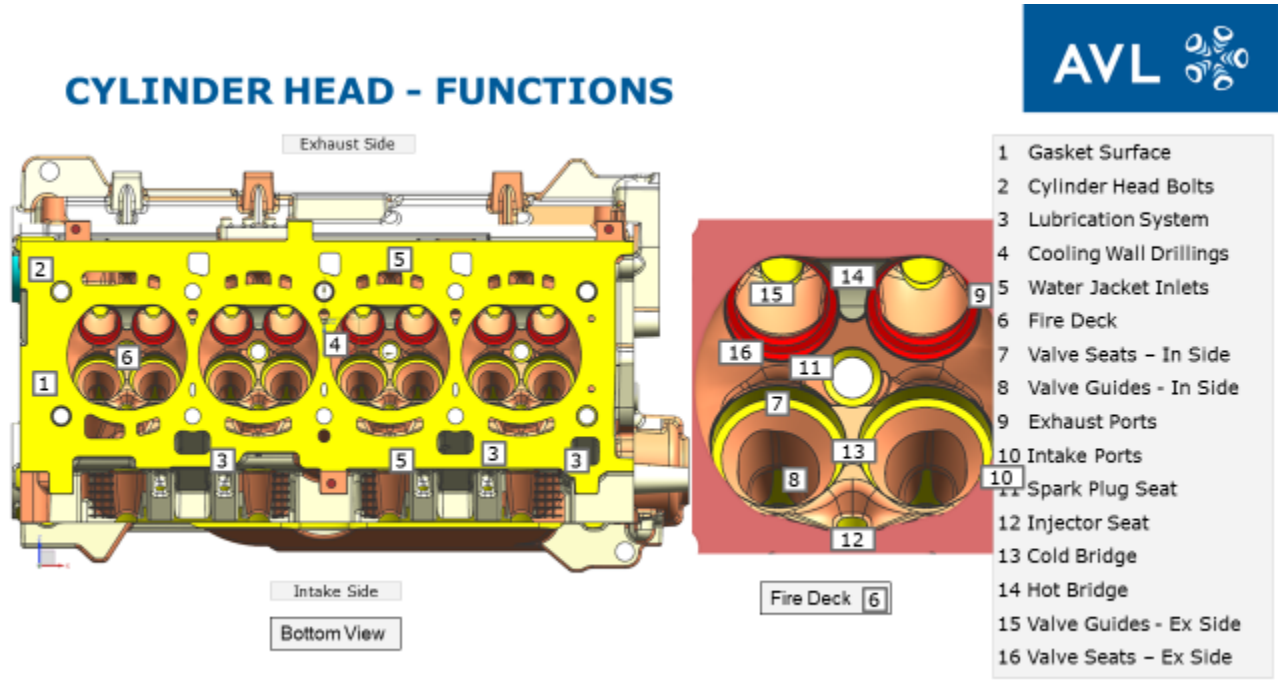


Figure 21: Cylinder Head Functions 3

### 3.1.7 Lubrication System

A Lubrication system is needed to lead the engine oil to the lubrication points (HLA, camshaft bearings...) and to drain it back to the crankcase. Furthermore, oil covered surface has an influence on heat transfer and therefore cooling, for example between valves and valve guides.

### 3.1.8 Gas Ventilation

The blow by gas and positive crankcase ventilation is usually lead through openings in the cylinder head (to the oil separator), which is usually in conflict with drain back openings for the lubrication oil. It is therefore imperative to include a sufficient number of openings with acceptable large cross section areas

## 3.2 Loads and Critical Regions

Load wise the most critical regions are hot spots around the fire deck. High temperatures around 300°C and changing pressure can lead to high cycle fatigue and thermal induced cracks. Due to position and limited cooling the bridge between exhaust ports, called the “hot bridge” is especially critical. Others are the exhaust ports themselves, especially the seats for the valve rings and the longitudinal bridge between hot and cold side. Due to the transient and often quickly changing load cycle current cylinder heads, especially those of engines with a high power to weight ratio, are highly critical components and designed at the limit of todays technical feasibility.

Hence for this thesis a high power density gasoline engine for a sports car is taken to demonstrate the potential of utilizing additive manufacturing. Actual load values for this cylinder head can be found later on in Chapter 6.3 (FEM Simulation) and while they can vary from head to head, they give a good general survey of today’s state of high tech car cylinder heads.

## 3.3 Current Production Technology

Nowadays passenger car cylinder heads are mainly casts from aluminum alloy. Additionally, heavier but stronger cast iron is an option. Applied casting technology depends on build numbers and implementation of the cylinder head. For truck and larger engines cast iron is the more common solution.

## 3.4 Restrictions due to Casting as Production Process

As for any casting process, certain design principles have to be followed to obtain suitable results. Most of them affect the achievable component structure, while some limit material selection.

### 3.4.1 Structure Constraints

Casting draft angles: In order to get cast components out of the cast form their surfaces have to be leaned towards the form. Undercuts can just be realized by further subdivided cast forms or lost form casts.

Minimal wall thickness: Minimal wall thickness attainable with casting processes used for cylinder heads is around 3 to 5mm.

Variation in thickness: abrupt jumps in wall thickness as well as bulks of material lead to cracks during the cooling process. So that steady changes in thickness and smooth, round designs are compulsory.

Surface quality: Depending on casting technique, form and cast material and cooling process surface quality varies a lot, but quality achievable is always limited.

Hollow parts: Hollow parts, cuts and openings have to be realized by cores. Since they are commonly made of form sand minimal thickness and structural complexity are limited. Furthermore, the possibility must be given to remove the sand cores after casting.

Heat transfer: Heat transfer in the cooling process should be considered in component design

Tolerances: Tolerances are a big issue with casting. Of course some casting technologies offer huge advantages over others but mainly due to the shrinking from liquid to solid stage and surface quality most touching and functional surfaces need machine finishing.

### 3.4.2 Material Constraints

Melting Temperature: Since the material has to be liquefied it must be heated above melting temperature and held there until the cast form is filled entirely. Considering that melting temperature of some metals is pretty high energy consumption on the one hand thermal load on the cast molds on the other must be handled.

Flow Properties: The liquid material has to fill the cast form entirely. Depending on the casting process and complexity of the component structure this calls for exceptional flow properties and surface moistening.

Thermal Conductivity: Has a huge influence on the cooling process.

Thermal expansion coefficient: Thermal expansion results in a direct proportional shrinking during the cooling process. In some cases, that can also lead to structural failure if the temperature differences in the component are considerably high in some areas.

Heat transfer Coefficient: HTC has a high influence on the cooling process.

Crystallization and Grain growth: Mechanical properties of the cast component are strongly influenced by its metallurgical structure, which is influenced by cooling speed, alloys, and component thickness and so on. Practically an isotropic grain structure with small grains is desired.

Alloys: Alloys can influence all the material characteristics above as well as mechanical properties, making casting easier or impossible.

It's possible to influence those constraints by certain measures, e.g. alloy additions, heated cast forms, pressure cast, heat treatment etc. but it's impossible to overrule all of them. Therefore, the sum of cast metals and their properties will always be limited.

# 4 Potentials Additive Layer Manufacturing on a cylinder head

## 4.1 Structure

Basically additive layer manufacturing allows to build any structure imaginable, as long as it stays within limits of the powder bed and minimal wall and layer thickness. However, depending on the additive manufacturing process, problems can occur with larger hollow spaces and backlogs under 45 degrees, which can be overcome by changing in layer direction or additive support structure which has to be removed afterwards.

So coming from a cast structure, which is pretty limited due to the production process, additive manufacturing offers the possibility to change the cylinder head topology to correlate the applied mechanical and thermal loads. Furthermore, some functional properties could be optimized due to the new possibilities. One of those is the cooling system, which will be covered later on.

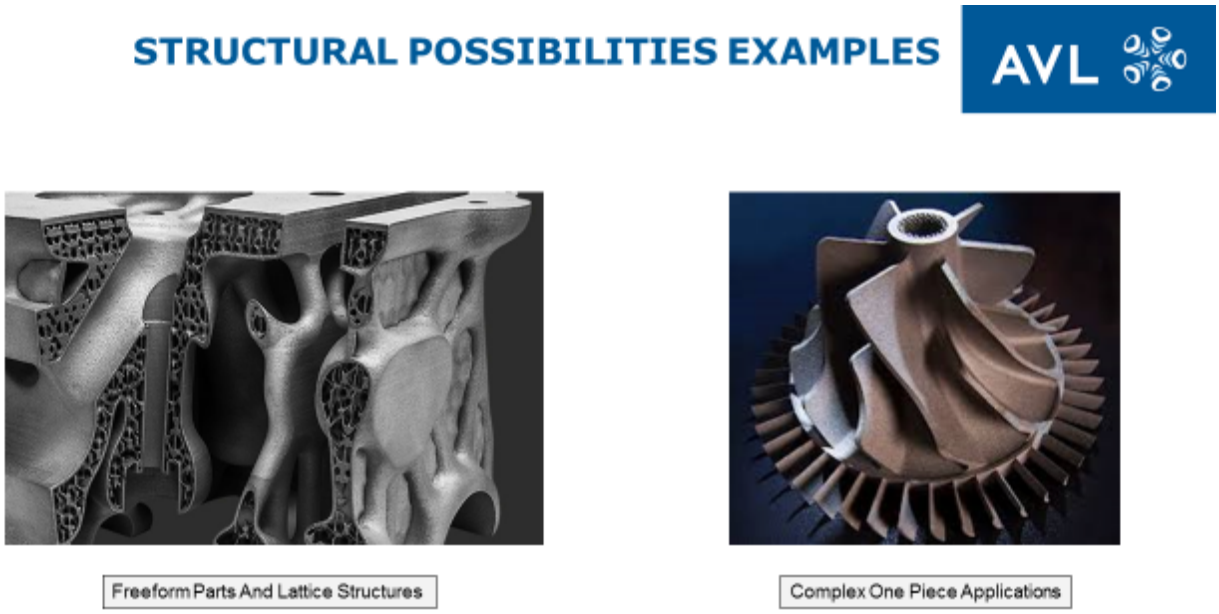


Figure 22: Examples for Structural Manufacturing Possibilities with AM

## 4.2 Materials

Although additive layer manufacturing offers a wide selection of materials which could be of interest for certain engine applications, the same aluminum alloy as used for the cast head is selected. Thus the result should be easy to compare. However, it is possible to reduce or eliminate some alloy materials which are necessary for casting but impair mechanical and/or thermal properties. For future application a known or specially created high strength aluminum alloy makes more sense.


Figure 23: Examples of AM Materials

## 4.3 Tolerances

Since tolerances of additive layer manufacturing considerably outperform standard cast cylinder heads, it is conceivable to reduce wall thickness in parts as well as the amount of post master forming treatment. Typical form tolerances of powder bed processes are around 0,2% of the part size for large parts and between 20-60 micrometers for small parts. Surface quality as build is around 4-20 µm Ra and 36-126 Rz depending on process, material, powder, machine and process parameters. Of course further surface treatment is possible. Minimal wall thickness is around 0,3-0,4 mm and layer thickness somewhere between 20-100 µm. For miniature parts Micro Laser Sintering is available with even closer tolerances. However, this process is very limited in size and therefore not of interest for a cylinder head application.

Table 5: Comparison Casting vs AM

| Process | Casting | Additive Manufacturing |
|---|---|---|
| **Structure** | | |
| limited by | change in diameter | min. layer thickness (> 20µm) |
| | draft angles | --> near net shape |
| | undercuts | |
| min. wall thickness | 3-5mm | 0.3 - 1mm |
| hollow sections | lower and structural limit set by sand cores | support structures for diameter > 8mm and > 45° |
| tolerances | depend on casting technology | 20-50 µm or 0.2% |
| **Material** | | |
| limited by | thermal properties | for most processes weldability |
| | flow properties | |

# 5 Model and Simulation

## 5.1 Current Cylinder Head

This simulation is based on a current high performance cylinder head developed by AVL GmbH for Alfa Romeo. It is a 4-cylinder direct injection gasoline engine which delivers 150 kilowatts per liter displacement. Ignition is placed in the middle, injection on the cold side and the 4 valves are driven by 2 camshafts on top. The cylinder head is cast from Aluminum alloy.

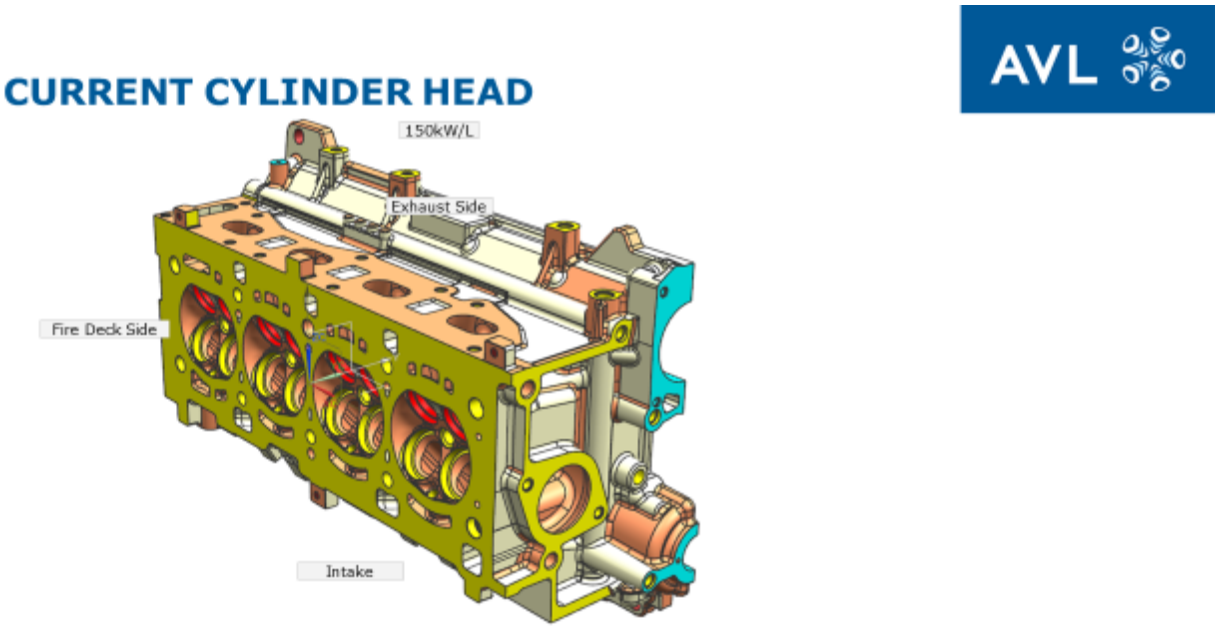


Figure 24: Current Casted Cylinder Head

## 5.2 Simplifications and Alterations

Most of the main features are taken from the original head without alterations. This refers to the fire deck, ignition, injection, ports, valve trail, lubrication system and head bolds. The cast related surfaces are simplified to create further design space for topology optimization. Largest alteration to the original head is the development of a completely new water jacket.

## 5.3 Cooling System

Main purpose of the water cooling system, also known as water jacket, is the transportation of heat from zones of high temperature. In a gasoline engine the classical hot spots are on the fire deck around the exhaust valves, the ignition plug and the bridges between those. Due to the casting process the water jacket has to be realized as a sand core. Therefore, the structural freedom is very limited. Compromises concerning ideal cooling and flow on one hand and producibility on the other have to be made, especially at the valve rings. Additive layer manufacturing opens a wide range of possibility to optimize the cooling system structural as well as hydrodynamic wise.

### 5.3.1 Current Water Jacket

The current water jacked is formed as a sand core. Therefore, it is voluminous and structural freedom is limited. Water flows longitudinal from one cylinder to another. Additionally, cold water is coming up from the crank case below cooling the valve seats. To meet casting requirements minimal wall thickness and minimal channel cross diameters are limited, so some areas of high cooling demand, like hot side vent seats cannot be reached because either diameters would be too small or production tolerances call for thicker walls. Other spots, like the hot side bridge, are cooled rather by a high amount of water flow then by an optimized spot cooling, since flow optimization of the surfaces is limited by casting constraints. However, it has to be said that this conventional water jacket would create some issues for additive manufacturing processes since some of the box section exceed diameters that can be produced without supporting structures. On the other hand this supporting structures can be realized as fins to improve flow. [46]

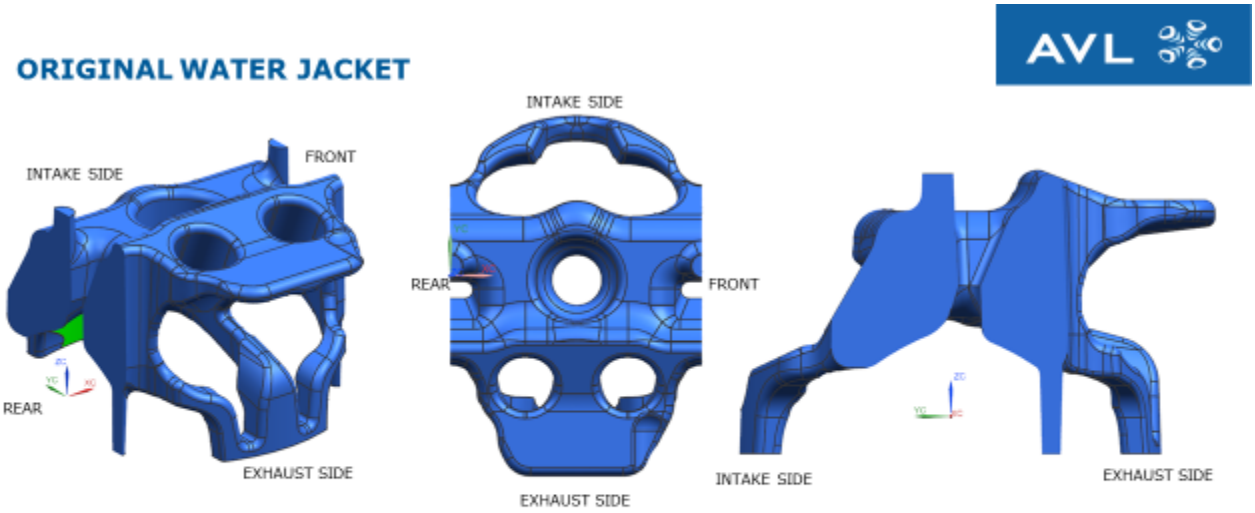


Figure 25: Sand Casted Water Jacket

### 5.3.2 Flow Optimized Water Jacket

In order to fully utilize the potential of additive manufacturing, a from scratch new water jacket has to be designed. Both, additional design space as well as superior cooling should be achieved. Second is of particular interest since the current cylinder head temperature at full load is borderline: So a direct comparison of both thermal simulations will show possible improvements.

The main idea was to build a water jacket which delivers cooling right to the hotspots while leaving other areas untouched to create design space for the topology optimization. Furthermore, the water jackets structure should keep flow, heat transfer and stability parameters in mind.

In collaboration with Robert Pöschl from AVL CFD department weak spots of the current water jacket were addressed and requests for an ideal water jacket were placed. The following new design ideas were proposed:

- Flow optimization and spot cooling: Instead of the current cast constrained form the new water jacket should consist of smaller streamline channels guiding the coolant directly to the hot spots instead of voluminous cross sections.

- Valve seat cooling: Exhaust port valve seats are a zone of high heat input but with limited design space for cooling, definitely too small of diameter to build working sand cores. A supposed redress here is a small channel directly around valve seats.
- Ignition plug cooling: Due due the high pressure from fire deck side and limited space a cooling close to the spark plug head is hard to realize with casting technologies. Bringing the cooling channels closer to the fire deck would be favorable.
- Structural and heat transfer optimized bridge cooling: Hot bridge is usually the hottest spot of the cylinder head and most likely to show thermal induced cracks. The strategy here so far is to get as close to fire deck as possible while keeping the minimal diameters necessary for casting. Mostly stability issues with the given casting diameters prohibit an improvement in cooling so far. Our new approach is to split this channel up into multiple channels to increase the surface on one while maintaining stability on the other. Furthermore, upper channels provide cooler water for the spark plug cooling.
- Valve guide cooling: Another spot of high heat input are the valve guides in the exhaust ports. As around the hot bridge getting the cooling channels as close to the heat input zones as possible is crucial here.
- Minimized diameters but increased surfaces: Generally smaller channels but due to their number an overall large surface.
- Cross sections: On the one hand smaller cross sections in areas of high temperature to increase flow velocity end turbulence for higher heat transport. Additionally, elliptical cross sections to increase surface compared circular ones and stability.

This leads to following design for the given cylinder head:

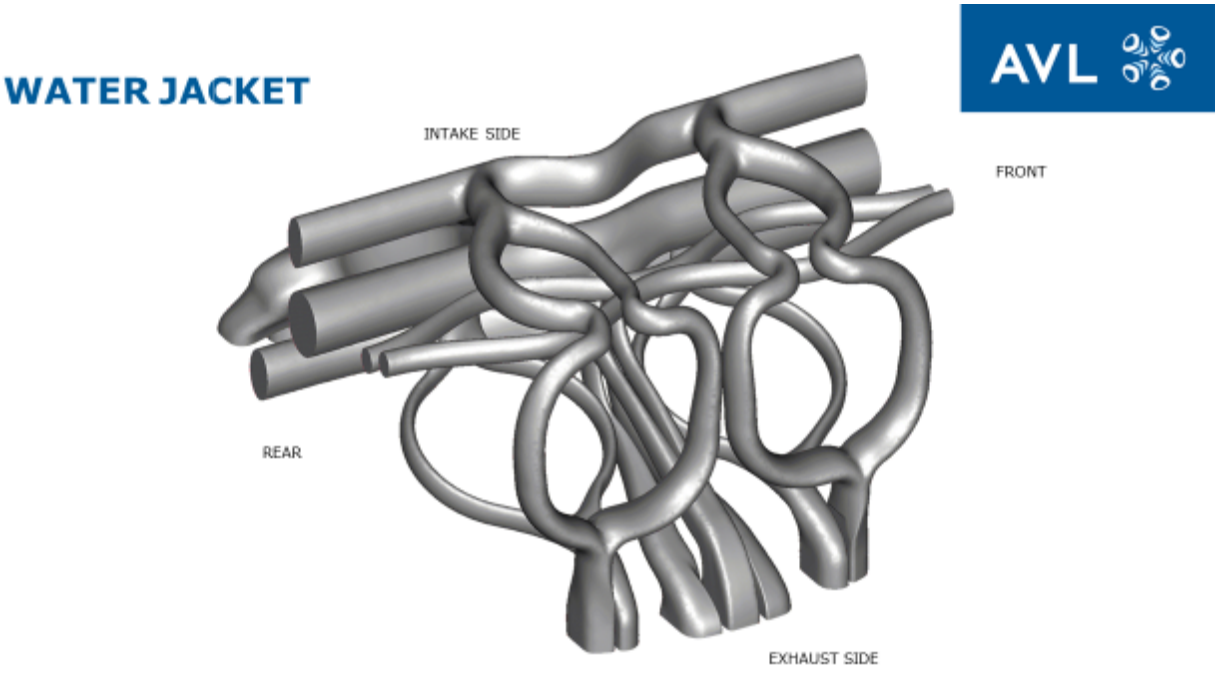


Figure 26: Additive Manufacturing Water Jacket

Intake side (cold side):

Incoming water flows around the injector to proceed in one canal trough cold bridge from where two channels build a ring around the ignition plug. The shorter part shows lower diameter to push flow towards the longer ring as well. Additional water comes from the front from the previous cylinder and is lead to the following cylinder in a collecting pipe in the middle bridge.

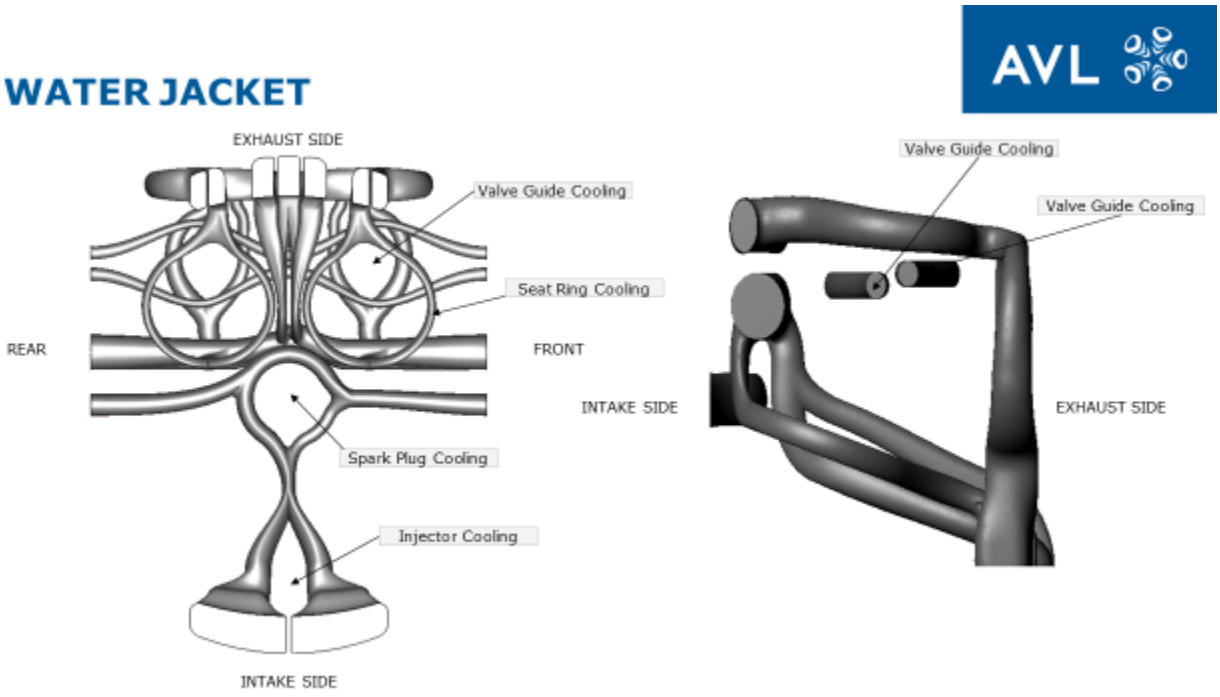


Figure 27: Additive Manufacturing Water Jacket – Functions

Exhaust side (hot side):

The exhaust side cooling jacket is divided into different areas, namely hot bridge, valve seat and exhaust ports/ valve guide. Hot bridge cooling is divided in four elliptical channels, offering large surface for heat transfer while keeping the volume low for mechanical stress and higher flow velocity. Those channels reunite in one collecting pipe close to the ignition plug. Diameters are also adapted to temperature, smaller at hot spots and wider in colder areas. Higher flow velocity and therefore turbulence increases the heat transfer coefficient.

Valve seat cooling is realized by a ring around the seats, formed by two canals separating on the exhaust side little closer to the hot bridge and joining right in the middle on the intake side of the valve seat. This should provide a little shorter channel on the hot bridge side to cope with the higher temperatures there. Overall diameters are also temperature related in this area.

Two extra pipes cut through the cylinder head longitudinally, cooling the valve guides. Last but not least further channels run around the exhaust ports from where they proceed to the valve seats and end up in a third collecting pipe.

Most cross diameters are elliptical for following reasons:

- Manufacturing: Elliptical walls lead to steeper angles which allow larger hollow sections without support structures with additive manufacturing technologies.
- Heat transfer: Larger surface for heat transfer while keeping the same volume compared to circular cross sections.

- Structural Stiffness: Proper orientated elliptical structures can increase stiffness.

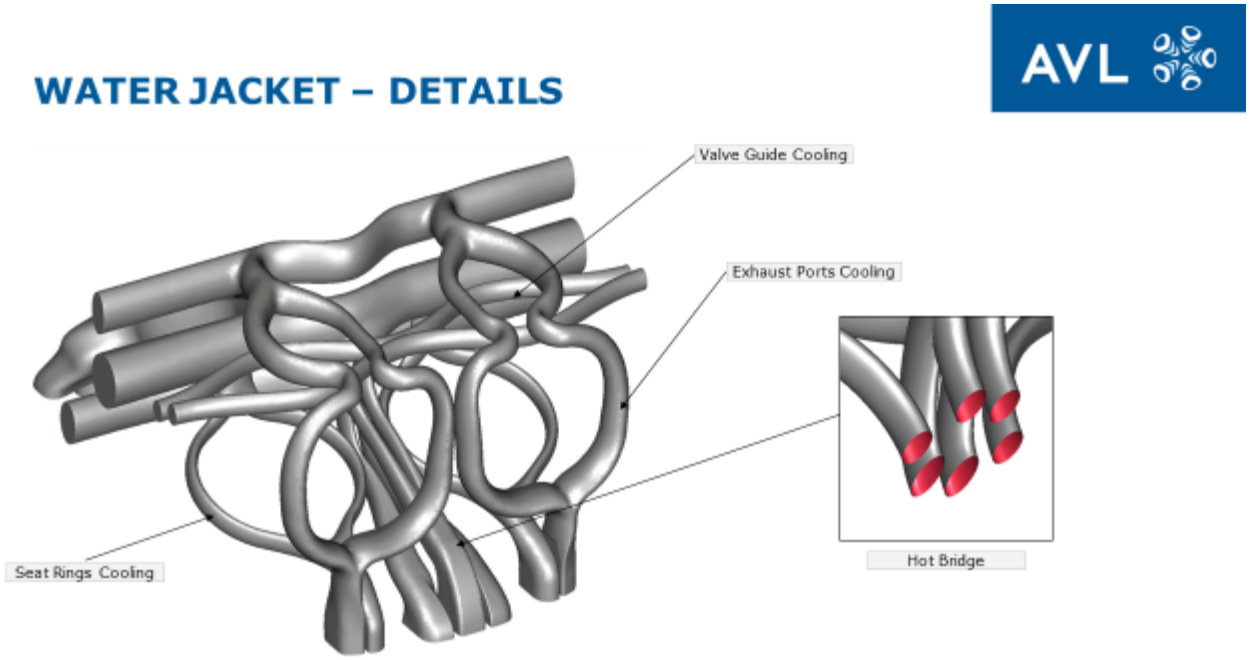


Figure 28: Additive Manufacturing Water Jacket – Detailed Hot Bridge

To facilitate the CAD design process longitudinal diameters of the the collecting pipes are kept constant, although it should increase with conflux. However, this conflux is not an appointed value at this point so it makes sense to do the diameter adaptation for collecting pipes at a future point.

# 6 Simulations Process

## 6.1 CFD Water Jacket

To prove that the designed water jacked can fulfill the given challenges, a CFD simulation based on the cast head was done. The main goal is not to optimize flow and cooling but rather the fundamental conformance to the given requirements should be shown. Further development for a working prototype is definitely necessary.

### 6.1.1 First Run

Analysis model is based on the cast engine, the additive manufactured water jacket is placed on the casted one from the crankcase.

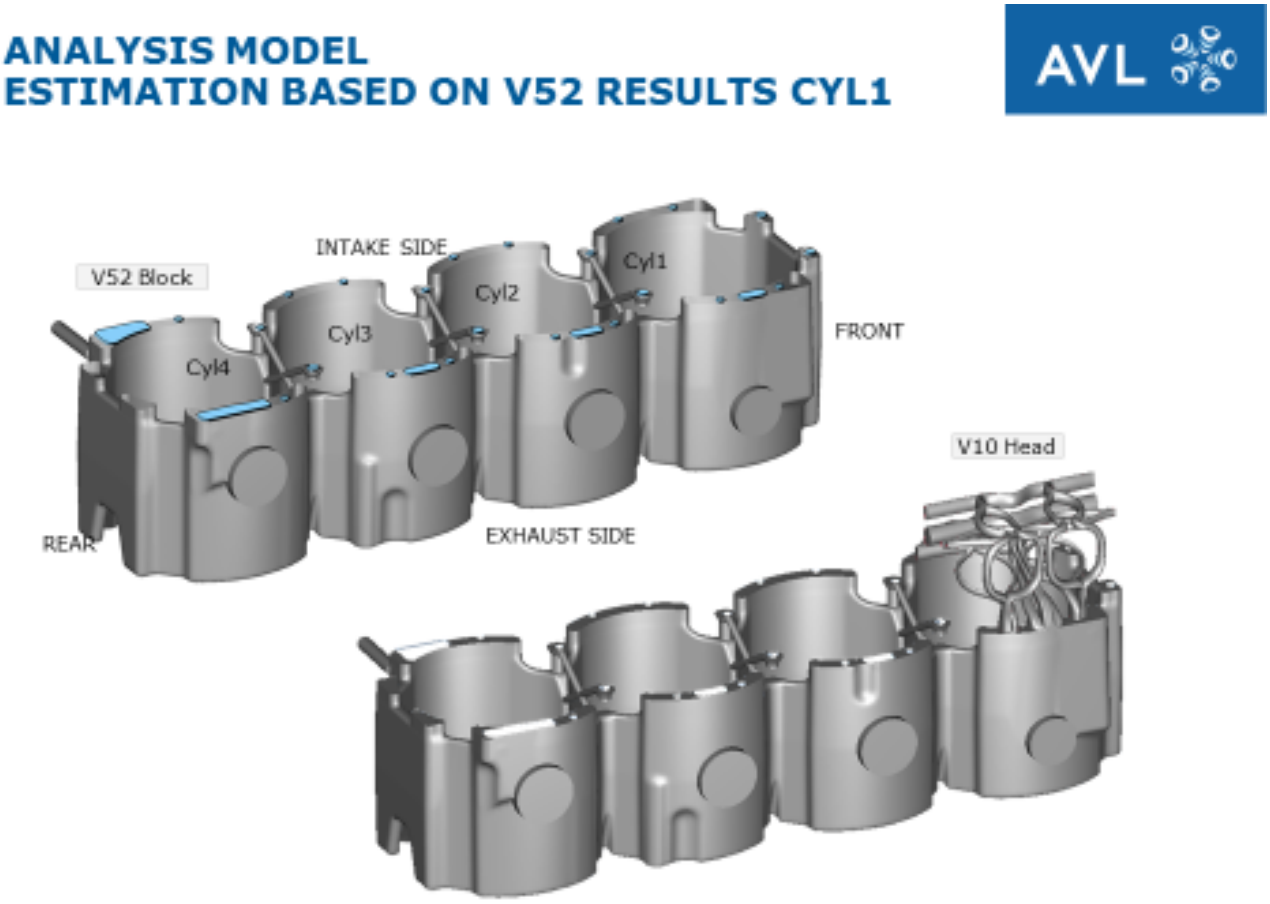


Figure 29: CFD Simulation: Analysis Model - Geometrical Set Up

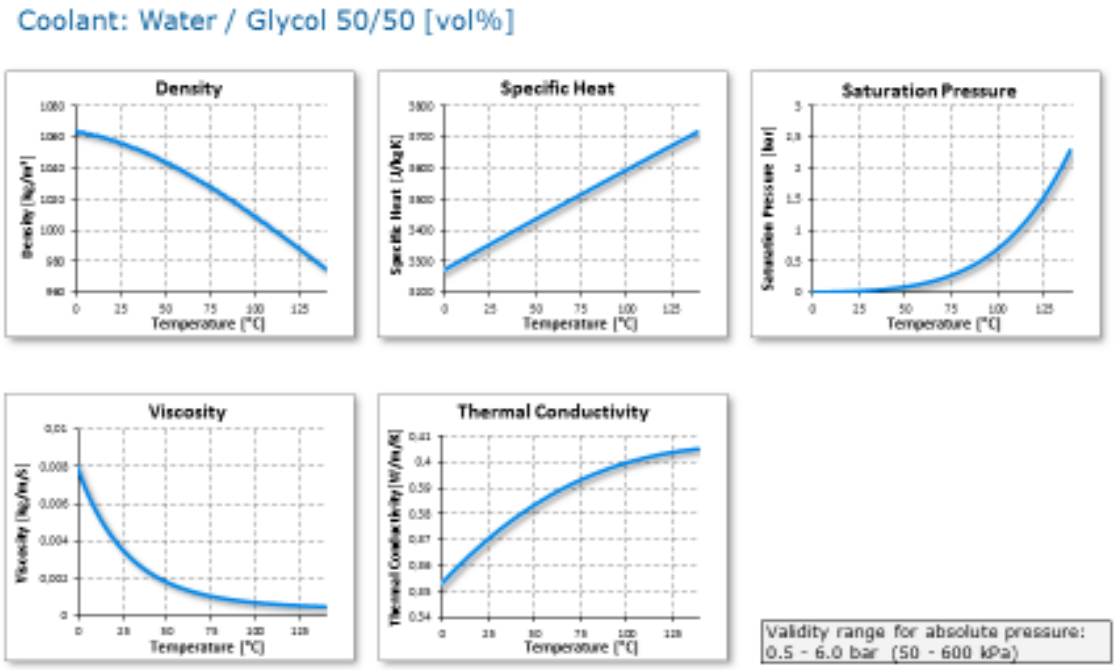


Figure 30: CFD Simulation: Coolant Properties

The complete documentation on that topic can be found in the appendix, following just a quick overview of the results

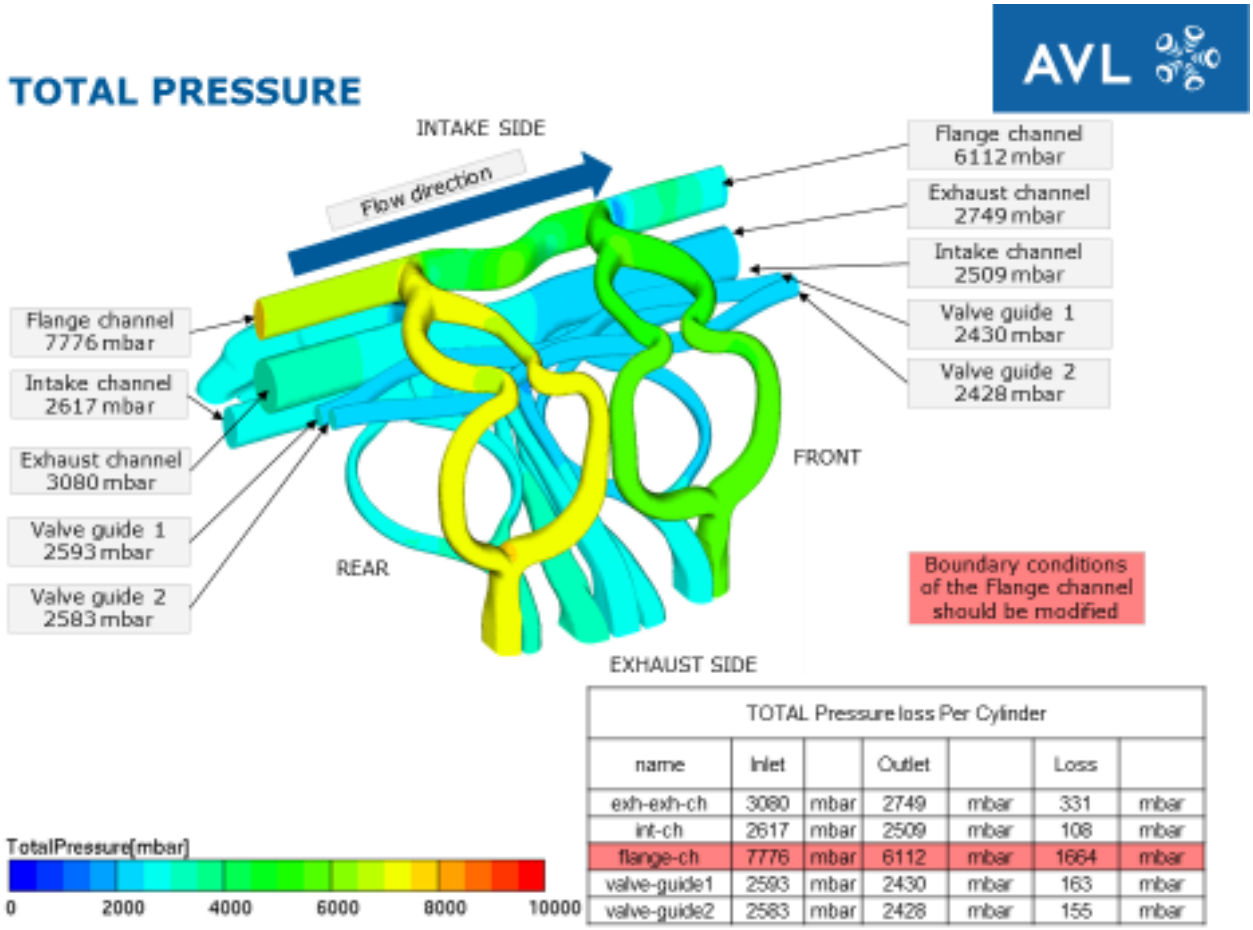


TOTAL Pressure loss Per Cylinder

| name | Inlet | | Outlet | | Loss | |
|---|---|---|---|---|---|---|
| exh-exh-ch | 3080 | mbar | 2749 | mbar | 331 | mbar |
| int-ch | 2617 | mbar | 2509 | mbar | 108 | mbar |
| flange-ch | 7776 | mbar | 6112 | mbar | 1664 | mbar |
| valve-guide1 | 2593 | mbar | 2430 | mbar | 163 | mbar |
| valve-guide2 | 2583 | mbar | 2428 | mbar | 155 | mbar |

Figure 31: CFD Simulation Boundary Conditions

Simulation for the total pressure or rather total pressure loss shows promising results except for the flange channel. Its diameter should be raised. Furthermore, all collecting pipes should increase in diameter in flow direction, which was not respected to ease the design process.

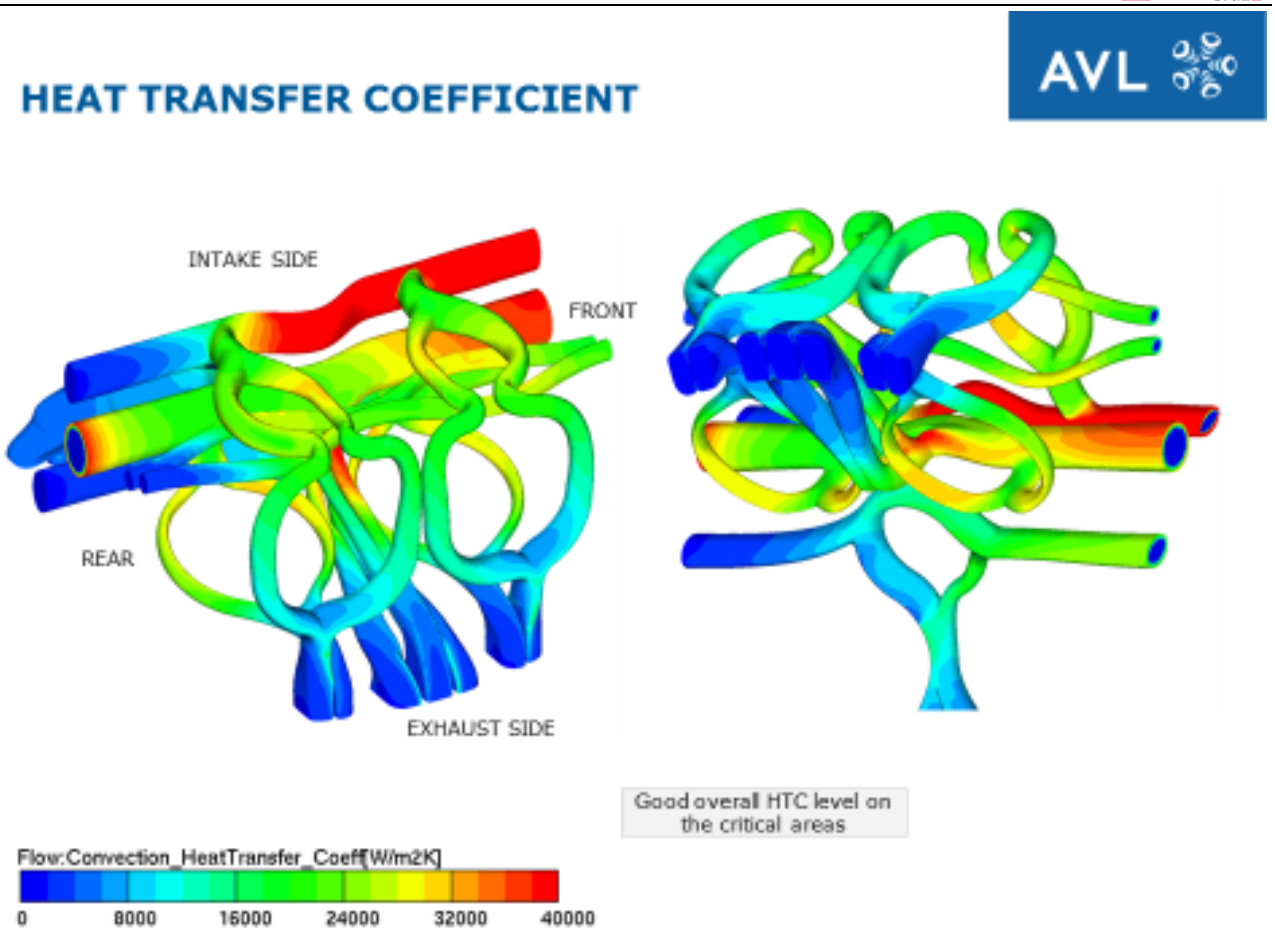


Figure 32: CFD Simulation Results: Heat Transfer Coefficient

The heat transfer coefficient is crucial for the water jackets job of cooling the cylinder head. It depends on flow velocity, turbulence and mass flow. One issue visible here, aside from the flange channel might by the difference between the right and left side channels in the hot bridge. Here the design could be changed to a point to equal heat transfer on both sides by either lengthen one side or a variation of diameter. Otherwise the results are satisfying. HTC is high around valve seats valve guide and hot bridge where high temperature and therefore heat input are expected.

## VELOCITY CONTOUR

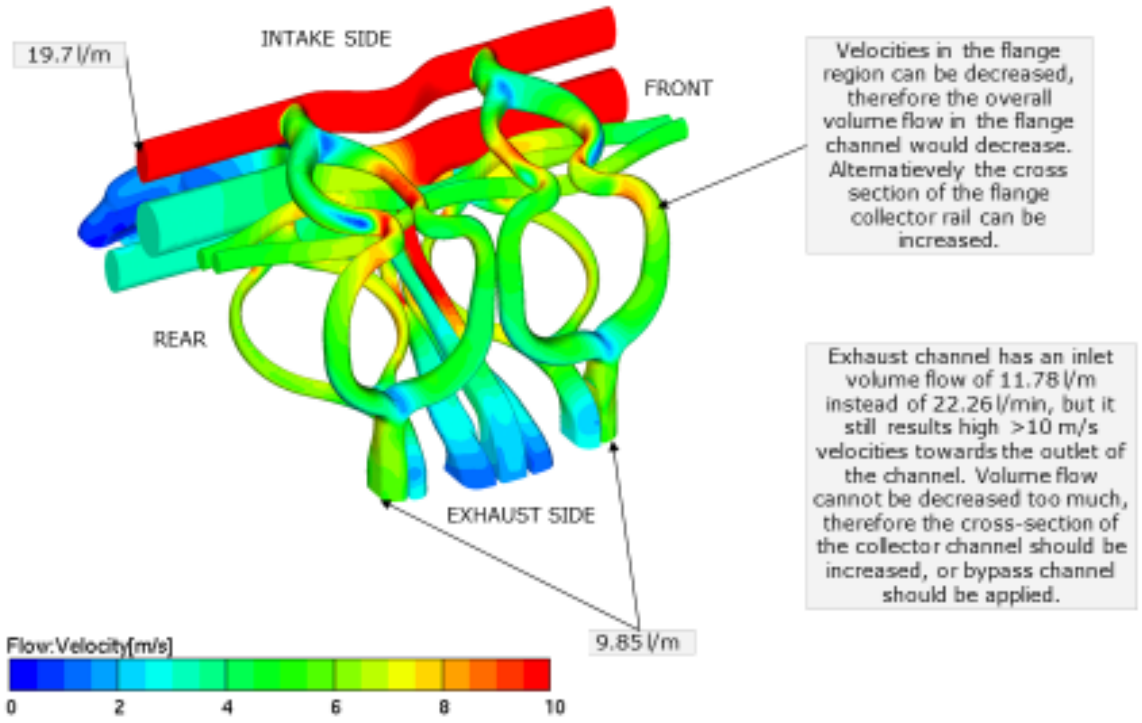


Figure 33: CFD Simulation Results: Velocity Contour - Top View

Looking at velocity results the connection between HTC and pressure loss becomes obvious. Zones of potential improvement are easy to find, especially flange channel and right side of hot bridge. Later should be adapted for symmetrical flow and HTC. The flange channel obviously has to increase in diameter while the curves on top exhaust ports to the valve guides should be smoothed. Also some other minor spots are visible which could be improved in future design.

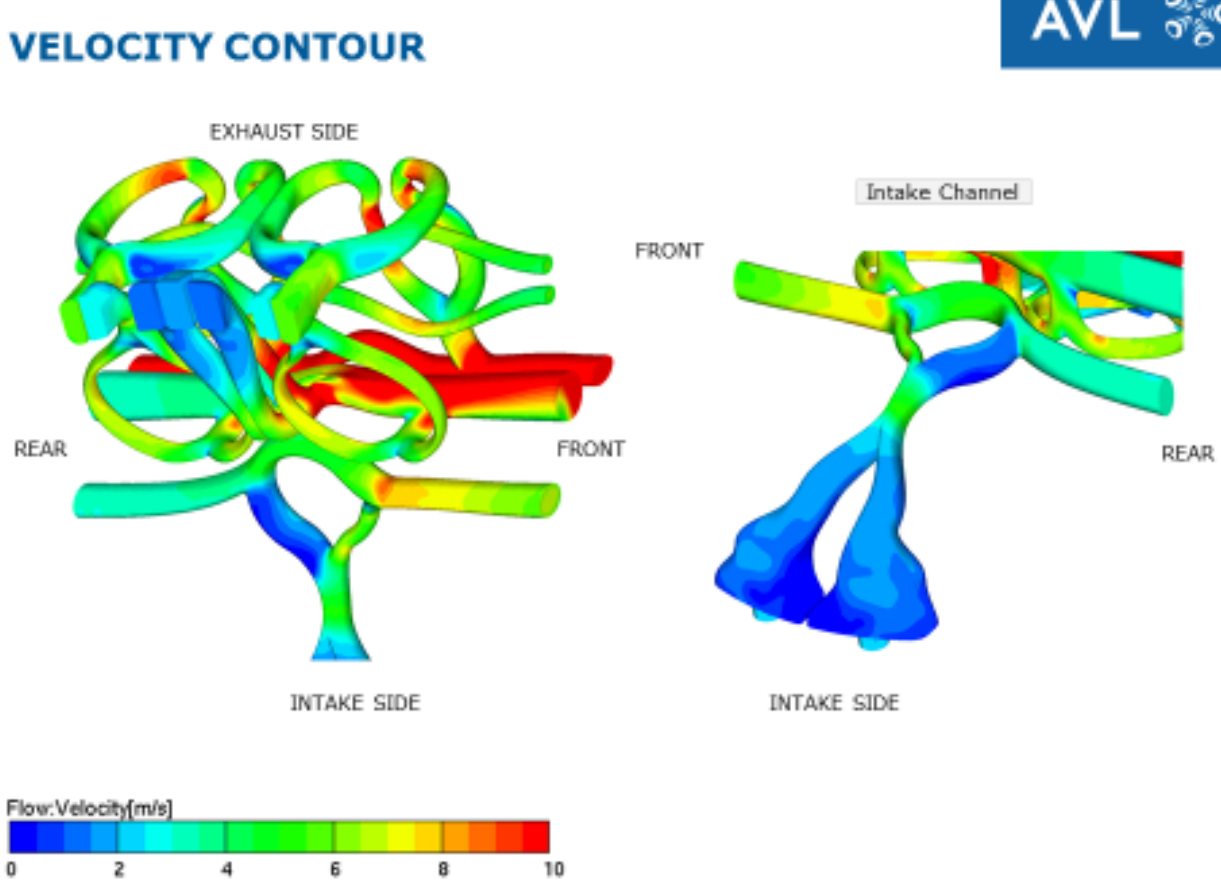


Figure 34: CFD Simulation Results: Velocity Contour – Bottom View

### 6.1.2 Second Run

To improve cooling additional channels between the cylinders are added, replacing cooling drillings there. Those channels then continue to the exhaust channels and end finally terminate in the valve guide cooling channels. Enclosed are results from the CFD analysis.

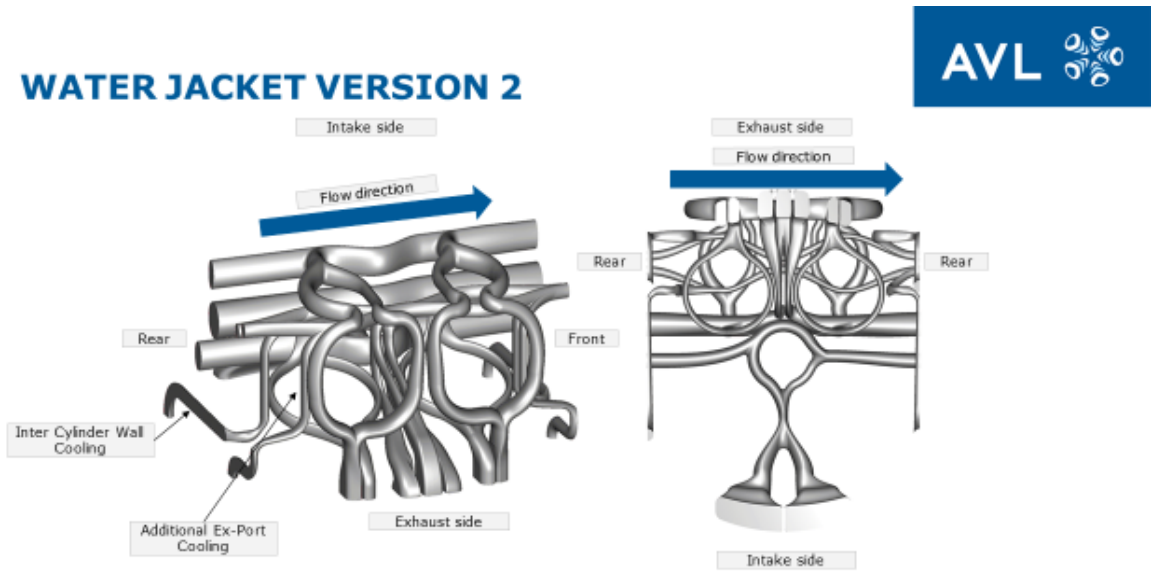


Figure 35: Updated Water Jacket with Wall Cooling between Cylinders

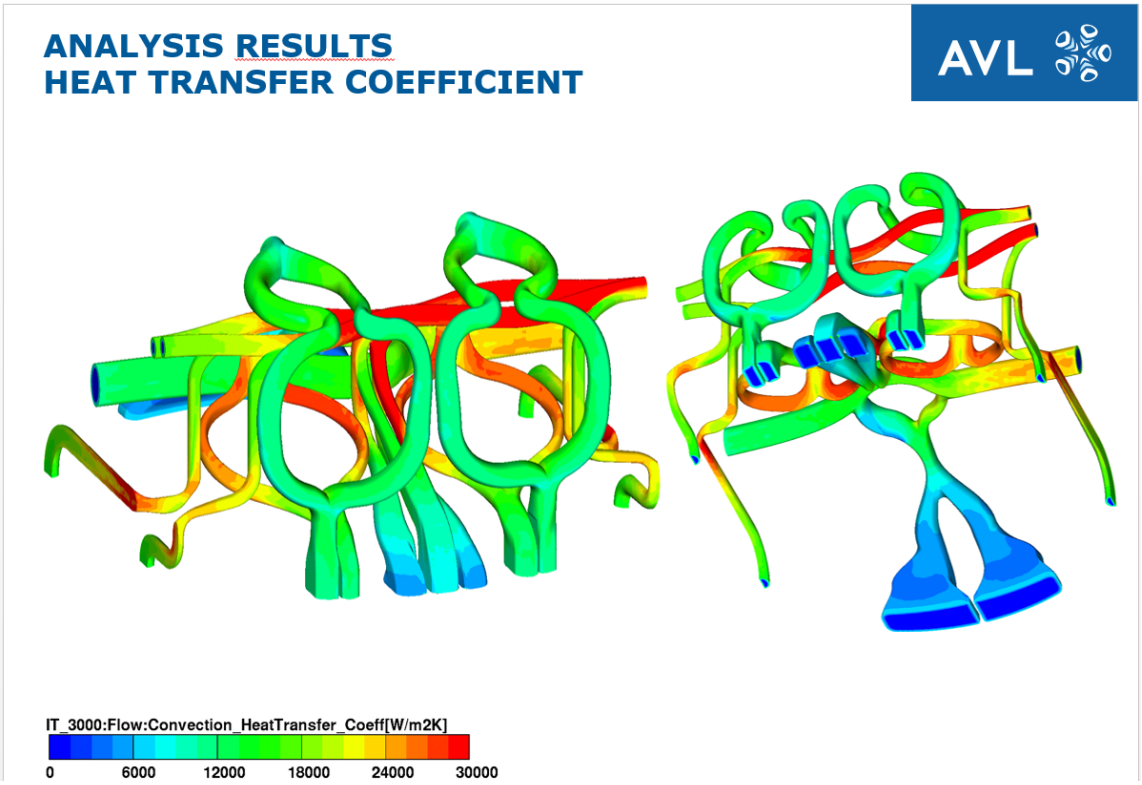


Figure 36: CFD Simulation Results: Heat Transfer Coefficient for Modified Water Jacket

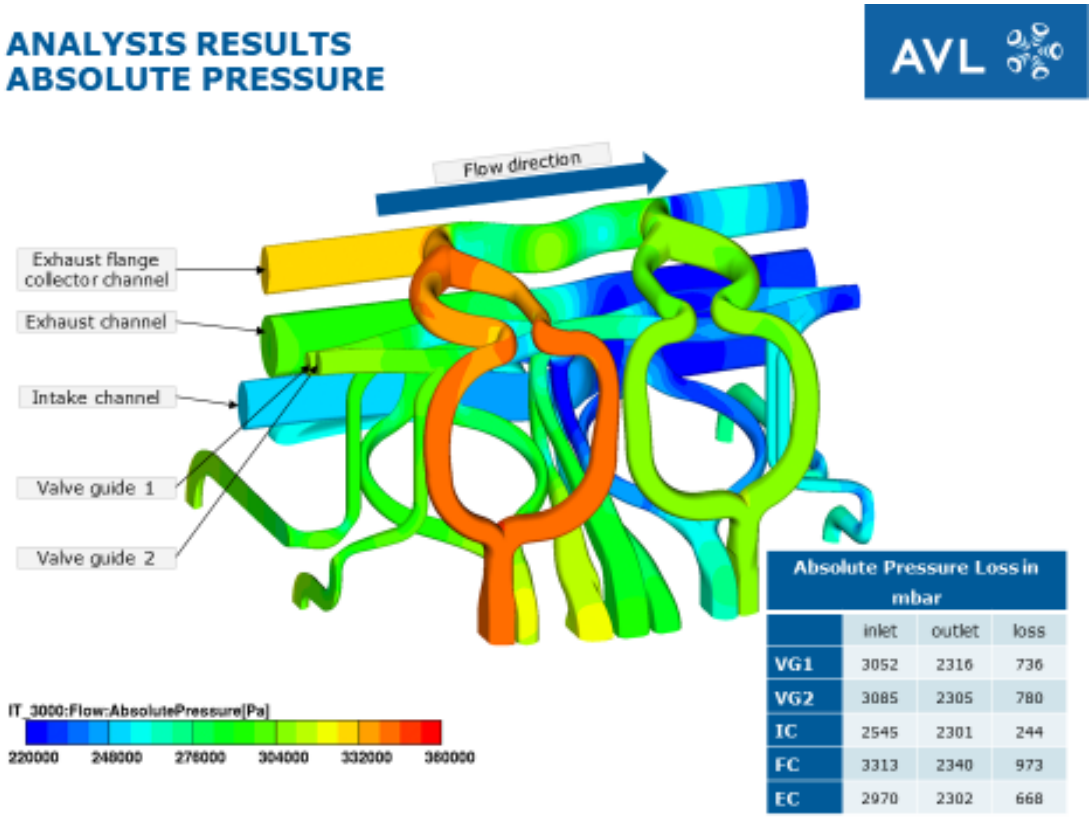


Figure 37: CFD Simulation Results: Absolute Pressure for Modified Water Jacket

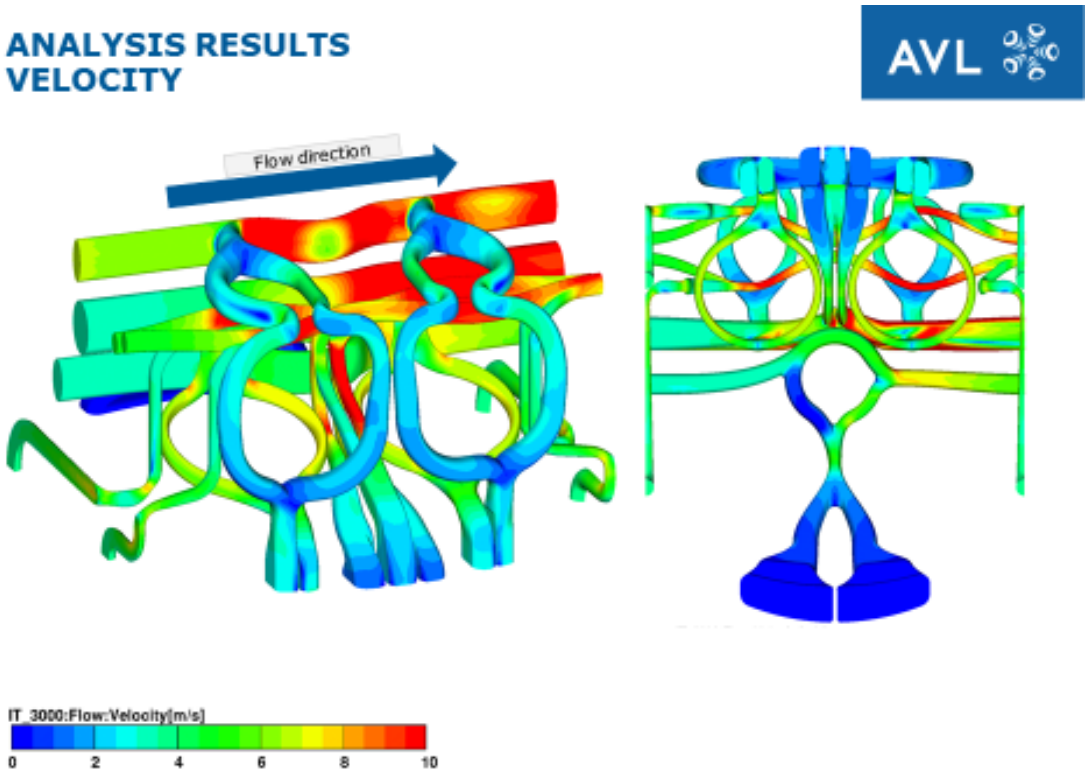


Figure 38: CFD Simulation Results: Velocity Modified Water Jacket

The results are even better in this particular case and the modification show the way were development could progress with additive manufacturing. However, for the added channels the longitudinal valve guide channels would either need an increase in diameter or connections to other channels to deal with the risen circulatory. It has to be mentioned that this simulation was used to test different methods of meshing.

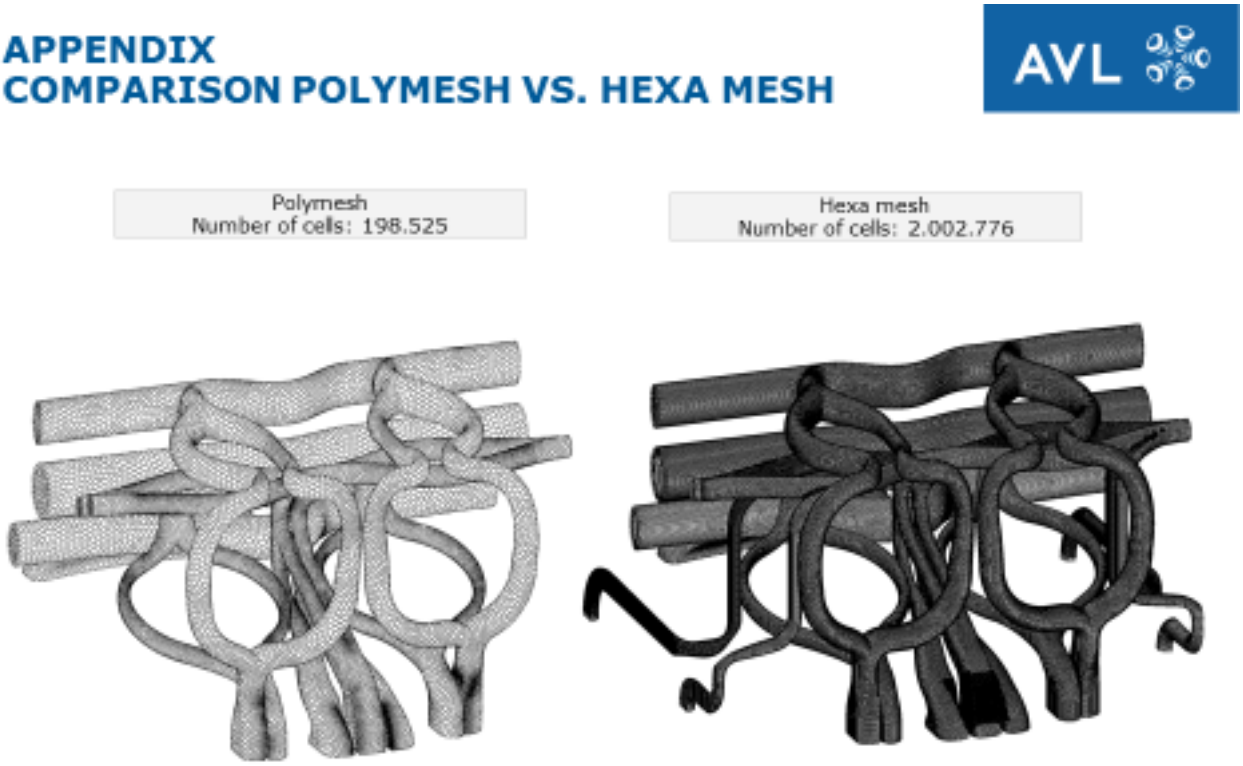


Figure 39: CFD Simulation: Polyhedron vs. Hexahedron Mesh

## 6.2 Mesh

A powerful mesh is crucial to any simulation based on finite elements or volumes, may it be FEM; CFD or topology optimization. First the elements have to represent the structure in a sufficient way, which calls for finer meshes as well as different elements as geometry gets more complex. Secondly mesh and elements must be able to deal with the physical requests the simulation is about. While a mesh which follows fluid dynamics is great for CFD, it is probably unfit for a mechanical load simulation. As for elements a geometry not able to bend, like 4 node hexahedrons, can not represent a bent part (e.g. instance a leaf spring).

So in the given case, the mesh should be able to deliver reliable results for the mechanical and thermal load simulation on one hand but on the other hand it must be able to perform the topology optimization. While the first can be archived quite easily, the latter is more challenging due to the following points. First, topology optimization finally removes whole elements, which consequently should not be too big in areas of high loads. Therefore, a finer mesh is required which leads to higher computing times. Secondly, experience with topology optimization on complex parts is limited. But as always, computing time should be kept to a minimum, which calls for fewer and simpler elements. Keeping all this in mind, finding the right mesh can be challenging.

In this case the idea is to use a boundary hexahedron dominant mesh. A boundary mesh consists more or less of two sections of elements. One matches with the surfaces, while the second one fills up the bulk sections. The complicated thing about it is the connection of those two sections by other types

of elements. Such a mesh is chosen for the following reasons: First, most of the surfaces are functional, and therefore mustn't be changed in optimization. A boundary mesh offers the possibility to keep this frozen layer thin and the mesh surfaces close to the original ones. Furthermore, a reduced model just consisting of these frozen surfaces can give an idea how far optimization and therefore reduction of volume can go. Hexahedrons on the other hand offer reliability and variability for many applications.

However, some disadvantages are as follows: This kind of meshing is time consuming. Between the boundary layer and the hexahedrons are transition elements of differing geometry. Some of those are far from ideal and can lead to problems. However, since in topology optimization alteration close the functional surfaces is expected to be negligible those elements should not be an issue. After several iterations, the following mesh is obtained.

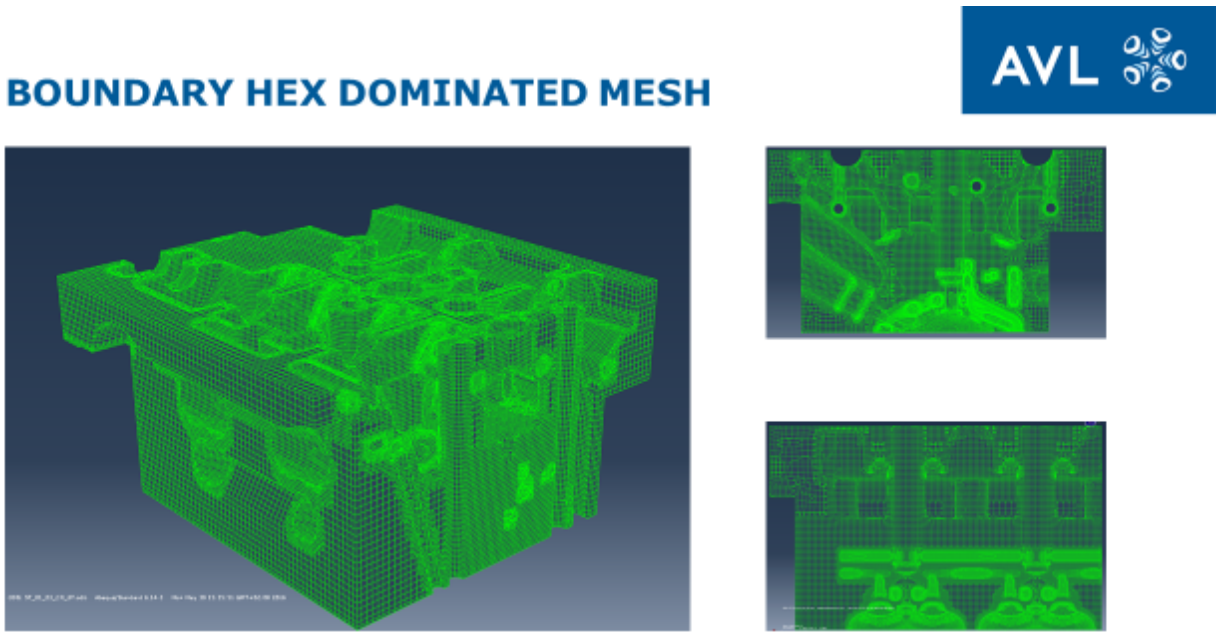


Figure 40: Hexagon Dominated Boundary Mesh

There are fine boundaries around the functional surfaces, especially those of complex geometry, while voluminous sections are replenished with hexahedrons, most of them even cuboids. In sections where high stress is expected, namely the area between fire deck and and cylinder head bold heads, the size of the hexahedrons is bisected to enable superior results in topology optimization. Transition layer elements are still not optimal for the task but the layer is quite fine and therefore should not cause any problems. As other drawbacks a slightly simplified surface and imperfect symmetry around ports and valve guides of both combustion chambers has to be mention. Also the bold hole for one cylinder head bolds has been lost during file conversions and is replaced by a set of air like elements for simulations.

## 6.3 FEM Simulation

Heat transfer as well as static load simulation are performed with the FEM program Abaqus from Simulia.

### 6.3.1 Heat Transfer Simulation

For the heat transfer model, hot gas loads are mapped from the current cast cylinder head simulation onto the new mesh. Water conditions are taken and mapped from the CFD simulation and oil surfaces set as boundary conditions. Valve guides, valve seats, sodium cooled valves, spark plugs and injector were put into the model to simulate heat transfer correctly. Although the mesh of those components is taken from the old model (and therefore are not coherent with the head mesh), this is not an issue with heat transfer.

Table 6: Components and Corresponding Materials

| Part | Material | |
|---|---|---|
| **Cylinder Head** | Cast Aluminum | NEMAK_G-AlSi7MGCU0C5 |
| **Valves** | Head: Ni- Superalloy | Nimonic 80A |
| | Shaft: Steel | ECMS-SIL1 |
| | Shaft Filling: Sodium | Sodium |
| **Valve guides** | Cast Iron | VG_PLS115 |
| **Valve Seats** | Steel | COMO12-600HWL |
| | Steel | DLTW019 |
| | Steel | FM_3010 |
| **Spark Plugs** | Steel | |

The simulation is performed for boiling as well as non-boiling conditions in the water jacket with either full heat transfer coefficient or a reduced one (factor 0,79).

#### 6.3.1.1 Set Up

To include the surrounding parts, contact definitions have to be set. In the case of Abaqus, the type of interaction has to be defined as well as either a conductance constraint or surrounding conditions.

Table 7: Contact Definitions Heat Transfer Simulation

| Interactions | Interaction Properties | Gap/ Conductance | Temp/HTC |
|---|---|---|---|
| **Cylinder Head - Spark Plug** | Surface to Surface | 0/1 | |
| **Cylinder Head - Spark Plug** | Surface to Surface | 0/1 | |
| **Cylinder Head - Valve Guide Exhaust** | Surface to Surface | 0/1 | |
| **Cylinder Head - Valve Guide Intake** | Surface to Surface | 0/1 | |
| **Cylinder Head - Valve Seat Exhaust Radial** | Surface to Surface | 0/1 | |
| **Cylinder Head - Valve Seat Exhaust Vertical** | Surface to Surface | 0/1 | |
| **Cylinder Head - Valve Seat Intake Radial** | Surface to Surface | 0/1 | |

| | | | |
|---|---|---|---|
| **Cylinder Head - Valve Seat Intake Vertical** | Surface to Surface | 0/1 | |
| **Oil** | Surface Film | | 130/0.00013 |
| **Valve Guide - Valve Exhaust** | Surface to Surface | 0/0.0015 | |
| **Valve Guide - Valve Intake** | Surface to Surface | 0/0.0015 | |
| **Valve Seat - Valve Exhaust** | Surface to Surface | 0/0.015 | |
| **Valve Seat - Valve Intake** | Surface to Surface | 0/0.015 | |

Boundary conditions for gas flow and temperature as well as water jacket are mapped on the model. For the water jacket, they are taken directly from the CFD results done on the additive manufacturing optimized one (c.f. chapter 5.3.1). On one hand, this includes the possible heat transport, while on the other hand the boiling conditions for the water inside the jacket, for simulation boiling should not occur under any circumstances.

Table 8: Mapped Boundary Conditions Heat Transfer Simulation

| Mapped Boundary Conditions | Note |
|---|---|
| **water jacked** | see chapter 5.3.1 “CFD Water Jacket” |
| **Gas temperature** | from current casted engine |

In addition including results from CFD, some parameters have to be set up. Those are some basic values of the cooling fluid (glycol fraction, boiling temperature, etc.) and geometrical parameters of the water jacket in the form of offset temperature and pressure. Later ones can be varied in this case to suit simulation results since geometry and surface are not final. However, they were kept set to zero since no adaptation was needed
For the gas temperature, results from the cast engine are taken since no conversions to any gas surfaces were made.

## GAS SIDE BOUNDARY CONDITIONS
## FIREDECK – 150kW/l @ 6000rpm

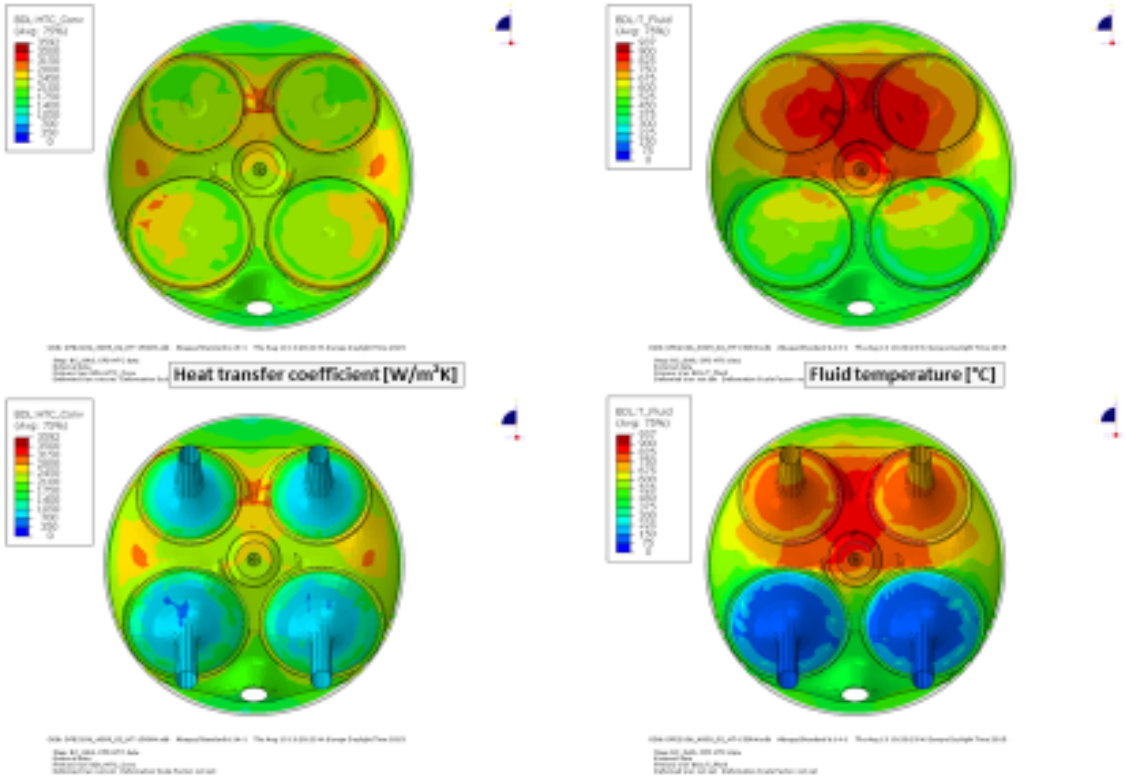


Figure 41: Boundary Conditions Heat Transfer Simulation – Fire Deck

On the fire deck highest temperature loads occur in the area between sparkplug and exhaust valves, including the exhaust bridge. Ports wise temperature on the intake side is low while it is logically higher on the exhaust side, especially on the outer curve between valve seat and valve guide.

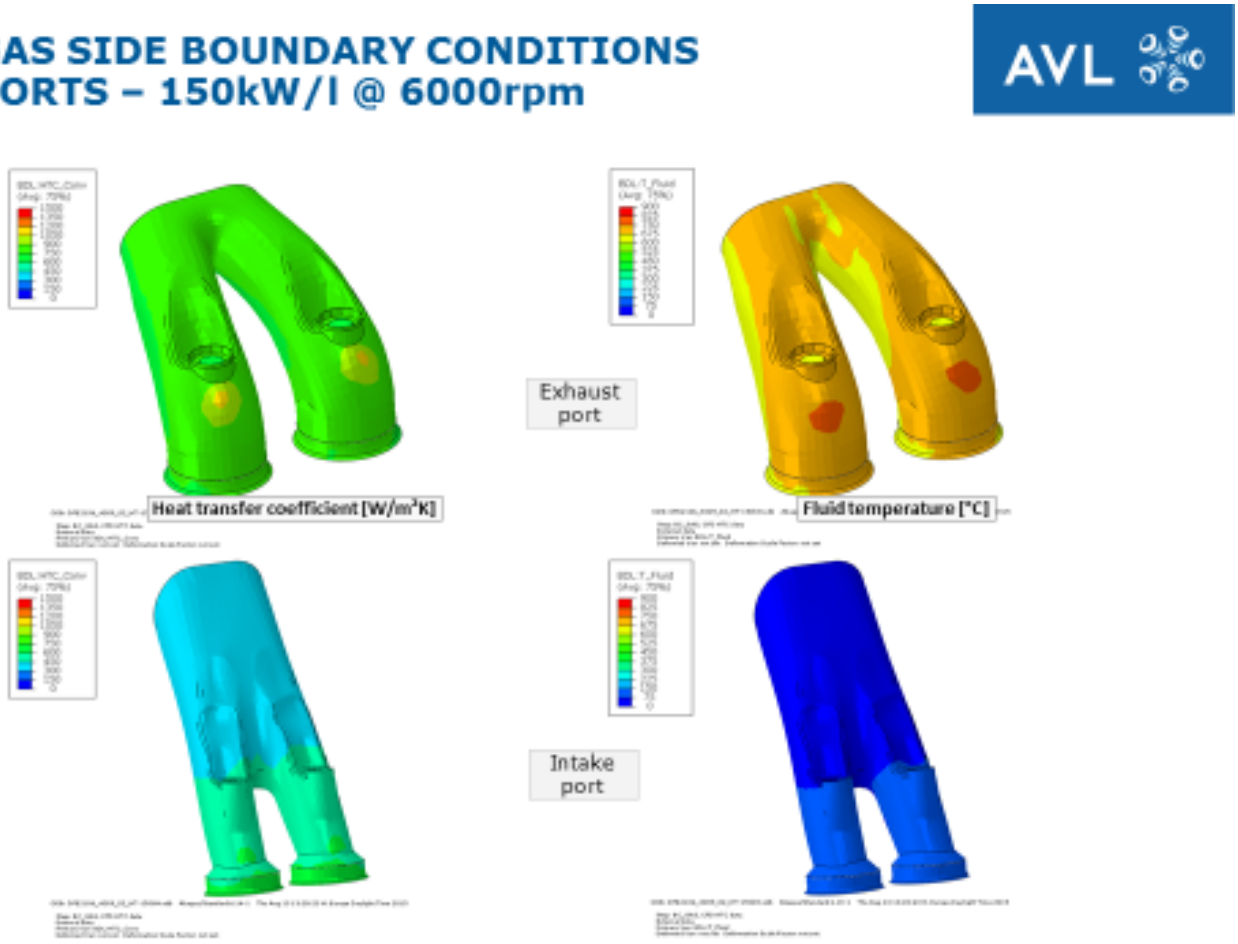


Figure 42: Boundary Conditions Heat Transfer Simulation – Ports

### 6.3.1.2 Results

The temperature fields achieved with an additive manufactured water jacket look more than promising. Simulation delivers a maximal temperature on the fire deck of 254° Celsius, which is a reduction of 47°C compared to the gasoline with a conventional cast water jacked. Fire deck temperature is a crucial limit for an Otto engine, since higher temperatures lead to knocking.
Temperature in other areas is also lower than with the conventional water jacket, especially in the valve guide region. Taking a closer look at heat distribution and gradients the results appear comprehensible and valid. As for the boiling simulation, temperature is -80°C bellow boiling which is much more than sufficient. For reduced HTC values the global temperature vary by around 2°C Celsius, which is surprisingly low.

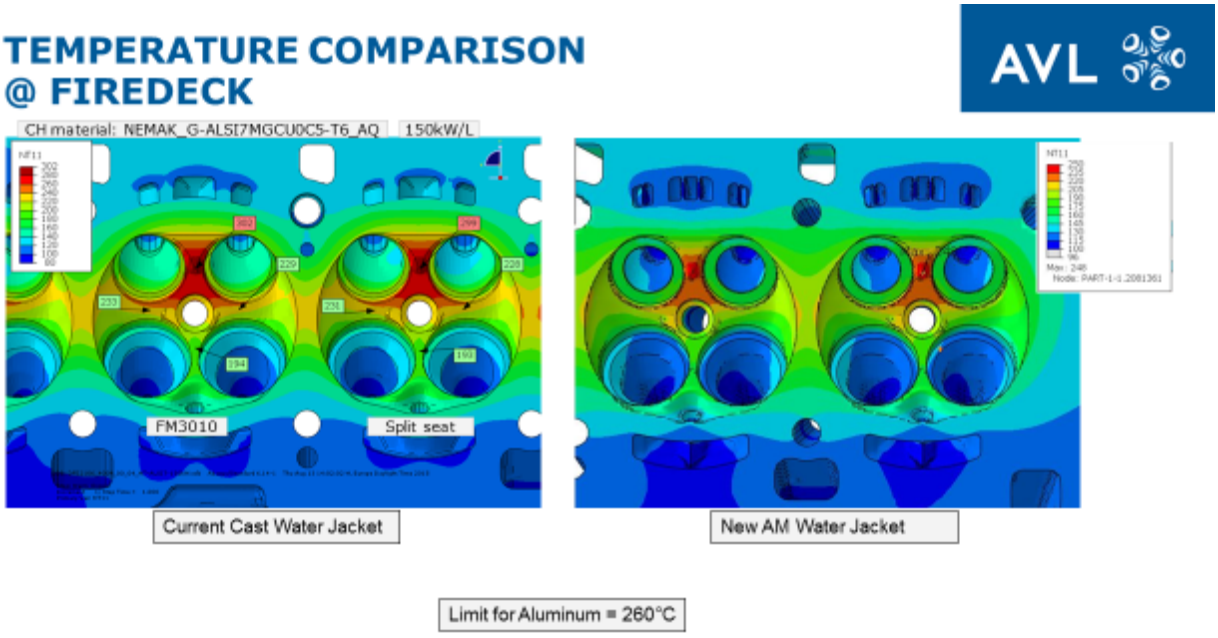


Figure 43: Results Heat Transfer Simulation – Temperature Fire Deck

The figures show a generally reduced temperature level. All problematic spots, like hot bridge, valve seats and cross bridge are colder than with the sand core based water jacket. Even the walls between cylinders, which have cooling holes drilled in the cast head, show lower temperature levels although no additional cooling is placed there. So the second version of the additive manufactured water jacket is not needed for the given loads but would reduce temperature even further, especially between cylinders and round the exhaust side.

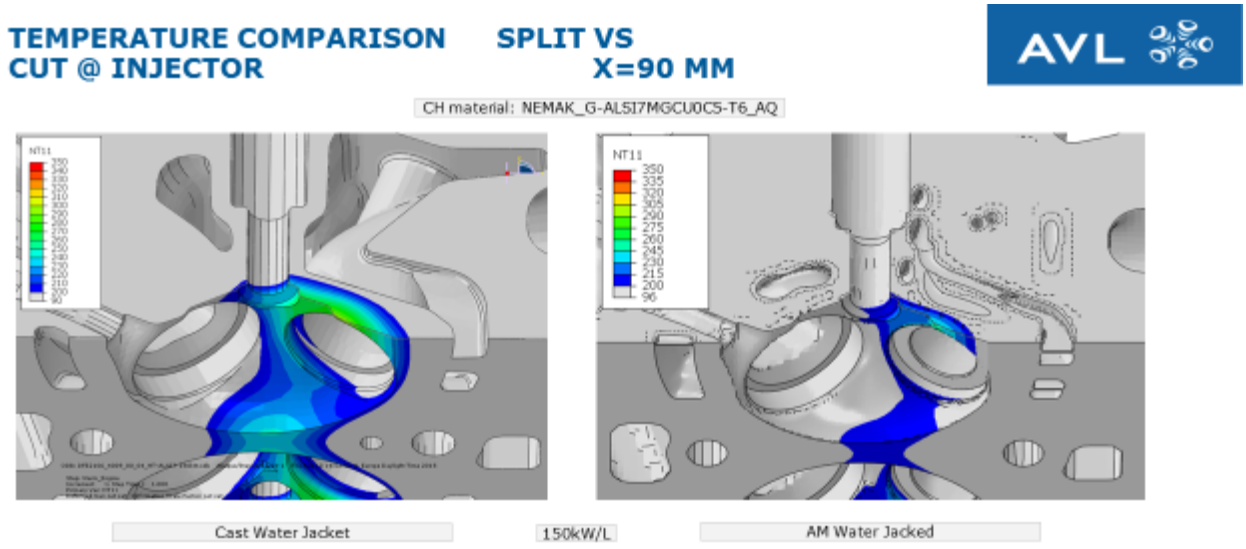


Figure 44: Results Heat Transfer Simulation – Temperature Injector

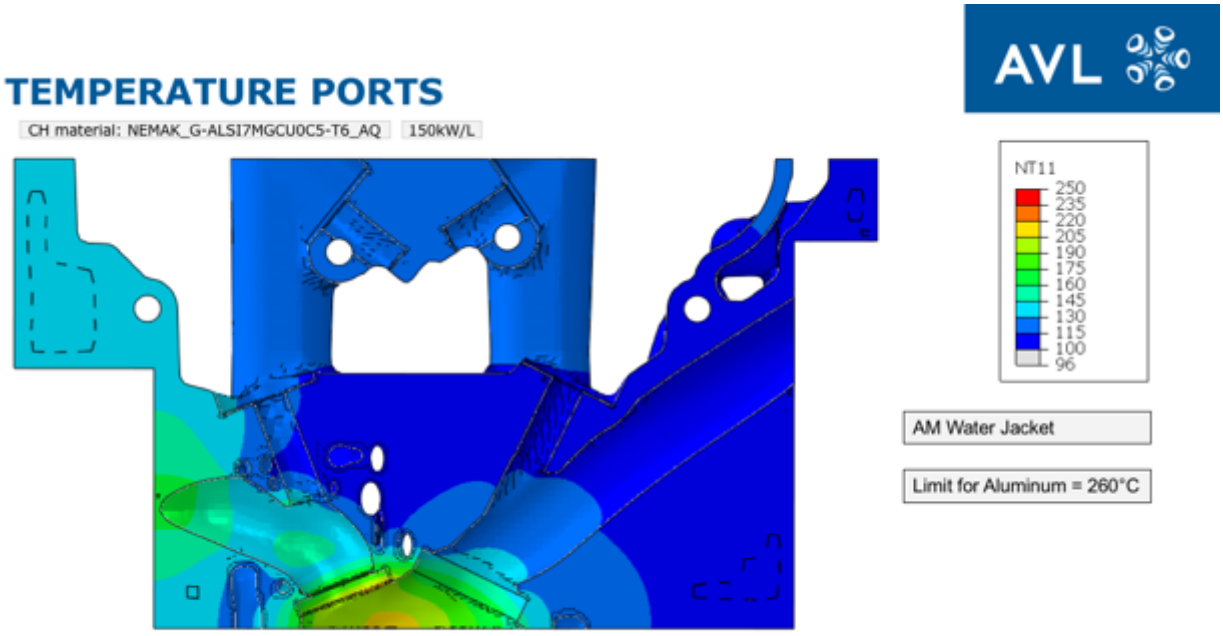


Figure 45: Temperature Distribution Ports

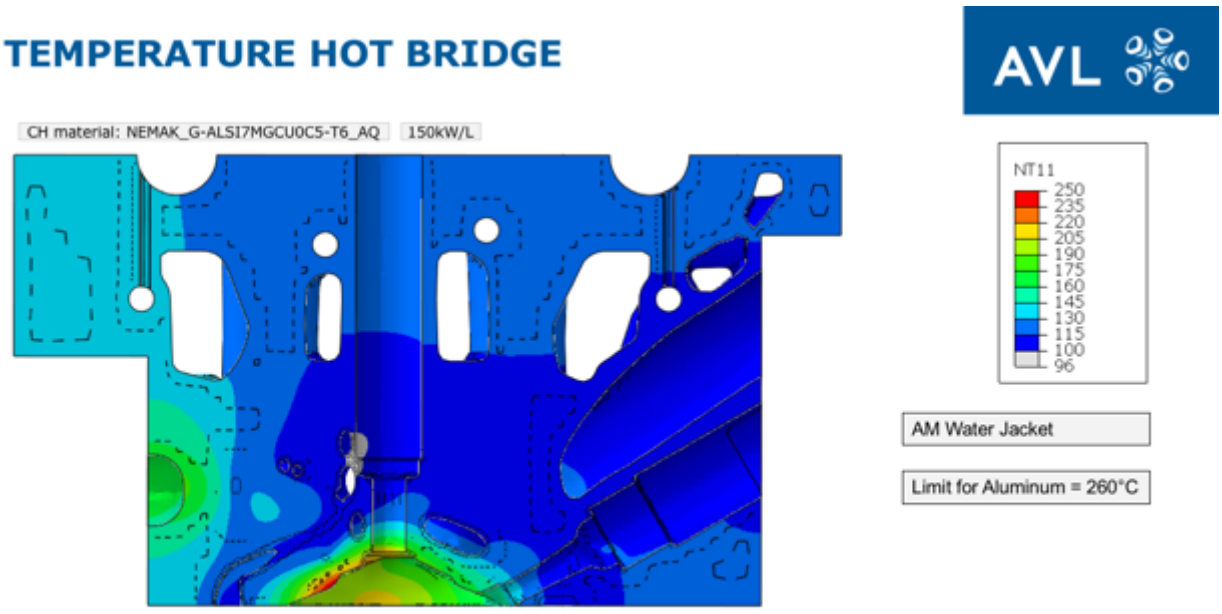


Figure 46: Temperature Distribution Hot Bridge

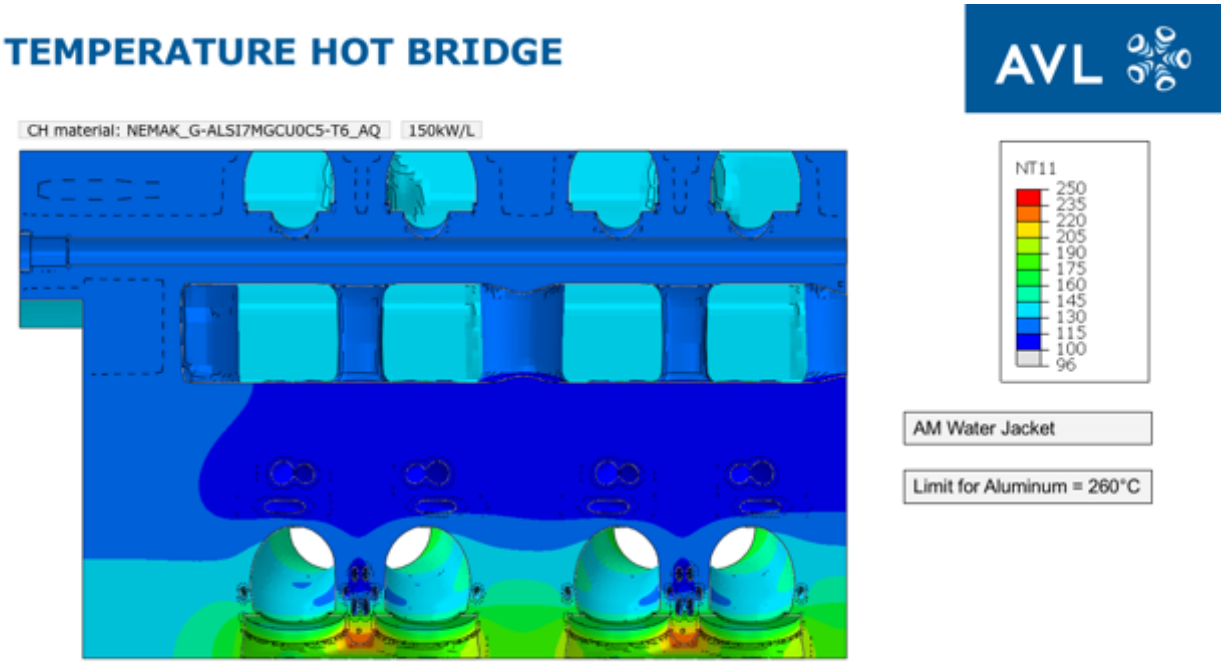


Figure 47: Temperature Distribution Hot Bridge 2

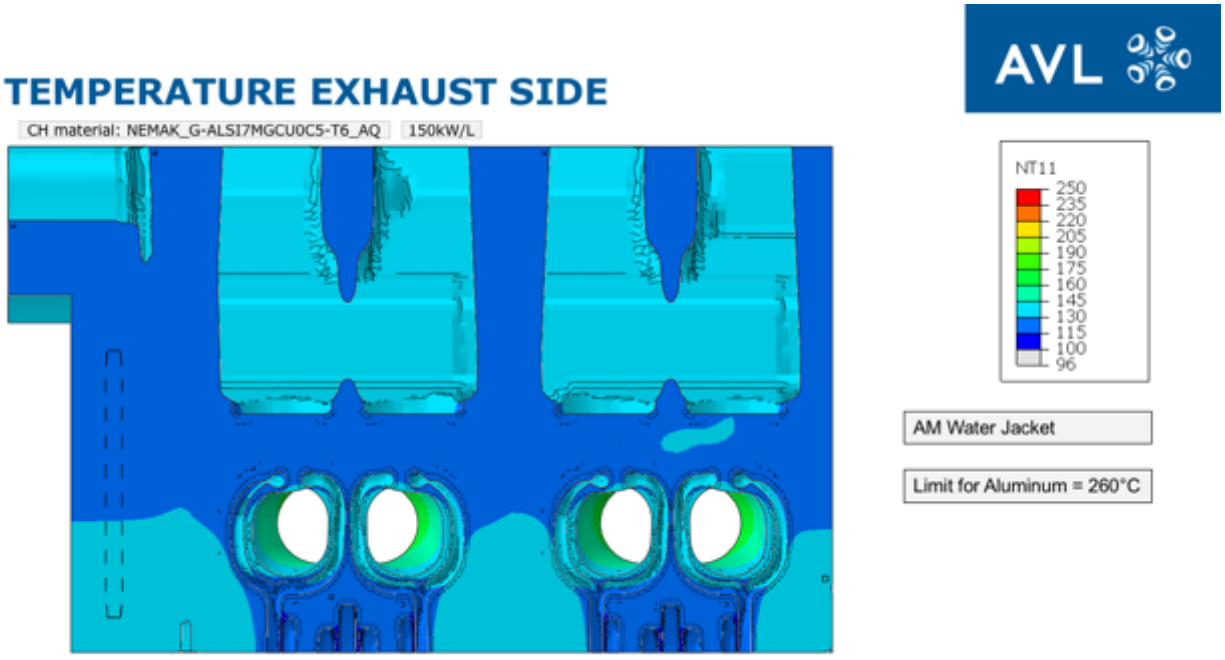


Figure 48: Temperature Distribution Exhaust Side

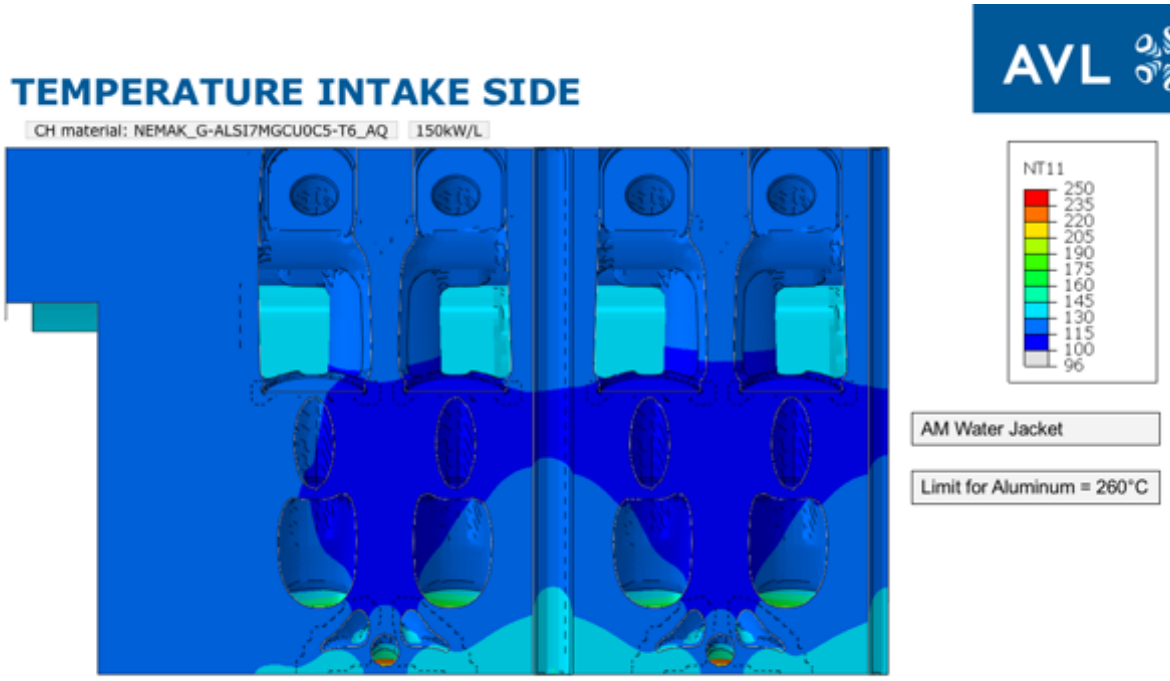


Figure 49: Temperature Distribution Intake Side

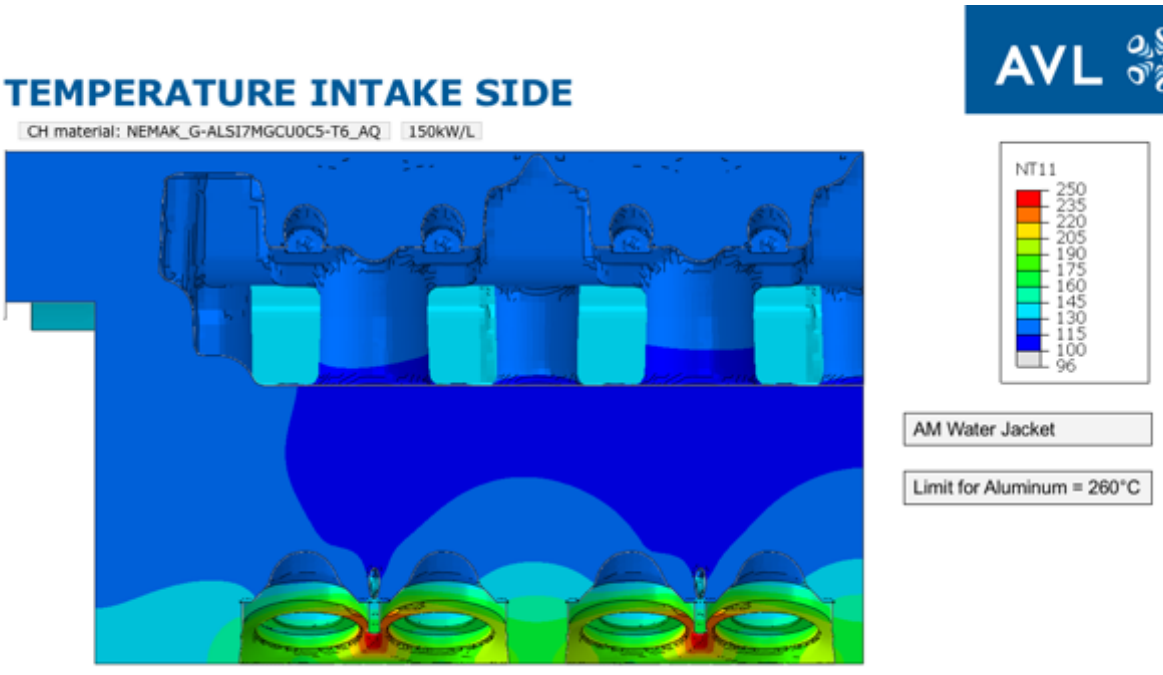


Figure 50: Temperature Distribution Intake Side 2

Raising the surface to volume ratio and the possibility to get the cooling cycle closer to the problem areas seems to be a promising way to achieve superior cooling. With further flow optimization and little design adaptations even better results are expected.

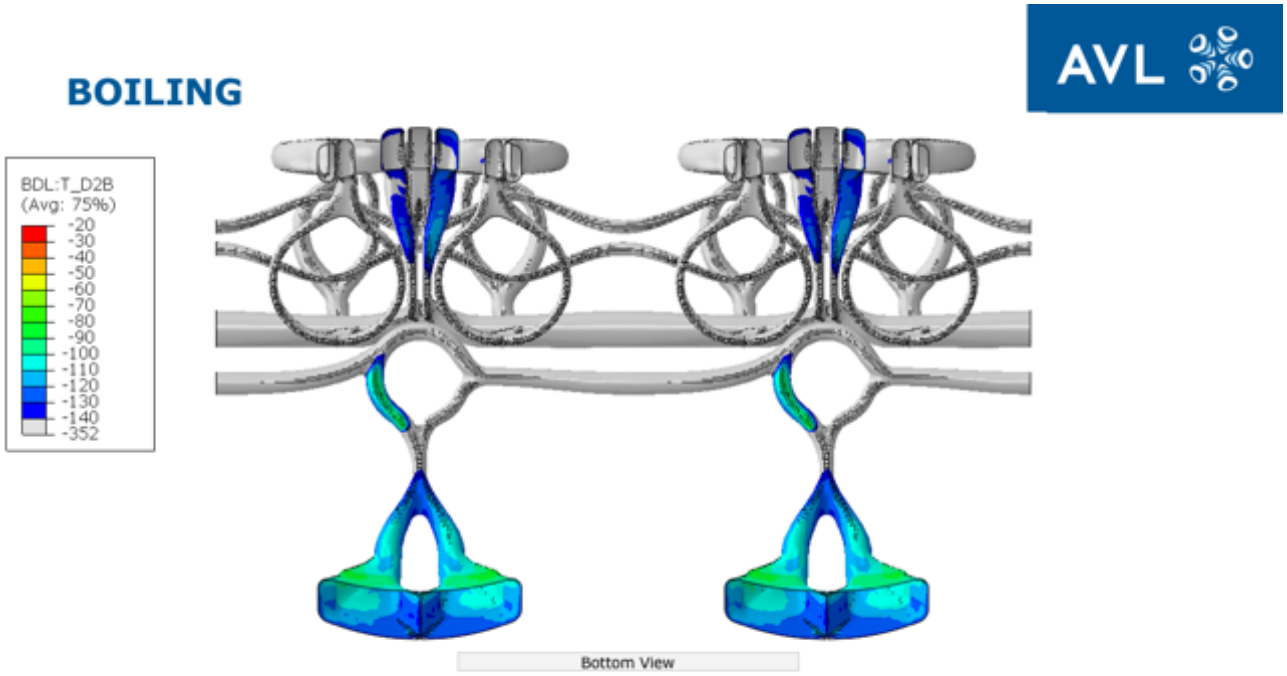


Figure 51: Temperature Below Boiling

As for boiling injector and spark plug cooling are the closest spots but they are far off, by 80° Celsius.

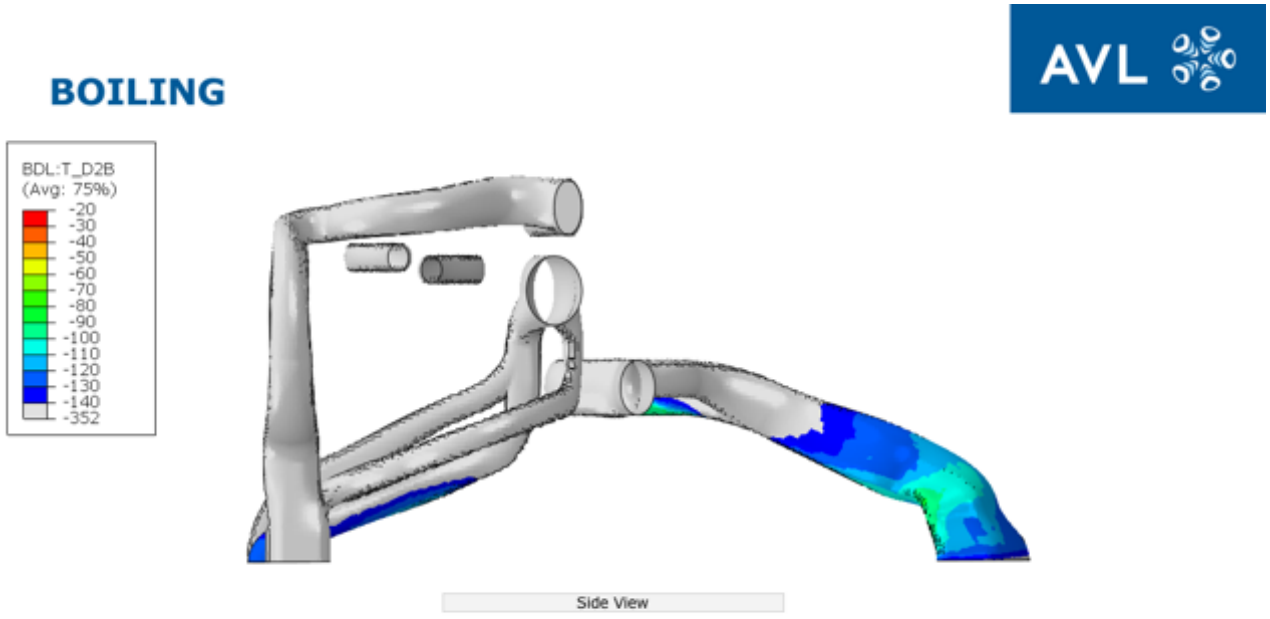


Figure 52: Temperature Below Boiling

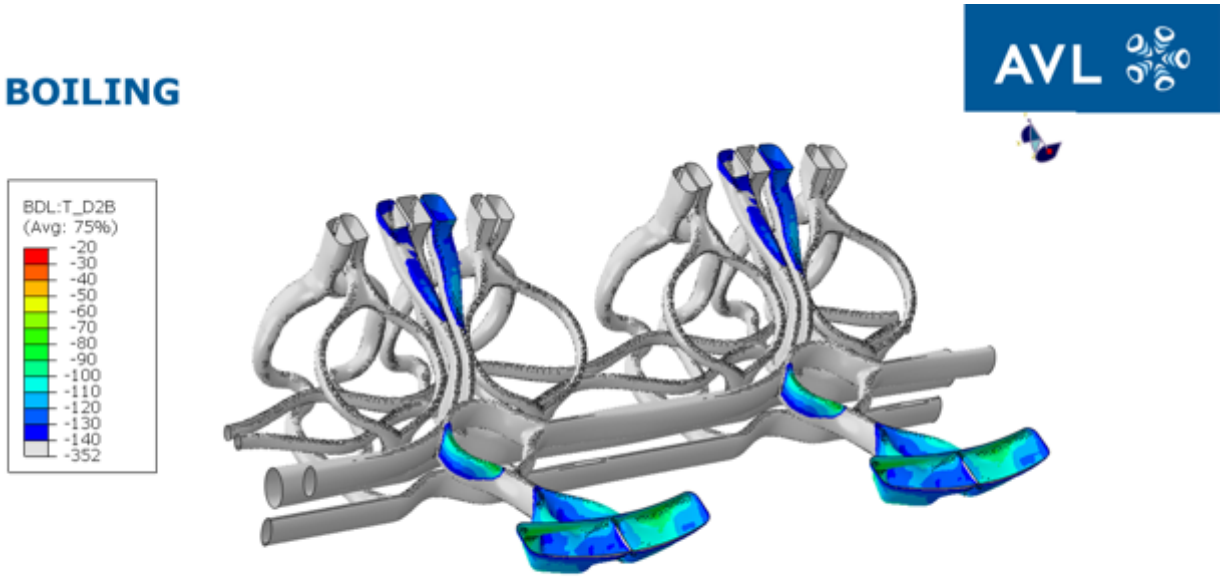


Figure 53: Temperature Below Boiling 3

### 6.3.2 Static Loads Simulation

Static load simulation set up is a little more challenging than thermal simulation keeping the future topology optimization simulation in mind. Since static load simulation has to be redone after every topology simulation step, it is crucial to keep computing time to a minimum. Unfortunately, the number of elements, which leads to longer computing times, has to be relatively high to meet the demands of topology optimization. Hence the model was reduced to the cylinder head only. Removing valves, seats, guides etc. and replacing them by surface pressure reduces the number of interactions and therefore computing time. However, this simplification comes with some drawbacks which have to be considered. For instance, if a guide is installed in a component and the pressure is too high, the material underneath will deform. The force on that spot will decrease then since the guide will distribute the pressure around the area. By using pressure in the simulation, a deformation of the material in an area will not reduce the force on it: Hence, it will deform until it reaches a stiffer structure. This has to be taken into account for channels close underneath valve guides and valve seats.

#### 6.3.2.1 Set Up

Most of the loads are taken from the current cylinder head model. Pressures on surfaces is read out and averaged manually, keeping realistic overall values in mind. Those are then applied on correspondent surfaces on the new model. In some cases that transaction is obvious, others provide troubles. Since models meshes are different some surfaces do not correlate perfectly. Furthermore, the new mesh is more smooth in some parts. Additionally, by removing bolts, gasket and other parts, interactions and contacts are eliminated. Therefore, when applying the loads, known result from the cast model has to be kept in mind. Since just the water jacked is changed, all loads not influenced by its structure should stay the same and logically the results should be similar. On one hand this implies that load input on former reaction surfaces, like between gasket and cylinder head, has to represent this contact reaction. In case of gasket to head contact, this leads to three split surfaces. For instance, the surface “Gasket Low Pressure” represents areas where gasket and head more or less just touch each other. “Gasket Medium Pressure” are around all sealing areas while “Gasket High Pressure

Cylinder 1 & 2" represent areas of high pressure around the fire deck. On the other hand, computed reaction forces should look similar to those of the cast model. Of course it takes several iterations to achieve this by adapting loads and surfaces they are applied on.
This is then performed for four different steps. By applying loads in different steps, an actual dynamic situation can be cut down to a static simulation. Step "Max Assembly" represents the maximal loads when the engine is assembled. "Warm Engine" includes the results from heat transfer simulation and therefor mechanical loads due to thermal input. Last but not least in the steps "Gas Load 1 and 2" combustion pressure on the equivalent cylinder is applied and accordingly some other loads, like those on valve seats and gasket, change their values.
Another issue that has to be covered is the absence of the cylinder head bolts. They are replaced by pressure from the gasket side and on the bolt head side by a boundary condition. Therefore, the area normally in contact with the bolt head is said to be unable to move in axial screw direction (z-axis). While the total load size can be compared to the cast cylinder head simulation results the elasticity of the bolt head touching the cylinder head can not be represented in this way.
Furthermore, some loads not taken into account in the cast model due to their small size are added, for instance bearing seats of the camshaft. This is to lesser extent for mechanical reasons than to archive better results later on in topology optimization. While regions with no load at all would be cut down to frozen areas, even a little load applied should lead to more useable structures
Due to the non symmetrical load input because of the not perfectly symmetric mesh (e.g. the cylinder surfaces the valve guides pressure is applied on) the usually punctual boundary condition in x- and y- direction are replaced by small areas to avoid punctual abnormalities.
Last but not least, surfaces in valve guides and around the gasket had to be adapted to work with pressure input. As said earlier, the reaction force when a guide is fitted will differ from an applied pressure because the guide's stiffness is not considered. If contact pressure under the guide for the material underneath it is too high, it will deform and pressure will drop since the guide itself will distribute it on the surrounding area. If just pressure is applied, the load size stays the same and can just be distributed by the material applied on. In this case, since it is an elastic-plastic simulation, this can lead to yield. So in areas this occurred, pressure surfaces are adapted. Of course this is not an optimal solution, however a justifiable compromise.

Table 9: Loads Static Load Simulation

| Load Areas | Loads per Step in MPa | | | |
|---|---|---|---|---|
| | Max Assembly | Warm Engine | Gas Load 1 | Gas Load 2 |
| **Bearing Screws** | 2,00 | 2,00 | 2,00 | 2,00 |
| **Bearing Seats** | 1,00 | 1,00 | 1,00 | 1,00 |
| **Gasket High Pressure Cylinder 1** | 170,00 | 170,00 | 120,00 | 150,00 |
| **Gasket High Pressure Cylinder 2** | 170,00 | 170,00 | 160,00 | 100,00 |
| **Gasket Midium Pressure** | 30,00 | 30,00 | 30,00 | 30,00 |
| **Gasket Low Pressure** | 1,00 | 1,00 | 1,00 | 1,00 |
| **Injectors Radial** | 1,00 | 1,00 | 1,00 | 1,00 |
| **Injectors Vertical** | 10,00 | 10,00 | 10,00 | 10,00 |
| **Pressure Firedeck 1** | 0,00 | 0,00 | 13,50 | 0,00 |
| **Pressure Firedeck 2** | 0,00 | 0,00 | 0,00 | 13,50 |
| **Spark Plugs** | 1,00 | 0,00 | 0,00 | 0,00 |
| **Valve Guide Exhaust Side 1** | 160,00 | 120,00 | 120,00 | 120,00 |
| **Valve Guide Exhaust Side 2** | 160,00 | 120,00 | 120,00 | 120,00 |

| | | | | |
|---|---|---|---|---|
| **Valve Guide Exhaust Side 3** | 160,00 | 120,00 | 120,00 | 120,00 |
| **Valve Guide Exhaust Side 4** | 160,00 | 120,00 | 120,00 | 120,00 |
| **Valve Guide Intake Side 1** | 170,00 | 160,00 | 150,00 | 150,00 |
| **Valve Guide Intake Side 2** | 170,00 | 160,00 | 150,00 | 150,00 |
| **Valve Guide Intake Side 3** | 170,00 | 160,00 | 150,00 | 150,00 |
| **Valve Guide Intake Side 4** | 170,00 | 160,00 | 150,00 | 150,00 |
| **Valve Seats Exhaust Radial Cylinder 1** | 60,00 | 65,00 | 80,00 | 65,00 |
| **Valve Seats Exhaust Radial Cylinder 2** | 60,00 | 65,00 | 50,00 | 100,00 |
| **Valve Seats Exhaust Vertical Cylinder 1** | 5,00 | 1,00 | 45,00 | 1,00 |
| **Valve Seats Exhaust Vertical Cylinder 2** | 5,00 | 1,00 | 1,00 | 45,00 |
| **Valve Seats Intake Radial Cylinder 1** | 45,00 | 60,00 | 60,00 | 45,00 |
| **Valve Seats Intake Radial Cylinder 2** | 45,00 | 60,00 | 40,00 | 50,00 |
| **Valve Seats Intake Vertical Cylinder 1** | 3,00 | 1,00 | 60,00 | 1,00 |
| **Valve Seats Intake Vertical Cylinder 2** | 3,00 | 1,00 | 4,00 | 60,00 |

### 6.3.2.2 Results

After several iterations it came to following results.

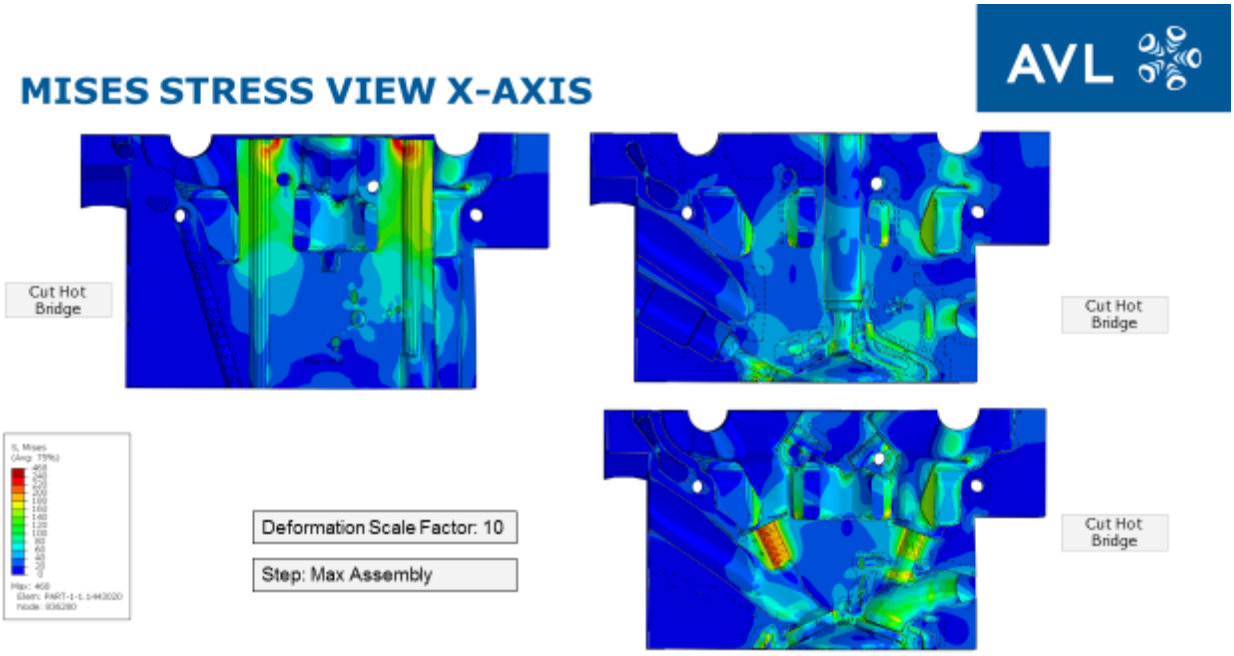


Figure 54: Results Static Load Simulation – Views Normal on x-Axis

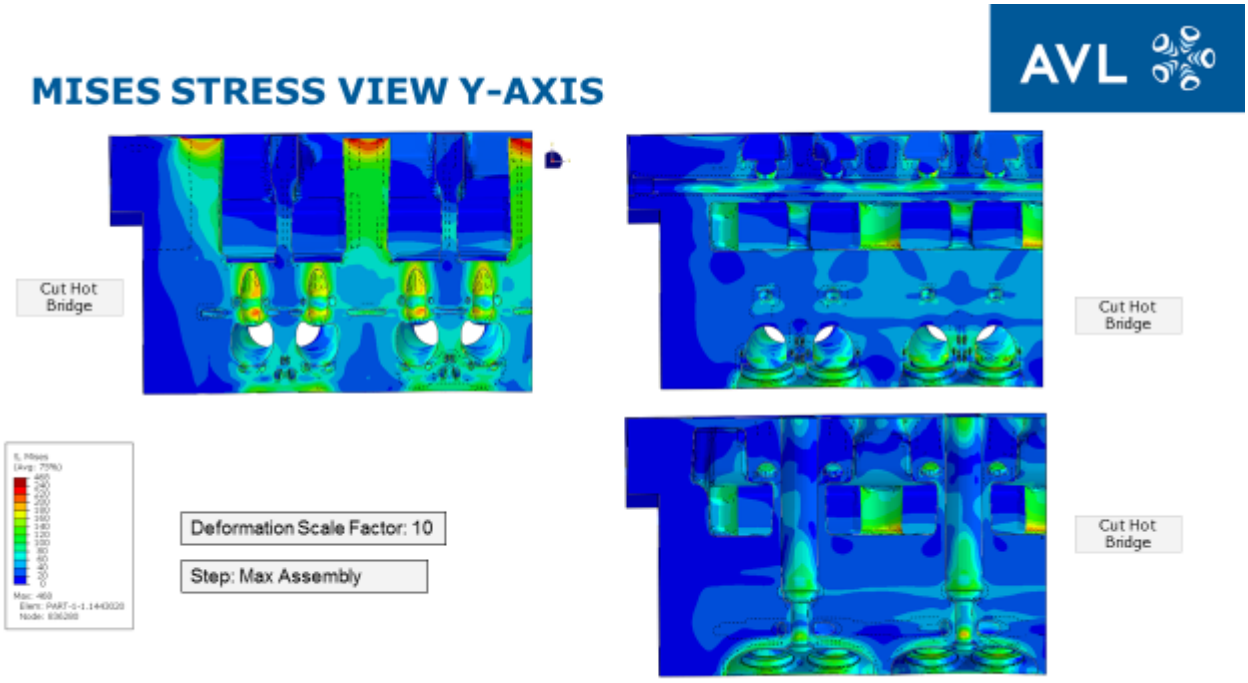


Figure 55: Results Static Load Simulation – Views Normal on y-Axis

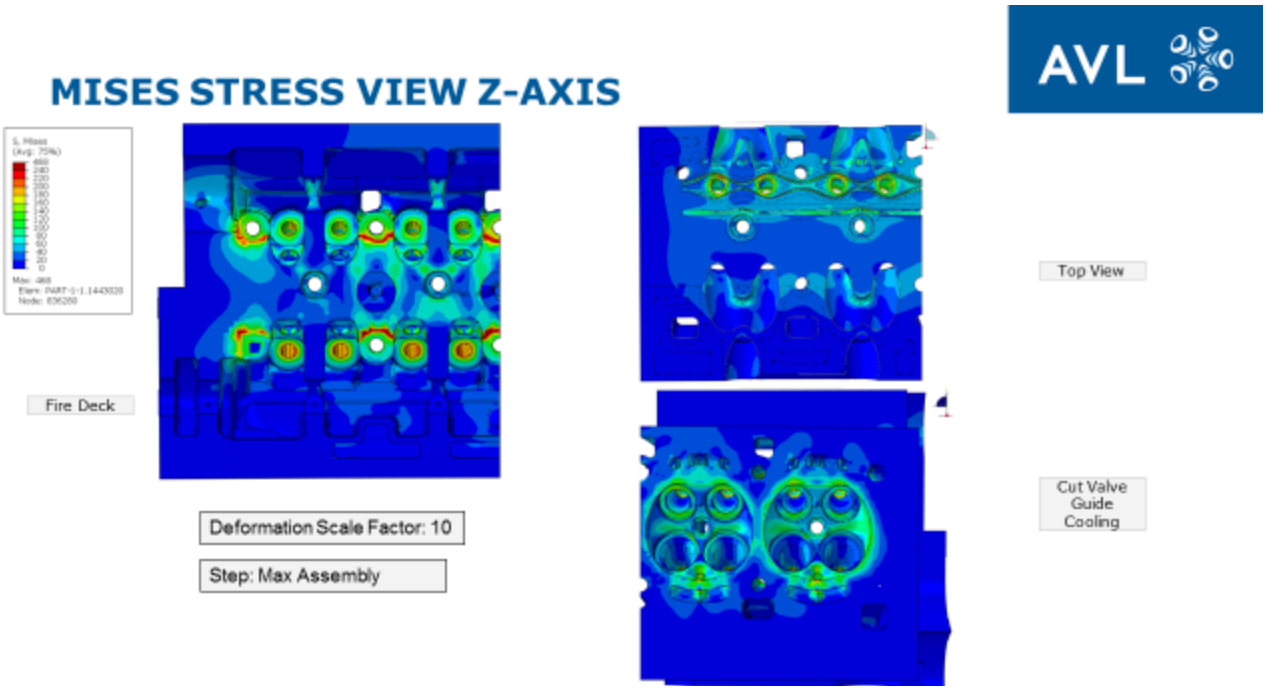


Figure 56: Results Static Load Simulation – Views Normal on z-Axis

The highest stress can be found in areas of the cylinder head bolts and the valve guides, both areas with a lot of simplifications in the model. Concerning the head bolts, they are modeled as a lateral fixation. While the real bold head and bold are elastic and can follow some deformation of the cylinder head, a fixation in the x-direction means that there is no movement in the area. Hence stress results vary from reality. They are less even and have elevated peaks, which might exceed yield limit in places because movement is blocked by the strong boundary condition. Due to this, the maximum

peaks in this area can be ignored. If compared to the previous simulation with the bolts included, overall stress is the same while peaks are higher with the fixed boundary condition. However, since cylinder head structure has not changed in the concerning areas and loads are the same, the stress distribution should be identical and actually could be taken from the old simulation too. For our given task of topology optimization, these peaks are negligible since the focus of optimization is set on other areas. Valve guides model simplification has already been discussed several times. Nonetheless, high stress leads to the conclusion to increase the distance of the valve guide cooling channels to enlarge wall thickness and thereby increase stiffness. The same applies for the seat ring and injector cooling. Stress distribution on the gasket side appears valid despite all simplifications. Difference to the original model is marginal.

In conclusion, static load simulation provides a valid model for the given task, and while some issues can be improved, reduction of computing time strongly supports the simplifications made.

### 6.3.3 Topology Optimization

For topology optimization, the Simulia tool Tosca is used, which is coupled with the Abaqus FEM solver. The basic idea behind it is to remove material not necessary for a load situation and given optimization constraints. Those given, Tosca reduces the density of elements not needed by creating new fictional materials. After every optimization run, a FEM run follows to verify the results. Step by step density of dispensable elements is reduced till they reach a set limit where they can be totally deleted.

Tosca provides two different solvers, a general and sensitivity based one. The former provides only volume and strain energy as design responses. Of those, only strain energy (and therefore by Hook's law stiffness) can be set as the objective function while volume has to be a given constraint. Basically a volume reduction is set, e.g. 50 percent, and then the output should be the stiffest possible structure for the remaining volume. Furthermore, the type of average determination of strain energy can be selected for both, steps and nodes. Either the maximal value or the middle sum can be taken.

In contrast, the sensitive based solver has preselected averaging for most design responses. The kind and number of those is however much larger. Nearly any numerical output value of static load simulation can be taken into account. For the sensitivity based solver in a first step design responses have to be set. Those are all the input values for the optimization which are taken from the basic FEM simulation.

In a second step, objective functions are set. Those are the functions which should be optimized, e.g. volume, stress, temperature and so on.

Third, constraints have to be set. They can either be based on the design responses or of geometrical nature. For instance, stress should be kept below a certain limit or there are some functional surfaces that must not be changed.

In order to reduce computing time and because of insufficient results with a plastic simulation during the first runs, material properties are set to elastic.

#### 6.3.3.1 Tosca Set-Up – Sensitive Solver

Table 10: Set Up Parameters Tosca Sensitive Solver

| Design Responses | Objective Functions | Constrains | Geometrical Restrictions | Parameters | |
|---|---|---|---|---|---|
| **Volume** | Minimize Volume | | Functional Surfaces | Soft Delete | if density < 0.05 |
| **Misses Stress** | | Misses stress <1 | Load Areas Frozen | Max Cycles | 80 |
| | | | Boundary Condition Areas frozen | Others | Default |

For the sensitivity based solver minimizing volume is set as the objective function while constraining the Mises stress below the original values. As with all following models areas where load is applied, boundary condition and functional surfaces are frozen as geometrical restrictions. Later areas include all surfaces in contact with water, oil, gas or other components as spark plugs, ignition etc.
Actually different constrains are tried, besides the Mises stress <1 varying fixed values for the same are used.

#### 6.3.3.2 Tosca Set-Up – General Solver – 70 percent volume reduction

Table 11: Set Up Parameters Tosca General Solver for 70 Percent Volume Reduction

| Design Responses | Objective Functions | Constrains | Averaging | | Geometrical Restrictions |
|---|---|---|---|---|---|
| | | | Part | Steps | Functional Surfaces |
| **Volume** | | 0.30 | | | Load Areas Frozen |
| **Strain Energy** | Minimize Strain Energy | | Sum | Sum | Boundary Condition Areas frozen |

For a first run with general solver volume should be cut down do 30% of the original model. Stiffness should be maximized while it's averaged over all steps. Number of iterations is set to 15, 30 and 50 to compare results. Geometrical restrictions are identical as with the sensitivity based solver.

#### 6.3.3.3 Tosca Set-Up – General Solver – 50 percent volume reduction

Table 12: Set Up Parameters Tosca General Solver for 50 Percent Volume Reduction

| Design Responses | Objective Functions | Constrains | Averaging | | Geometrical Restrictions |
|---|---|---|---|---|---|
| | | | Part | Steps | Functional Surfaces |
| **Volume** | | 0.50 | | | Load Areas Frozen |

| | | | | | |
|---|---|---|---|---|---|
| **Strain Energy** | Minimize Strain Energy | | Sum | Sum | Boundary Condition Areas frozen |

A second run is set up with only 50 percent of volume reduction and 15 iterations

# 7 Results

## 7.1 Tosca General Solver

The Tosca General Solver delivered results that give an idea of how force makes its way through the component and where material is necessary to bear those loads. For the two cases performed, a 50 and a 70 percent volume reduction, following structures where received.

### 7.1.1 30 Percent Volume Reduction

The optimization output is a strongly reduced structure, basically following flux of force from the cylinder head bolds to the gasket. Those are obviously the areas with the highest unidirectional load input. Additionally, there is a lot of supporting materials around the valve guides to take care of the high contact forces. Furthermore, there is a kind of a framework around the exhaust ports while intake ports are reduced to the frozen areas, as is most of the oil covered surface, injector and spark plug seats. This radical cut down is due to the negligence of thermal loads on the one hand and the minor load input on the other. Just in the bearing seats some extra lattice connection on the inside stays for additional stiffness. However, that aspect points out how much unnecessary material there is due to the casting process.

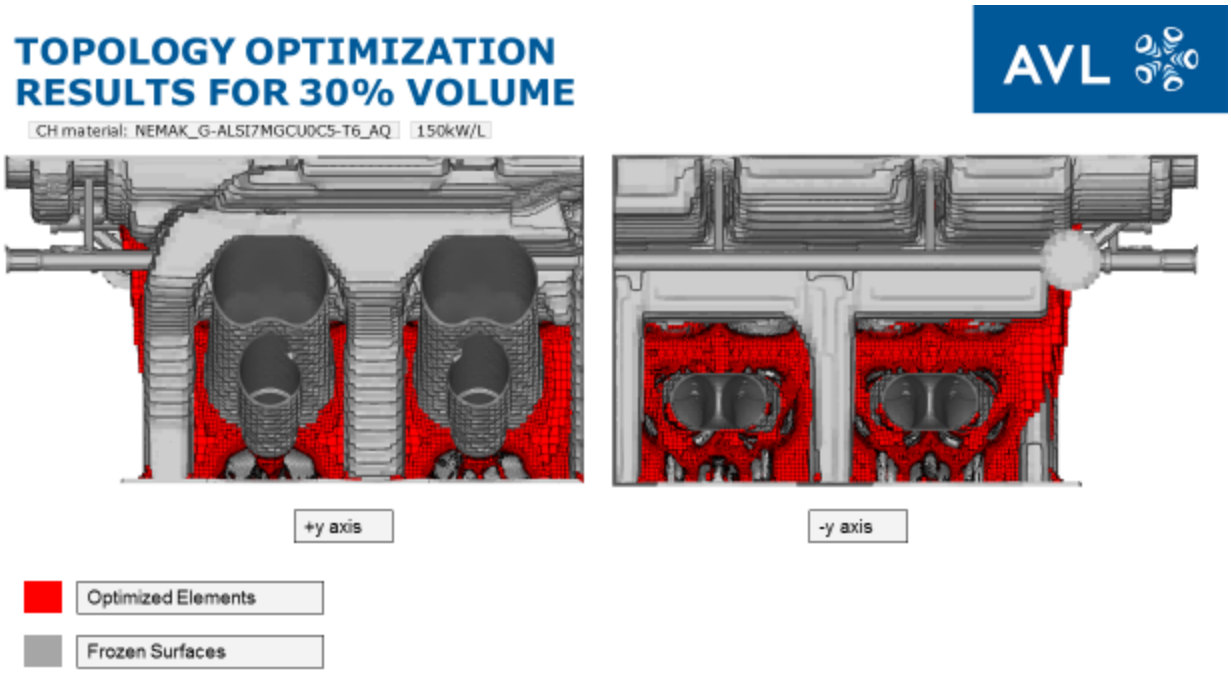


Figure 57: Results Topology Optimization - General Solver – 30 Percent Volume Reduction

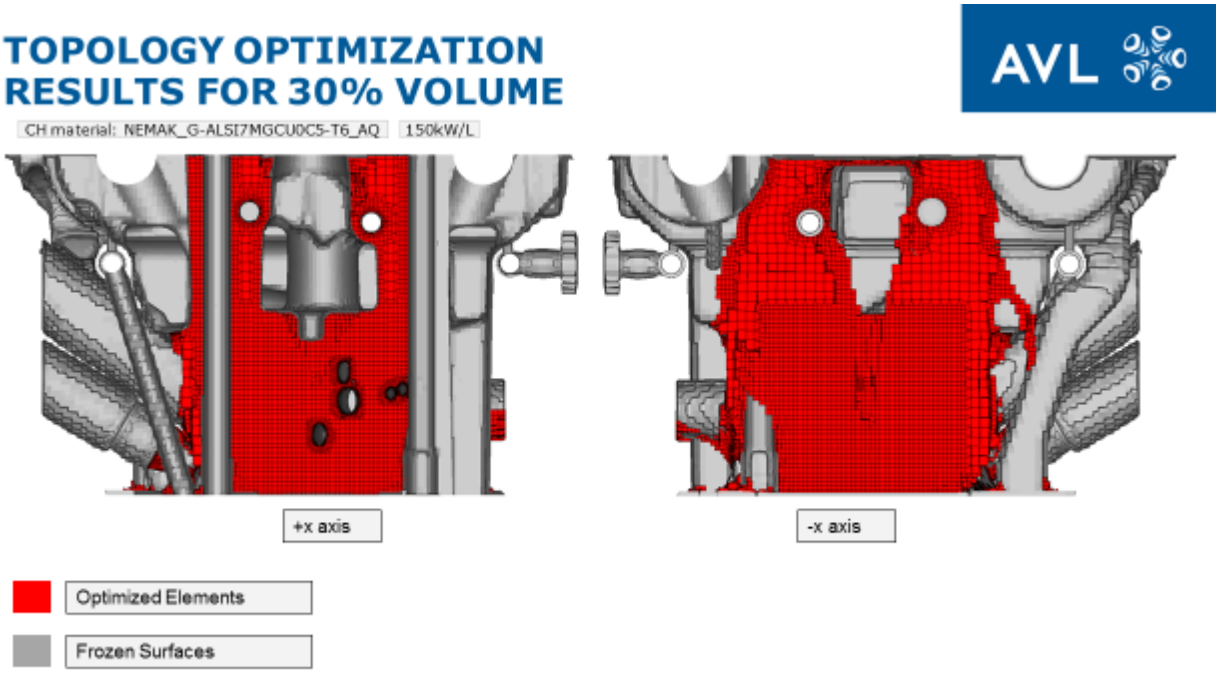


Figure 58: Results Topology Optimization - General Solver – 30 Percent Volume Reduction

Stress levels are within limits for most parts of the head. Exceptions can be found in the valve guides and around and the cylinder head bolds. As mentioned before, the first is due to replacing the contact force of real valve guides by pressure. Second by using a fixed boundary condition instead of the bold head.

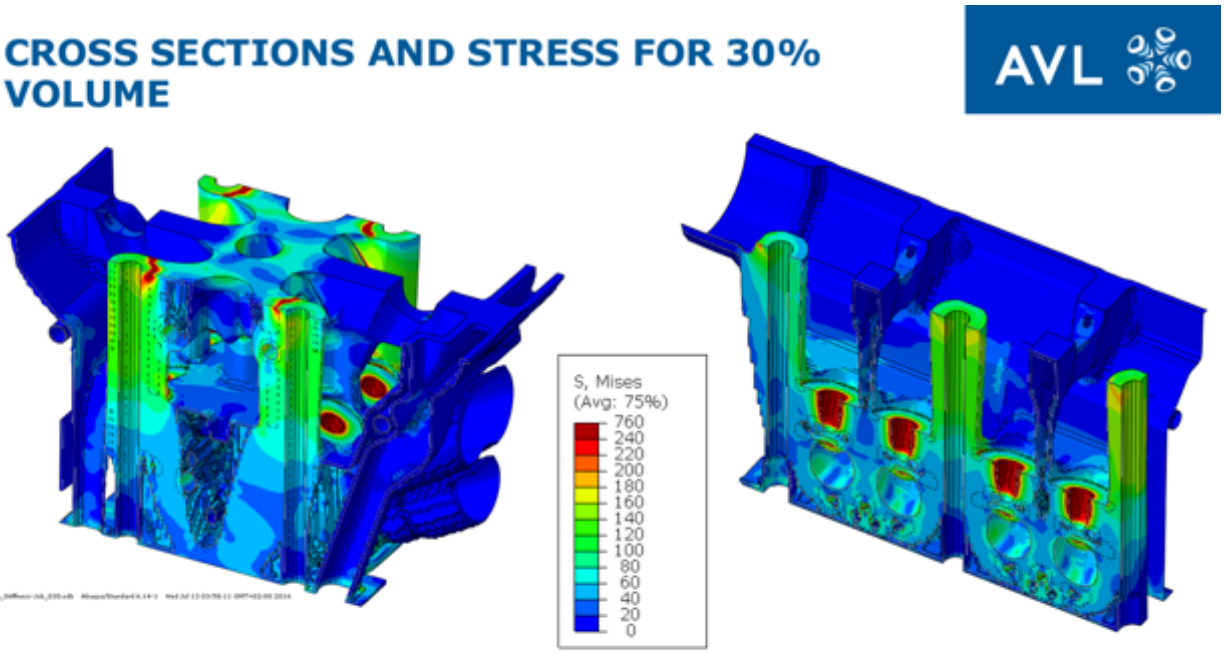


Figure 59: Stress and Structure for 30% Volume

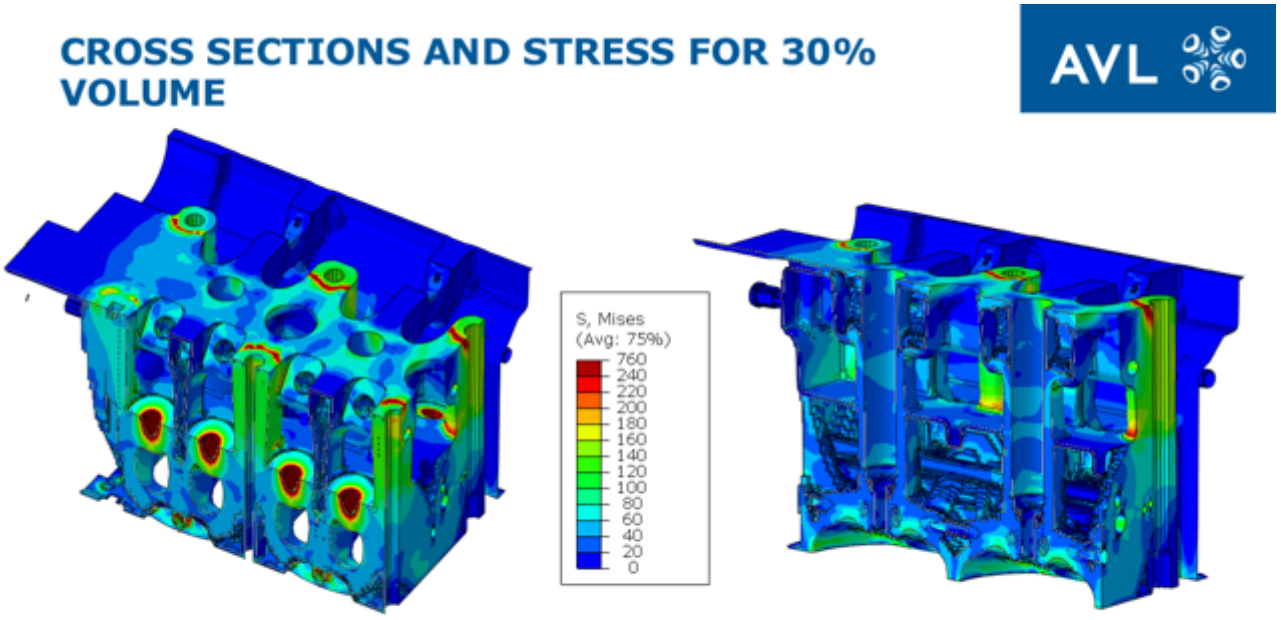


Figure 60: Stress and Structure for 30% Volume

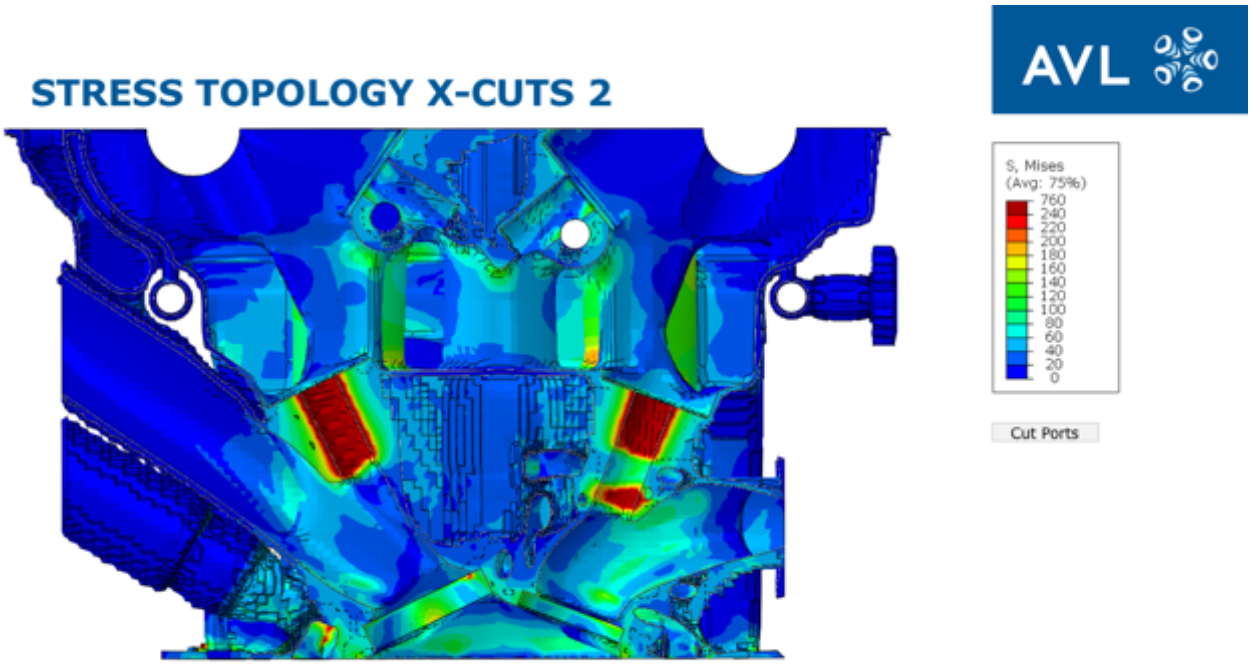


Figure 61: Misses Stress Results Topology Optimization - General Solver – 30 Percent Volume Reduction – Views Normal on X-Axis

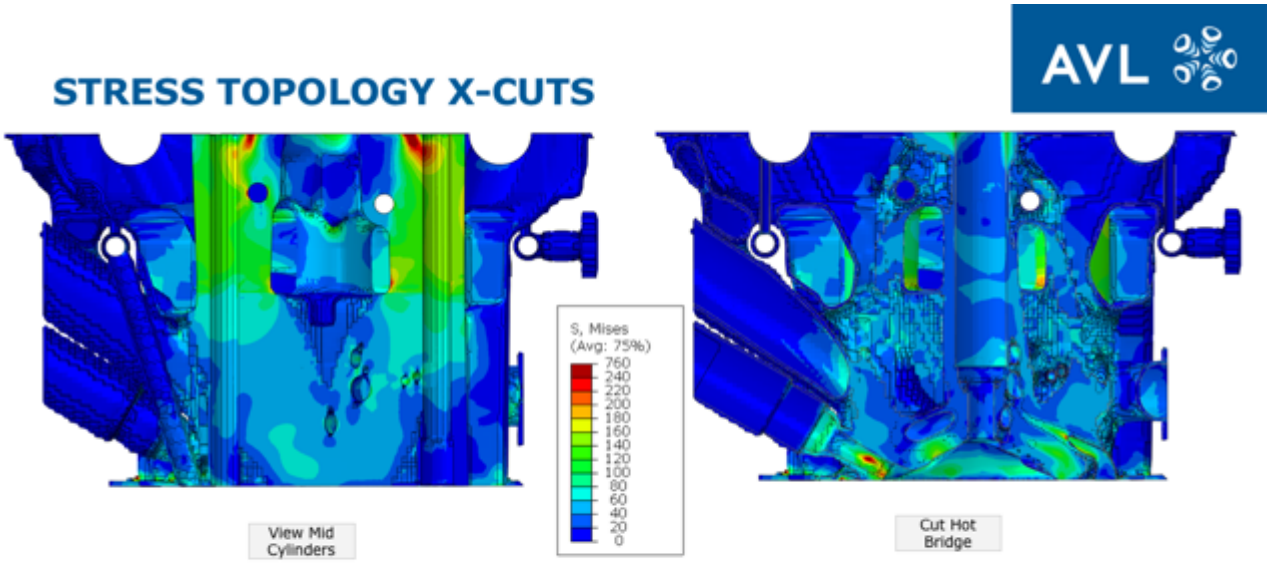


Figure 62: Misses Stress Results Topology Optimization - General Solver – 30 Percent Volume Reduction – Views Normal on X-Axis

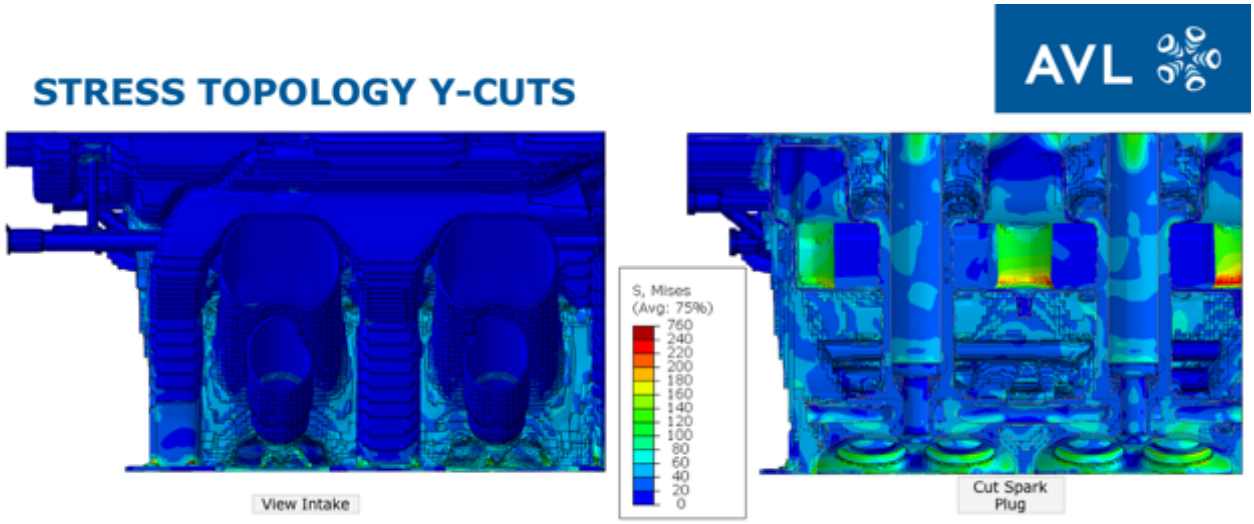


Figure 63: Misses Stress Results Topology Optimization - General Solver – 30 Percent Volume Reduction – Views Normal on y-Axis

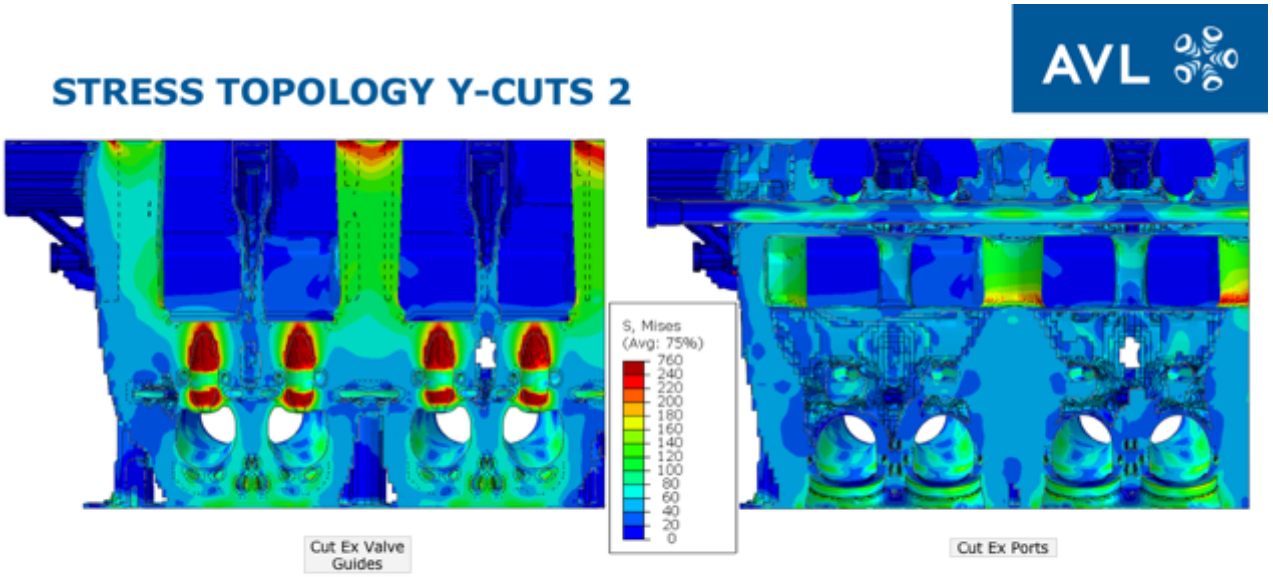


Figure 64: Misses Stress Results Topology Optimization - General Solver – 30 Percent Volume Reduction – Views normal on y-Axis

Both effects can be seen in the static load simulation of the full volume model too which indicates the validity of the Tosca results. The slight deviation in numbers is probably due to the change from a plastic model with yield to an elastic one. This causes different stress results in areas of high mechanical loads. In addition, excluding thermal loads might play its part in that too. Still some small changes in the water jacket around valve guides, seat rings and injector might help to prevent future complications.

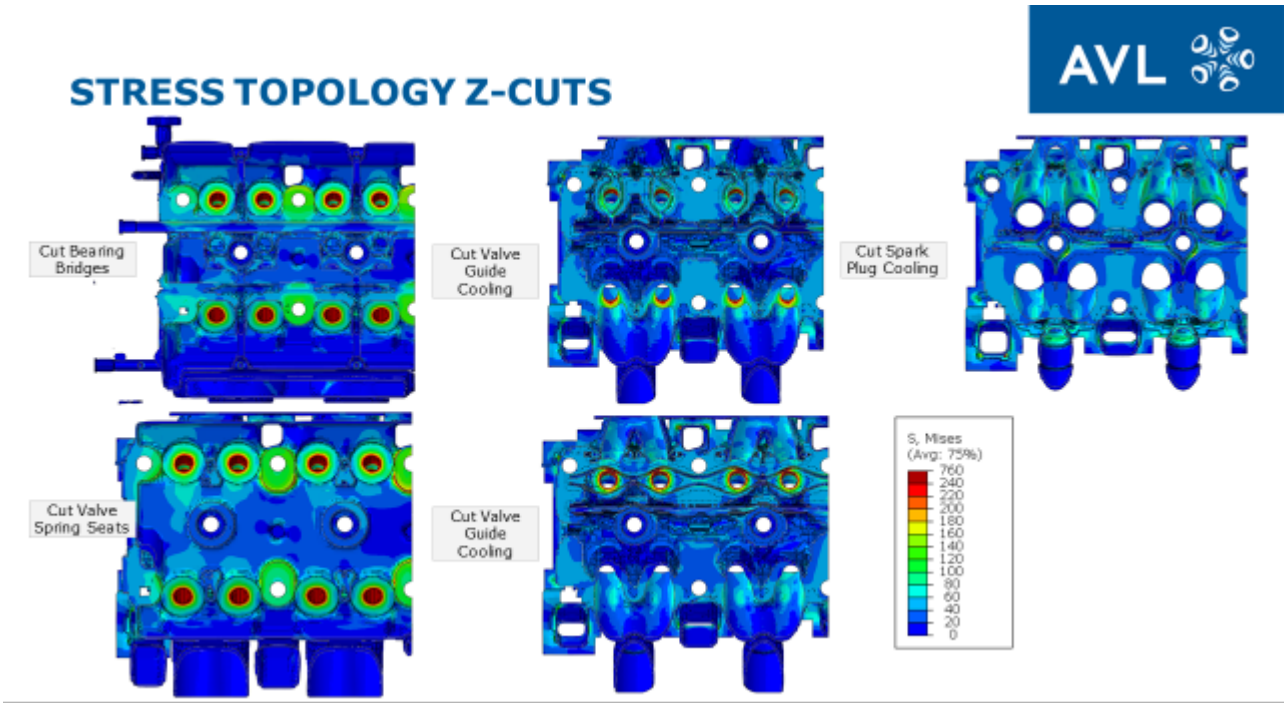


Figure 65: Misses Stress Results Topology Optimization - General Solver – 30 Percent Volume Reduction – Views normal on z-Axis

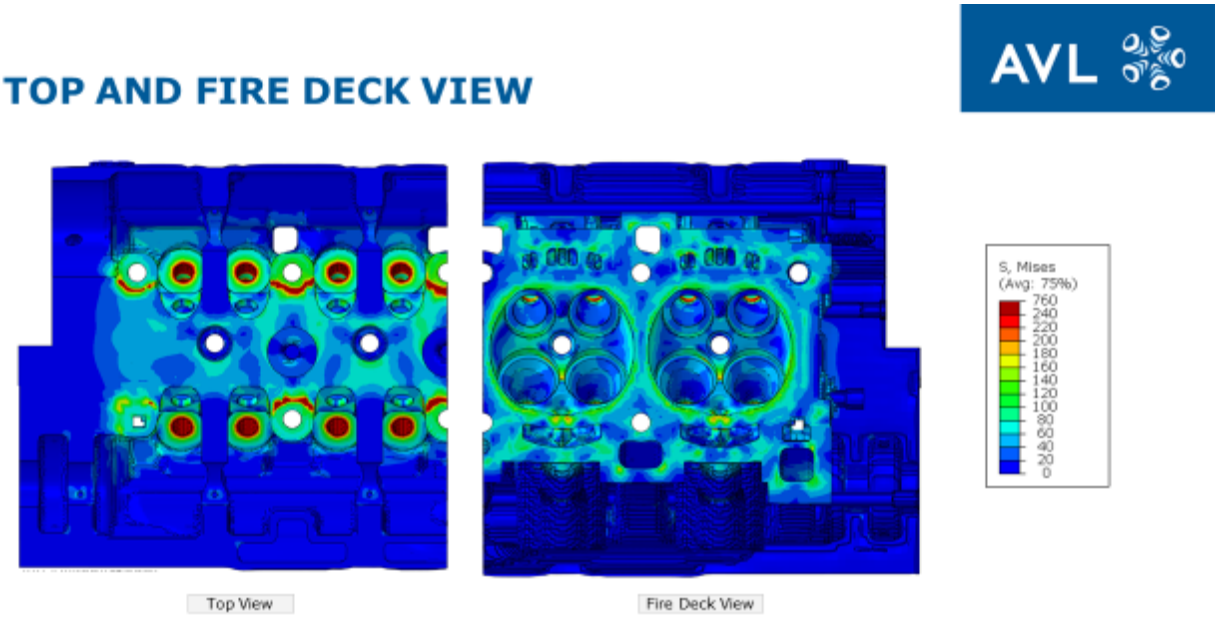


Figure 66: Misses Stress Results Topology Optimization - General Solver – 30 Percent Volume Reduction – Top and Fire Deck

However, it has to be kept in mind that some functional structures, especially the oil gallery, are far from ideal for the weight reduced design and actually need at least a partial redesign do be integrated in the new structure. Also connection to neighbor components and neglected heat load might call for both a different and thicker structure. This topic will be discussed more detailed in chapter 8.

### 7.1.2 50 Percent Volume Reduction

For a 50 percent volume reduction, the results are pretty similar to the 70 percent one, with the exception of course being that structures are thicker in places. However, improvement of static load simulation results is marginal. So for the loads applied further reduction of volume is actually the way to go.

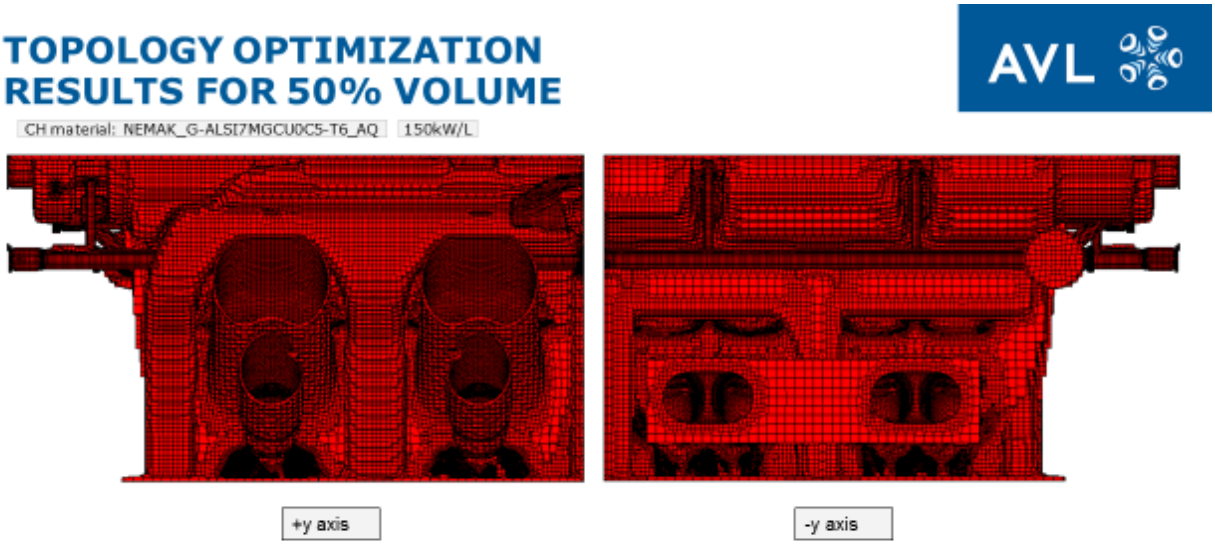


Figure 67: Results Topology Optimization - General Solver – 50 Percent Volume Reduction – Views Normal on y-Axis

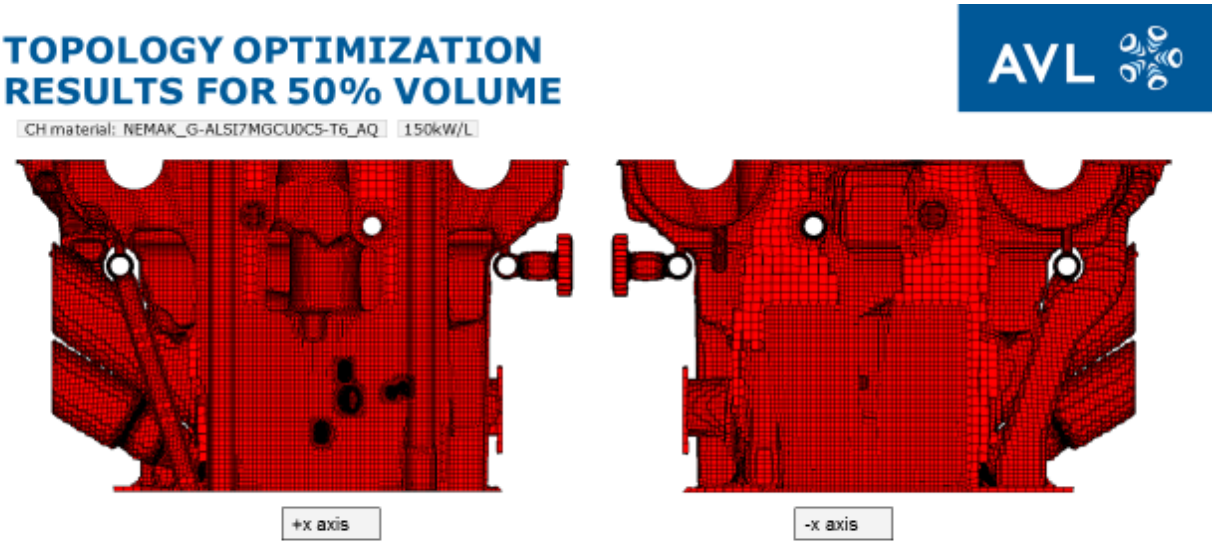


Figure 68: Results Topology Optimization - General Solver – 50 Percent Volume Reduction – Views Normal on x-Axis

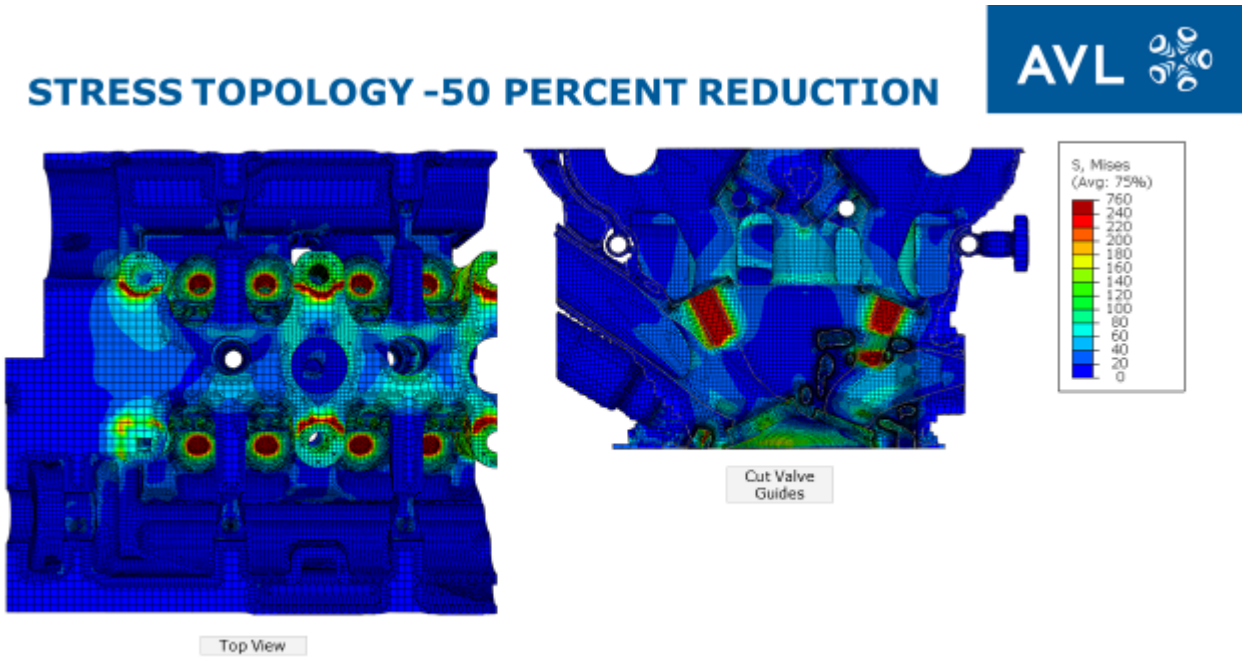


Figure 69: Misses Stress Results Topology Optimization - General Solver – 50 Percent Volume Reduction

## 7.2 Tosca Sensitivity based Solver

No satisfying results could be archived with the sensitivity based solver, although many variations and variables were tried.

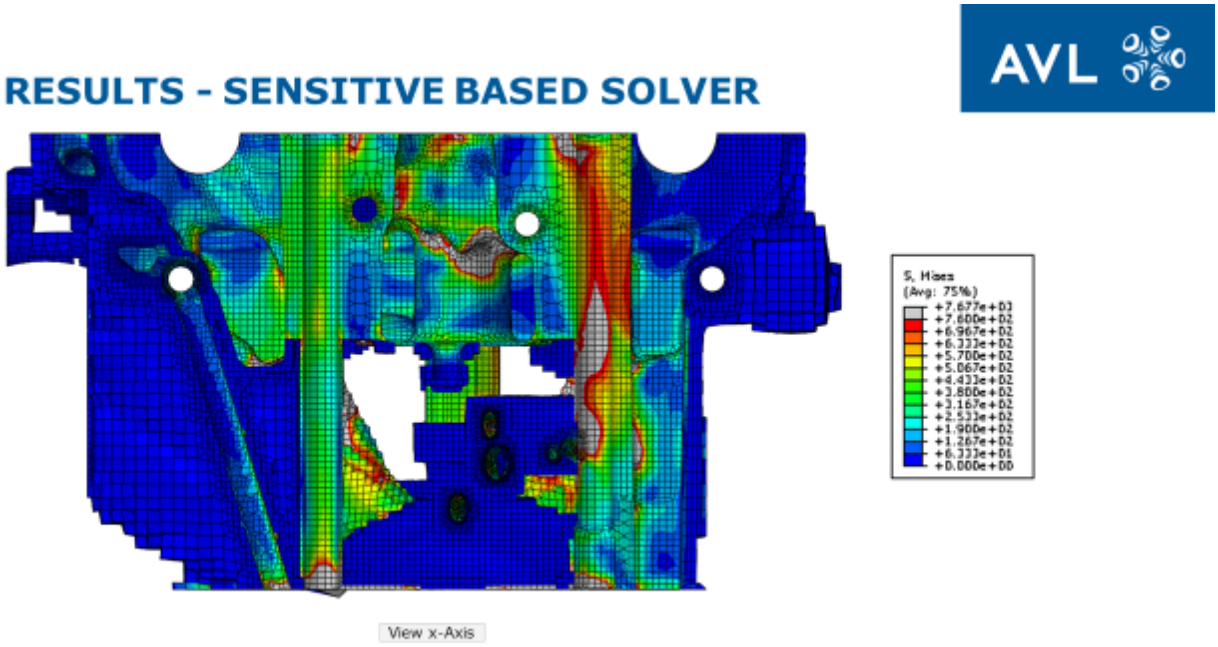


Figure 70: Sensitivity Based Solver Results

In the best of sensitivity based results areas of high stress are cut away massively while those under minor load stay basically untouched. Valve guides, surfaces in contact with the gasket and even cylinder head bolt holes, are actually the areas under highest loads and are reduced to the frozen surfaces in many places while areas around the outer ports, ignition etc., (where mechanical loads are negligible) are even untouched at some points. Furthermore, some features around the top are even unconnected to the main model. Of course this results in stress levels high above material limits, hence this results are inapplicable.

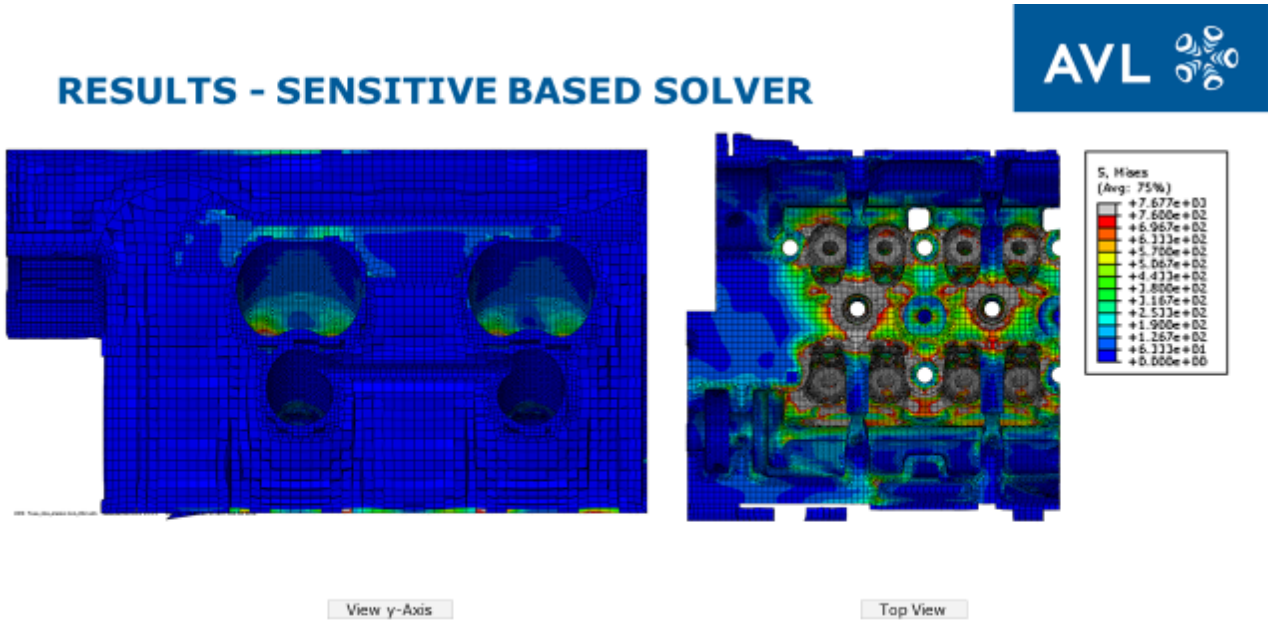


Figure 71: Misses Stress Results Topology Optimization - Sensitivity Solver – 30 Percent Volume Reduction

However, it shows some of the limitations and complications with topology optimization and finding the reasons for them might help with future projects.

### 7.2.1 Issues with Sensitivity Based Solver

#### 7.2.1.1 Mises Stress

First of all, choosing Mises stress as a design response and constraint makes things complicated for the solver. While technically a simple and valid way to show a component's design limitations and weaknesses, it messes around with Tosca topology optimization in more than one way.

First and primarily because of its definition and how it is processed in FEM, it has to be computed for every step. The Abaqus FEM solver does this at all the nodes, which mainly are situated on element edges and corners, depending on element type. As for a standard mesh and simulation there is full material between the nodes and outside surfaces should be smooth or rather representing the real life component, so there can be a straight flux of force between the nodes and a valid stress value can be computed easily.

Now using that for topology optimization leads to the following problem. Assume the case of a right angled hex mesh where some elements are not needed and can be totally cut away, resulting in steps between the other elements. Therefore, between the outer nodes straight force flow is prohibited. The steps act like cuts, weakening the structure and leading to unrealistic higher stress levels, since the future components surface will be smoothed and unlikely look like the steps from cut out elements. Thinking this through, the same effect will appear with varying magnitude on other element geometries and elements of different density, keeping in mind that Tosca uses changes in material density to simulate structure changes.

To avoid this issue, Tosca uses an algorithm to move the contact point for Mises stress from outside nodes to the center of the element. While this artificially smoothens steps of cut out elements, it is a numerical operation that needs computing power on one hand and can preclude convergence on the other. Furthermore, step size has to be cut down drastically to archive any results. Unfortunately, that just diminishes the problem but does not totally solve it.

Secondly, the type of constraint used with Mises stress can cause problems. Using the same or smaller constraint than the original, two issues arise. Firstly, cutting away elements directly leads to higher stress in other areas. Secondly, using a smaller start density, which reduces computing time, also leads to higher stress. And thirdly, areas of high stress, as found in the bold head, can set the maximum stress level too high. This may be avoided by not including those areas in the design space.

This is also crucial when setting an absolute Mises stress value as the design constraint. While for sensitivity based solvers, the Mises stress as a design constraint is actually always approximated over a bulk of elements to avoid unrealistic peaks having areas of high stress in the design area forces for a absolute averaged value higher than the highest existing value. However, that can lead to the problem that this value is higher than wanted for the other elements.

#### 7.2.1.2 Start Density

The default start density of all but the frozen elements for the sensitivity based solver is set at 50 percent. While this may lead to a result in an elastic simulation it will not work in plastic and yield simulation for high mechanical loads. Raising the start density to above 90 percent is then necessary for plastic material models but it also seems to improve convergence with elastic simulation. However, a lower start density would improve computing time.

#### 7.2.1.3 Soft Delete

Using sensitivity based solver Tosca reduces density of unnecessary elements to a level close to zero. However, these elements still stay in the model. Using the Soft Delete function, a limit can be set below which elements are deleted permanently. For instance, it is set to 0.05 then elements reaching a density below 0.05 of the original density are removed from the model. This improves computing time and helps with visualizing results. However, Tosca is not able to add elements, so if a once deleted element would be useful in a further simulation step it cannot be recovered. Hence, it is recommended to run the same simulation in both modes, with and without soft delete.

#### 7.2.1.4 Design Space

Of course it would be perfect to just get ideal structure results for the whole model. However, reducing the design space can help to improve results. On one hand, reducing the design space will reduce computing time. On the other hand, areas which probably will not see that many structural changes but have a high load input or abnormalities, can be cut out to make it easier to set design constrains for the model. Furthermore, in some cases an optimized structure in some areas is obvious. Taking them out of design space will then reduce computing time and can improve results on the remaining design space.

#### 7.2.1.5 Model Size

Obviously computing time strongly depends on the size of the model, including number of elements, materials and complexity of loads and boundary conditions. The latter can be reduced by simplifications at some point, which will not necessarily lead to worse results. The number of elements however is crucial. Using too few elements will not deliver any valid result, taking topology optimization the chance to create fine enough structures. But increasing the number of elements will add up in computing time. It is therefore all about the middle way and finding a compromise between computing time and a mesh fine enough.

## 7.3 Limitations

### 7.3.1 Thermal Optimization

While originally intended to take temperature and thermal loads directly into account in the topology optimization, they were neglected since it is unfortunately impossible to implement with Tosca. Even using temperature dependent material data will lead to convergence problems. Furthermore, since Tosca alters the structure by changing element density creating new fictive material, new thermal properties would have to be set at each step for multiple materials. Also uneven surfaces due to the cut out elements will not lead to valid heat fluxes. Hence, thermal load issues can just be taken into account for separate simulations, e.g. the base model for the initial step and finally for smoothed results of the topology optimization.

### 7.3.2 Yield – Plastic Behavior

Although working with yield and plastic behavior is possible, it is highly recommended not to do so. First, computational time rises. Secondly, it leads to more degrees of freedom which directly lead to convergence problems. An element yielding at one point in the simulation because neighbor elements are changed is very unlikely to return to a stable state in the next steps even if the structure would provide it. This is mainly because until then, the deformation is in most cases so big that a change of structure does not have any impact any more. And last starting with a lower start density will directly lead to yield and therefore inhibits a running simulation.

# 8 Discussion

## 8.1 Topology Optimization

Although topology optimization doesn't deliver a perfect model that can be realized by additive manufacturing yet, it definitely shows the potential of the technology. A set volume reduction of 70 percent might not dispense a technically feasible cylinder head but a structure that's able to cope with the given loads and still offering all functional surfaces. So by redesigning mainly the oil gallery and lubrication circuit, a huge weight saving seems to be achievable. Of course topology optimization results are quite radical in places, may it be to simplifications, the high given reduction by 70 percent or not included thermal forces.

Taking the thermal loads simulation into account, it is obvious that not only weight can be reduced but further more functionality can be improved massively. In this case, only the water jacket was adapted to additive manufacturing but the same can be done to the whole lubrication cycle as well.

## 8.2 Material

For this simulation the same material as for the original cast head, the aluminum alloy AlSi7MgCu0C5-T6, was used. All material properties are taken from the cast material. While it shouldn't be an issue to work with this aluminum alloy in additive manufacturing, properties definitely are not the same. Taking into account that most scientific papers on this topic show better material properties for additive manufactured components than cast ones, it seems valid to take those properties for a first simulation. However, especially data on thermal properties end high cycle fatigue is insufficient at the moment so some test are inevitable for future steps. For an optimal result the use of a high-strength alloy would be the way to go but more about that in chapter 9.3.

## 8.3 Weight Comparison

Table 13: Weight and Volume for the Cylinder Head – 2 Cylinders

| | Model | Tosca 30% | Tosca 50% | Original Head | Functional Surface |
|---|---|---|---|---|---|
| Volume [l] | 4,05 | 1,22 | 2,03 | 2,65 | 0,37 |
| Weight [kg] | 10,95 | 3,28 | 5,47 | 7,16 | 0,99 |
| Percent of Model | 100,00 | 30,00 | 50,00 | 65,45 | 9,04 |
| Save to original in % | +52,79 | -54,16 | -23,61 | 0,00 | -86,19 |
| Save to original in kg | +3,78 | -3,88 | -1,69 | 0,00 | -6,17 |

Comparing cylinder head weight, it has to be considered that the model used for simulations is actually heavier than the cast cylinder head. This is due to different reasons. First it has to be said that the cast head is weight optimized too. Nobody wants a non-stationary engine to be heavier than it has to be in order to achieve superior drive dynamics as well as a lower fuel consumption by a reduced overall mass. Of course the sweet spot between costs and further weight saving has to be found. Creating the model for this simulation some material was added to obtain a simpler mesh as well as more design space for topology optimization. As mentioned, topology optimization just removes elements and cannot add any. Therefore, it is pointless to optimize cast structures if the chosen

production technology is additive manufacturing, so the added material offers possibilities to achieve flux of force optimized structures for this production process.

The same applies similarly to the reduced inner volume of the water jacked. By adding bulk material in areas that formerly were needed for the water jacket mass of the model increases but that offers a chance for better overall results in topology optimization

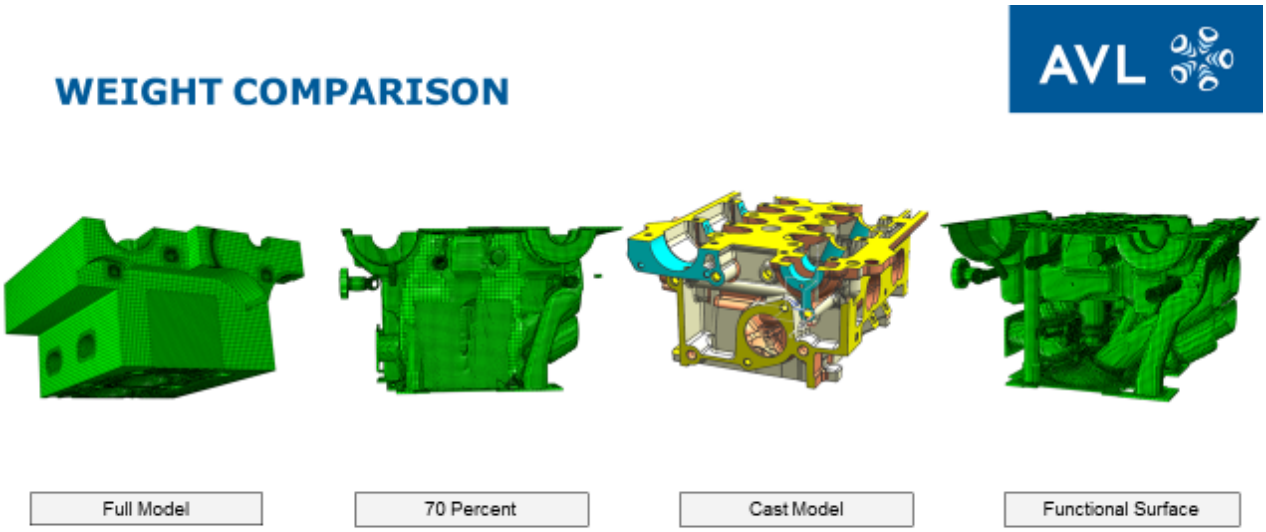


Figure 72: Overview of Model, Topology Optimization Result, Casted Cylinder Head and Functional Surfaces

Topology optimization with the set target of 70 percent volume reduction actually translates to a roughly 50 percent reduction from the original cast model, which is still quite massive. Although the simulation result is not a final useable component, it definitely shows the potential additive manufacturing has for this application. Keeping in mind that functional surfaces alone make up nearly one quarter of the cut down version, the possibilities become even more obvious. Considering more redesigning, especially of the oil covered surfaces and oil gallery, a volume reduction of at least 40 percent should be possible.

# 9 Future Prospect

Although many further steps are necessary to produce a working high power cylinder head, it should nonetheless be feasible to achieve. Some of those steps are covered here.

## 9.1 Redesign

First of all, it has to be said that the results of topology optimization are mainly an impulse for a new design. In reality, a new structure has to be created that follows the idea of the result, but takes all parameters into account that were not included in the topology optimization making it an early step in a design cycle.

Two different approaches could be taken from here on. First taking the head available and change at least those areas needed to archive a producible structure for additive manufacturing processes. Furthermore, all not connecting surfaces could be optimized to get to even better results. Second, a complete new design optimized to additive manufacturing could be taken into account.

### 9.1.1 Redesign Based on Current Cylinder Head

Starting with the first approach, it is easy to see which areas need redesigning. First thing that strikes the eye is the lubrication circuit. Looking at Tosca results, most of it seems to hang around in open space. So including those channels in the structure is the first step. As they are just drillings they are not optimized to either flow or structural objects. Adapting their form and location then might improve both mechanical and thermal properties of the cylinder head as well as function of the oil channels. The same applies to most other oil surfaces. Their main job is to get lubrication oil to moving parts, like valve guide and drive. However, the surface form is manly defined by casting parameters, meaning a redesign could help to enhance oil supply while reducing further volume. It has to be said though that oil covered surface plays a crucial part in cooling, since it has a different heat transfer coefficient than air covered areas. Therefore, it must be considered in thermal simulation and at some places an increase of volume in order to get better cooling by oil covered surfaces might be preferable.

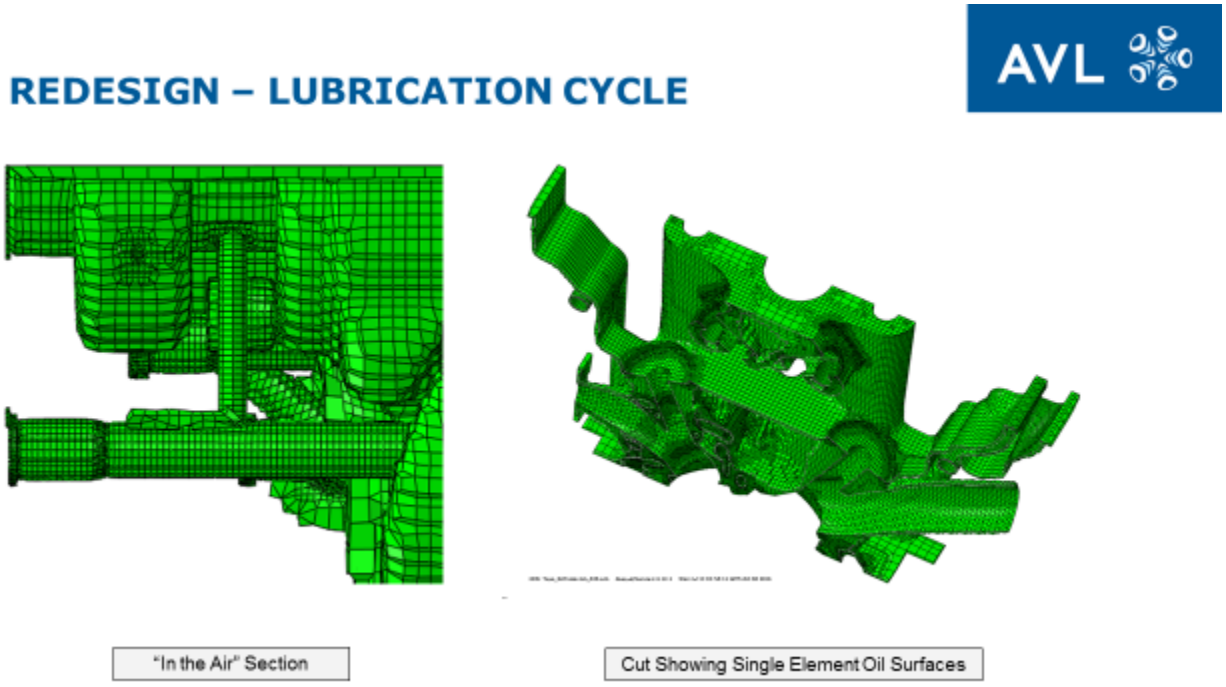


Figure 73: Problem Areas – Oil Gallery

Redesigning oil surface also opens the possibility to change side walls and bearing seats. Later ones however are not considered in standard cylinder head simulation due to the small loads. In this case, a fictional load is applied. However, for an equitable optimization this load should be considered with their actual magnitude. Another topology optimization in just this area might come up with new design ideas too.

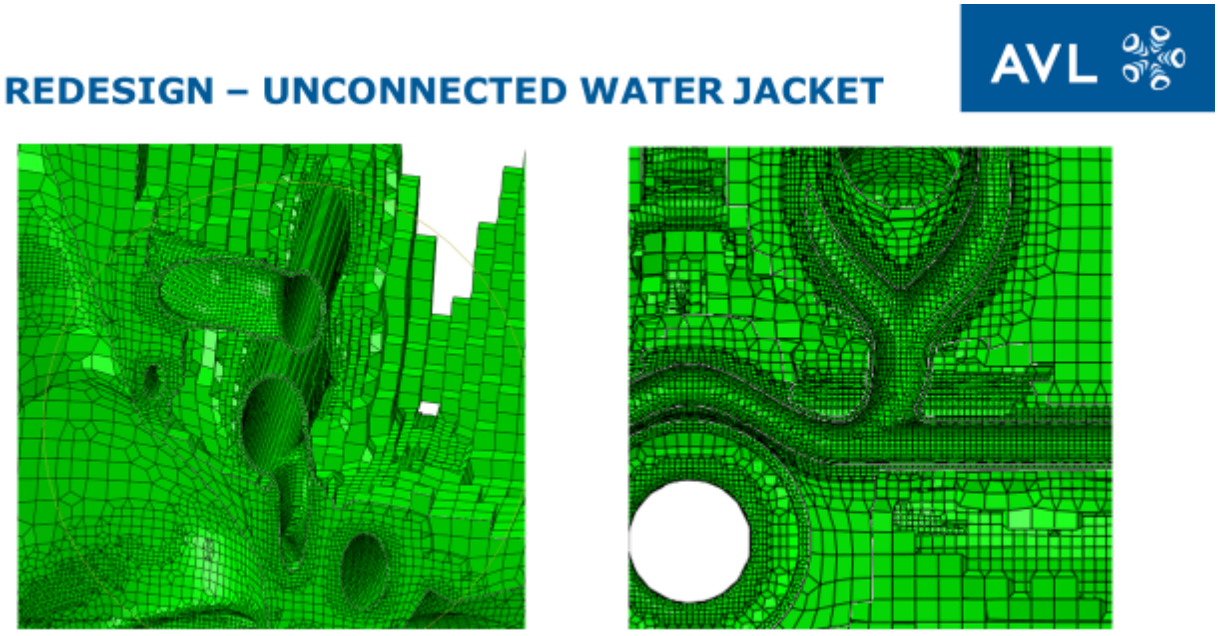


Figure 74: Problem Areas – Water Jacket

As for thermal loads, another round of thermal simulation should be done with the model achieved from topo simulation to see if there are any new problem spots. An obvious issue without any simulation is that the water jacket at some places isn't directly connected to the structure underneath anymore. This may lead to inferior cooling as well as problems with thermal strain. This means that structures have to be filled and smoothed to provide heat transport from hot spots to the water jacket. Additionally, added fins could improve cooling too, on the inside structures as well as on the outside surfaces.

### 9.1.2 Complete Redesign – New Cylinder Head

The other approach would be a total redesign of the cylinder head. Since in many areas structure is dictated by casting constraints a complete redesign might lead to better results, taking the step from form follows production process to a mainly functional based design. Obtaining the functions as the original head had following approach might be taken. Fire deck and ports seem to have few limitations in design by the casting process, so they would basically be left untouched. The water jacket could be based on the one developed here. Keeping the camshaft and valve drive in the same position, it is obvious that these areas need structural support too. While loads around the valve guides are quite high, those at the camshaft bearings are low, so a massively reduced structure could deal with those. Since the highest end-to-end loads run from gasket and fire deck to the cylinder head bolts, it makes sense to take a closer look at this area. Perhaps a relocation or shortening of the bolts can lead to reduction in mass. In order to maintain enough stiffness around the fire deck, a lattice structure could help. For the oil gallery, the same approach applies as for a partial redesign. Focus on getting the oil where it is needed for lubrication in a flow optimized way and reduce the oil covered surfaces when cooling is not an issue.

Further savings could be realized by replacing sidewalls and cap by an integrated plastic part. Since thermal and mechanical loads are low and the cap and wall act as a seal to the surrounding environment this can be an ideal application for plastics. However, there are some points that have to be considered. First, an enduring seal has to be found. Secondly, fire resistance might be a challenge. Furthermore, aging be problematic with plastics and chemical constancy to oil and other fluids that might make contact with the component which must be addressed. However, this could help to achieve both a reduced weight by using a lower density material and reduced costs due to reduced build size, build time and metal powder consumption.

## 9.2 Further Simulations

Whatever decision is made, a complete simulation - thermal and mechanical - of the cylinder head is inevitable, including most of the connecting parts and contacts. In particular, thermal simulation should be done early in the development process since this loads are not directly considered in topology optimization. Therefore, also material tests are important since simulation depends on the quality of the input data.

However, a new mesh should be designed for this simulation to shorten computing time and for more accurate surfaces. Also the inclusion of surrounding parts is advisable for the next static load simulation.

In addition, simulation of the production process is of high interest. On one hand it will help to optimize the production process for the given component, on the other hand it might shows problem points which can be avoided by changes in design. However, simulation and process control of additive manufacturing are in its beginnings but a lot of development can be seen there. So it can be expected that there will be a selection of simulation tools available in foreseeable future. This may lead to better adapted designs as well as less waste in production and lower costs as a result.

## 9.3 Materials

As previously mentioned, the same material properties as for the cast material were used in this simulation. This leads to both issues as well as a lot of opportunities. Issue number one is that material properties of an additive manufactured part are not the same as those of same component produced by casting. While static mechanical material properties of additive manufacturing outclass those achieved with casting information on thermal properties and high cycle fatigue are rare. So material tests are mandatory for a working prototype. Secondly, it is not sure that the exact alloy is available as powder. While it is technically no problem to powder nearly any material, it is questionable from an economics standpoint as well as technical point of view. As said before, cast materials have a lot of limitations due to the production process. So using the same material for additive manufacturing might be a good first step to point out the structural advantages that can be achieved. However, in order to use the full potential of additive manufacturing, a superior alloy should be used. As of today there are already some high-strength aluminum alloys available which would allow for even more radical structures and therefore weight savings. However, the final step is the development of a new alloy, optimized for both, the given application and the additive manufacturing process. Eventually this is the way to go if the full potential of this technology should be exploited. Although it is state of the art, the selection of aluminum should be questioned at some point and the possibility of applying other materials should be taken into consideration, such as titanium alloys. While not as light as aluminum alloy, it offers great strength. Another approach are extremely reduced structures with high strength materials like nickel alloys.

## 9.4 Further Ideas

Following some possibilities which could be of interest in years to come but are either not yet feasible or demand some evolution steps to get there.

### 9.4.1 Hybrid Materials

Significant development in additive manufacturing is being made in the direction of hybrid materials, different materials properties in different areas of a single material as well as material combinations. Some of these projections and their potentials are explained here.

#### 9.4.1.1 Single Material Gradients

Material gradients can be archived with either one single material or a material combination. Single material gradients might be just by structural design or reached by changing process parameters. The first can be achieved easily by lattice structures and is feasible as of today. Different directional stiffness as well as weight reduction are possible to some extent. However, the material properties are the same throughout the component - it is just a gradient by design made possible by the near net shape structure doable with additive manufacturing processes.

The real difference in material properties can be realized by changing process parameters. Varying those differences in porosity, stiffness, ductility and hardness are possible. However, strict adherence of the component must be ensured and some variation might just be possible in the build direction and small difference per layer. It’s remains to be mentioned that process control for this is complex and therefore still in development.

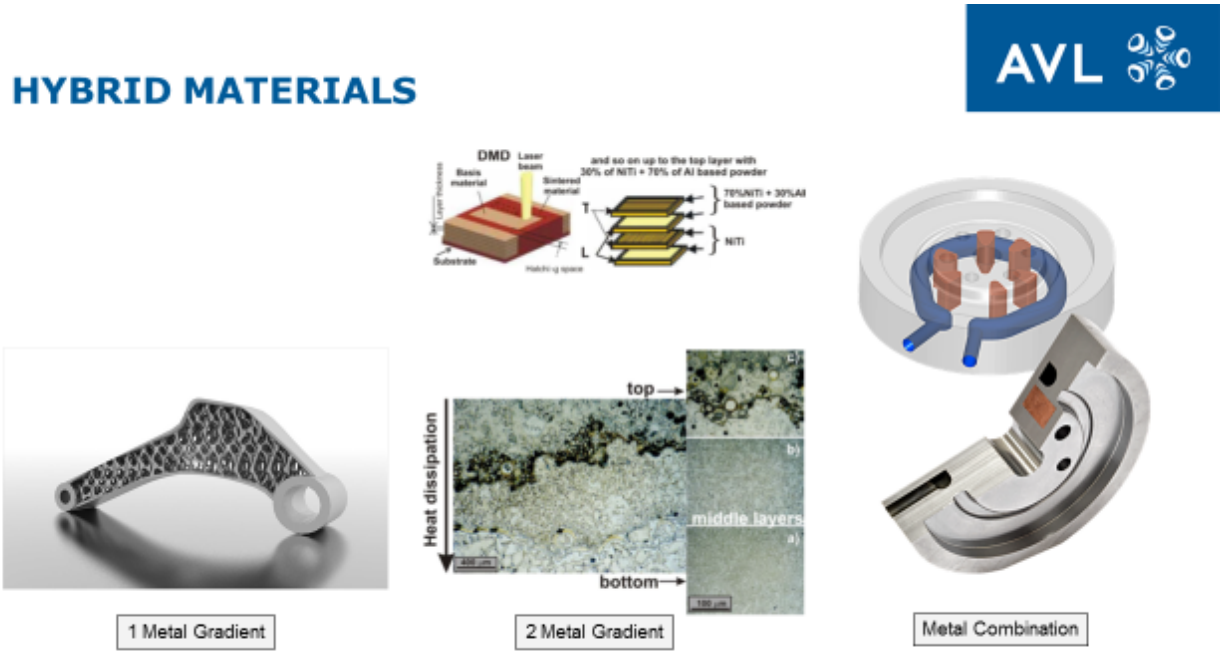


Figure 75: Additive Manufacturing – Hybrid Materials [10] [6]

### 9.4.1.2 Two Metal Gradients and Metal Combinations

Combinations between two metals can either be with a gradient transition or building one metal directly on another. Powder bed processes allow for just the first one in the build direction by applying a varying powder mixture with every layer. Logically this means that the material gradient in powder bed processes can just vary in only one direction. Freeform fabrication allows for both, a complete as well as a gradient change in material in any build direction. While powder based free form fabrication offers both material gradients and combinations, wire based process are limited, since gradients with two different wires are more challenging than mixing two powders.

However, while theoretically possible, feasibility is still very limited. Since most processes are similar to welding, the same issues occur as with welding two different materials. In addition to that there is a lot to think about when designing a component using two materials, especially under thermal load.

But as development continues, these technologies might help to replace valve guides and valve seats in a cylinder head. In addition, cooling could be supported by adding parts of material with different thermal properties or by changing thermal and mechanical properties in build direction which can make sense looking at a cylinder heads heat distribution. [10]

### 9.4.1.3 Metal Matrix Ceramic - MMC

Instead of combining two different metal powders, a ceramic powder is added in small doses to a metallic matrix. This influences mechanical as well as thermal properties. As far as literature study for this master thesis showed no sophisticated results on strength and thermal properties could be achieved yet, although a change in tribology to a lower coefficient of friction can be seen. This could help to increase dry lubrications for certain components. [24]

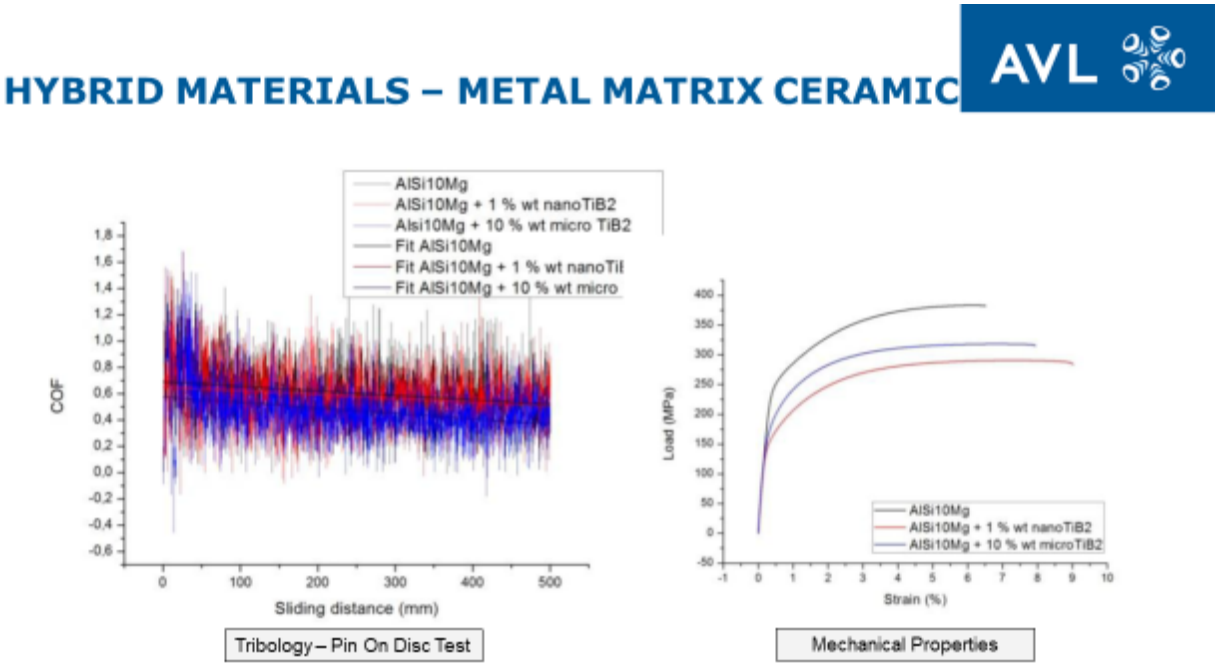


Figure 76: Additive Manufacturing – Metal Matrix Ceramics [24]

### 9.4.2 Hybrid Production Processes

In some cases, it might be a good idea to combine advantages of different production processes, like low costs of casting for high production numbers with high structural freedom of additive manufacturing. This might be done by using a cast substrate for additive manufacturing process, reducing build size and time and therefore costs, which could be of interest for higher production numbers. Also a build on high strength forged substrates could make sense, for instance for pistons with integrated oil galleries.

### 9.4.3 System Integration

With increasing build size, it might be possible to integrate further functions into the cylinder head. That could be part of the exhaust system and supercharger as well as or oil circuit or injection. While this may create problems with established standards, it would reduce connections and transitions and therefore reduce size and weight as well as optimize function (e.g. flow). In the end an additive manufactured motor block, piston and other engine parts should be considered too. Although they lack the potential and functional complexity of the cylinder head some weight and functional optimization certainly can be realized.

# 10 Appendix

## 10.1 Table Material Properties

| Materials | | Process | | | Physical properties |
|---|---|---|---|---|---|
| Materials | Process | Machine | Source | Note | Density [g/cm$^3$] |
| Aluminum Alloys | | | | | |
| EOS Aluminum AlSi10Mg | DMLS | EOS | EOS | no heat treatment | 2.98 |
| EOS Aluminum AlSi10Mg | DMLS | EOS | EOS | heat treatment | 2.98 |
| EOS Aluminum AlSi10Mg (200°C) | DMLS | EOS | EOS | build on preheated platform (200°C) | 2.67 |
| AlSi12 | SLM | SLM Solutions | SLM Solutions | no Heat treatment, 50µm layer | |
| AlSi10Mg | SLM | SLM Solutions | SLM Solutions | no Heat treatment, 50µm layer | |
| AlSi7Mg | SLM | SLM Solutions | SLM Solutions | no Heat treatment, 50µm layer | |
| AlSi9Cu3 | SLM | SLM Solutions | SLM Solutions | | |
| AlMg4,5Mn0,4 | SLM | SLM Solutions | SLM Solutions | | |
| AlSi12 | SLM | Concept Laser | Concept Laser | | |
| AlSi10Mg | SLM | Concept Laser | Concept Laser | | |
| Scalmalloy | SLM | Concept Laser | Toolcraft/Airbus | | 2.7 |
| AlCu7 | EBF$^3$ | NASA | Nato | as build | |
| AlCu7 | EBF$^3$ | NASA | Nato | Heat treatment T62 | |
| AlCu7 | wrought | | Nato | O typical | |
| AlCu7 | wrought | | Nato | T4 | |
| AlCu7 | wrought | | Nato | t62 | |
| AlCu5Ni1.5CoSbZr | cast | | Gifu Assets | heat treatment | |
| AlSi10Mg | cast | | Gifu Assets | heat treatment | |
| AlSi10Mg | DMLS | | Gifu Assets | heat treatment | |
| Scalmalloy | DMLS | | Gifu Assets | heat treatment | |
| Al + SiC | DMLS | | Gifu Assets | heat treatment | |
| Al + SiC | DMLS | | Gifu Assets | heat treatment | |
| Al + SiC | DMLS | | Gifu Assets | heat treatment | |
| Titanium Alloys | | | | | |
| TiAl6V4 | SLM | SLM Solutions | SLM Solutions | no Heat treatment, 30µm layer | |
| TiAl6Nb7 | SLM | SLM Solutions | SLM Solutions | Heat treatment | |

| | | | | | |
|---|---|---|---|---|---|
| Ti | SLM | SLM Solutions | SLM Solutions | no Heat treatment, 30µm layer | |
| EOS Ti64 | DMLS | EOS | EOS | | 4.43 |
| EOS Ti64 ELI | DMLS | EOS | EOS | no heat treatment, 50µm layer | 4.41 |
| EOS Ti64 ELI | DMLS | EOS | EOS | heat treatment, 50 µm layer | 4.41 |
| Grade 2 Ti | EBM | ARCAM | ARCAM | | |
| Grade 2 Ti | Cast | | ARCAM | casted | |
| TIAl6V4 ELI | EBM | ARCAM | ARCAM | HIP for | |
| TIAl6V4 ELI | Cast | | ARCAM | casted | |
| TiAl6V4 | EBM | ARCAM | ARCAM | HIP | |
| TiAl6V4 | Cast | | ARCAM | casted | |
| TiAl6V4 | Wrought | | ARCAM | wrought | |
| TIAl6V4 ELI | EBF[3] | NASA | Nato | | |
| TiAl6V4 | | | Nato | Std. grade, AMS4999 | |
| TiAl6V4 | | | | | |
| TiAl6V6 | EBM | ARCAM | [48] | | |
| TiAl6V6 | Wrought | | [48] | | |
| TiAl6V6 | EBM | ARCAM | Euro PM2015 | HIP, Heat Treatment (Dif. HT see Paper) | |
| Steels | | | | | |
| EOS Stainless Steel GP1 | DMLS | EOS | EOS | stress relieved | 7.8 |
| EOS Stainless Steel PH1 | DMLS | EOS | EOS | | 7.8 |
| EOS Stainless Steel PH1 | DMLS | EOS | EOS | hardened | 7.8 |
| EOS Maraging Steel MS1 | DMLS | EOS | EOS | | 8.0-8.1 |
| EOS Maraging Steel MS1 | DMLS | EOS | EOS | age hardening | 8.0-8.1 |
| 12.709 | SLM | SLM Solutions | SLM Solutions | no Heat treatment, 30µm layer | |
| 1.4404 (316L) | SLM | SLM Solutions | SLM Solutions | no Heat treatment, 30µm layer | |
| 1.2344 (H13) | SLM | SLM Solutions | SLM Solutions | Heat treatment, 30µm layer | |
| 1.4540 (15-5PH) | SLM | SLM Solutions | SLM Solutions | Heat treatment, 30µm layer | |
| 1.4542 (15-5PH) | SLM | SLM Solutions | SLM Solutions | | |
| 1.2344 (H13) | MPA | Hermle | Hermle | | |
| 12.367 | MPA | Hermle | Hermle | | |
| 1.4404 (316L) | MPA | Hermle | Hermle | | |
| 17-4HP | SLM | | Euro PM2015 | | |
| 17-4HP | DMLS | | Euro PM2015 | | |
| 17-4HP | wrought | | Euro PM2015 | | |
| Titanium Aluminide | | | | | |
| | EBM | | Acram | | |

| | | | | | |
|---|---|---|---|---|---|
| Nickel Alloys | | | | | |
| EOS Ni HX | DMLS | EOS | EOS | as build | 8.2 3 |
| EOS Ni HX | DMLS | EOS | EOS | heat treatment | 8.2 |
| EOS Ni IN718 | DMLS | EOS | EOS | as build | 8.2 |
| EOS Ni IN718 | DMLS | EOS | EOS | solution anneal, age hardening ams5662 | 8.2 |
| EOS Ni IN718 | DMLS | EOS | EOS | solution anneal, age hardening ams5662 | 8.2 3 |
| EOS Ni IN625 | DMLS | EOS | EOS | as build | 8.4 3 |
| EOS Ni IN625 | DMLS | EOS | EOS | stress relieved | 8.4 |
| Hastelloy X | SLM | SLM Solutions | SLM Solutions | no Heat treatment, 30µm layer | |
| Inconel 625 | SLM | SLM Solutions | SLM Solutions | no Heat treatment, 30µm layer | |
| Inconel 718 | SLM | SLM Solutions | SLM Solutions | no Heat treatment, 30µm layer | |
| Inconel 939 | SLM | SLM Solutions | SLM Solutions | no Heat treatment, 30µm layer | |
| Inconel 738 | SLM | SLM Solutions | SLM Solutions | | |
| Inconel 939 | SLM | | Euro PM2015 | as build | |
| Inconel 939 | SLM | | Euro PM2015 | HIP, Solutioning 1150/4, Agening 850/16 | |
| Inconel 939 | Cast | | Euro PM2015 | Solutioning 1150/4, Agening 850/16 | |
| Cobalt-Chrome | | | | | |
| EOS CoCr MP1 | DMLS | EOS | EOS | | |
| CoCr | SLM | SLM Solutions | SLM Solutions | no Heat treatment, 30µm layer | |
| ASTFM F75 | EBM | ARCAM | ARCAM | as build | |
| ASTFM F75 | EBM | ARCAM | ARCAM | heat treatment | |
| Others | | | | | |
| Elektron MAP+43 | DED | custom | Euro PM2015 | T6 + HIP | |
| | SLM | SLM 125 | Euro PM2015 | | |
| | cast | | | T6 | |
| Copper | EBM | ARCAM | [48 ] | | 8.84 |
| | wrought | | [48 ] | | 8.9 |

| Materials | | Mechanical Properties | | | | | | | |
|---|---|---|---|---|---|---|---|---|---|
| Materials | Process | Ultimate Tensile Strength | | | | Yield Strength (rp 0.2) | | | |
| | | Horiz-ontal [Mpa] | Vari-ation | vertical [Mpa] | Vari-ation | horizontal [Mpa] | Vari-ation | vertical [Mpa] | Vari-ation |
| Aluminum Alloys | | | | | | | | | |
| EOS Aluminum AlSi10Mg | DMLS | | | 340 | ±40 | | | 250 | ±15 |
| EOS Aluminum AlSi10Mg | DMLS | | | 315 | ±20 | | | 260 | ±15 |
| EOS Aluminum AlSi10Mg (200°C) | DMLS | 360 | | 390 | | 220 | | 210 | |
| AlSi12 | SLM | | | 409 | ±20 | | | 211 | ±20 |
| AlSi10Mg | SLM | | | 397 | ±11 | | | 227 | ±11 |
| AlSi7Mg | SLM | | | 294 | ±17 | | | 147 | ±15 |
| AlSi9Cu3 | SLM | | | | | | | | |
| AlMg4,5Mn0,4 | SLM | | | | | | | | |
| AlSi12 | SLM | | | 317 | ±8 | | | 170-220 | |
| AlSi10Mg | SLM | | | | | | | | |
| Scalmalloy | SLM | | | 490 | | | | 450 | |
| AlCu7 | EBF³ | | | 280 | | | | 110 | ±10 |
| AlCu7 | EBF³ | | | 410 | | | | 290 | ±5 |
| AlCu7 | wrought | | | 175 | | | | 80 | |
| AlCu7 | wrought | | | 340 | | | | 175 | |
| AlCu7 | wrought | | | 400 | | | | 280 | |
| AlCu5Ni1.5CoSbZr | cast | | | 220 | | | | 210 | |
| AlSi10Mg | cast | | | 269 | | | | 220 | |
| AlSi10Mg | DMLS | | | 345 | | | | 230 | |
| Scalmalloy | DMLS | | | 490 | | | | 450 | |
| Al + SiC | DMLS | | | 500 | | | | 430 | |
| Al + SiC | DMLS | | | 560 | | | | 490 | |
| Al + SiC | DMLS | | | 620 | | | | 570 | |
| Titanium Alloys | | | | | | | | | |
| TiAl6V4 | SLM | | | 1286 | ±57 | | | 1116 | ±61 |
| TiAl6Nb7 | SLM | | | >972 | | | | >865 | |
| Ti | SLM | | | >290 | | | | >180 | |
| EOS Ti64 | DMLS | | | 1150 | ±60 | | | 1030 | ±70 |
| EOS Ti64 ELI | DMLS | 1260 | ±40 | 1250 | ±50 | 1125 | ±65 | 1130 | ±75 |
| | | | ±30, min | | ±30, min | | ±40, min | | ±40, min |
| EOS Ti64 ELI | DMLS | 1075 | 860 | 1080 | 860 | 1000 | 795 | 1005 | 795 |
| Grade 2 Ti | EBM | | | 570 | | | | 540 | |
| Grade 2 Ti | Cast | | | 345 | | | | 275 | |
| TIAl6V4 ELI | EBM | | | 970 | | | | 930 | |

| | | | | | | | | | |
|---|---|---|---|---|---|---|---|---|---|
| TIAl6V4 ELI | Cast | | | 860 | | | | 795 | |
| TiAl6V4 | EBM | | | 1020 | | | | 950 | |
| TiAl6V4 | Cast | | | 860 | | | | 758 | |
| TiAl6V4 | wrought | | | 930 | | | | 860 | |
| TIAl6V4 ELI | EBF³ | | | 790 | | | | 680 | |
| TiAl6V4 | | | | 810 | | | | 750 | |
| TiAl6V4 | | | | | | | | | |
| TiAl6V6 | EBM | | | | | | | 950 | |
| TiAl6V6 | wrought | | | | | | | 860 | |
| TiAl6V6 | EBM | | | 1010 | ±5 | | | 900 | ±5 |
| Steels | | | | | | | | | |
| EOS Stainless Steel GP1 | DMLS | 1050 | ±50 | 980 | ±50 | 540 | ±50 | 500 | ±50 |
| EOS Stainless Steel PH1 | DMLS | 1150 | ±50 ±100, min | 1050 | ±50 ±100, min | 1050 | ±50 ±100, min | 1000 | ±50 ±100, min |
| EOS Stainless Steel PH1 | DMLS | 1450 | 1310 | 1450 | 1310 | 1300 | 1170 | 1300 | 1170 |
| EOS Maraging Steel MS1 | DMLS | | | 1100 | ±100 | | | 1000 | ±100 |
| EOS Maraging Steel MS1 | DMLS | | | 1950 | ±100 | | | 1900 | ±100 |
| 12.709 | SLM | | | 1015 | ±34 | | | 854 | ±50 |
| 1.4404 (316L) | SLM | | | 654 | ±49 | | | 550 | ±39 |
| 1.2344 (H13) | SLM | | | 1730 | ±30 | | | | |
| 1.4540 (15-5PH) | SLM | | | 1100 | ±50 | | | 1025 | ±25 |
| 1.4542 (15-5PH) | SLM | | | | | | | | |
| 1.2344 (H13) | MPA | 1800 | | 1500 | | 1150 | | 1150 | |
| 12.367 | MPA | | | | | | | | |
| 1.4404 (316L) | MPA | | | | | | | | |
| 17-4HP | SLM | | | 1150 | ±100 | | | 600 | ±100 |
| 17-4HP | DMLS | | | 1075 | ±100 | | | 670 | ±100 |
| 17-4HP | wrought | | | 1050 | | | | 550 | |
| Titanium Aluminide | | | | | | | | | |
| | EBM | | | | | | | | |
| Nickel Alloys | | | | | | | | | |
| EOS Ni HX | DMLS | 850 | ±40 | 720 | ±40 | 675 | ±50 | 570 | ±50 |
| EOS Ni HX | DMLS | 730 | ±40 | 690 | ±40 | 330 | ±50 | 330 | ±50 |
| EOS Ni IN718 | DMLS | | | 980 | ±50 ±100, min | | | 634 | ±50 ±100, min |
| EOS Ni IN718 | DMLS | | | 1400 | 1276 | | | 1150 | 1043 |

| | | | | | | | | | |
|---|---|---|---|---|---|---|---|---|---|
| | | | | | ±100, min | | | | ±100, min |
| EOS Ni IN718 | DMLS | | | 1380 | 1241 | | | 1240 | 1034 |
| EOS Ni IN625 | DMLS | 990 | ±50 | 900 | ±50 | 725 | ±50 | 615 | ±15 |
| | | | | | ±100, min | | ±100, min | | ±100, min |
| EOS Ni IN625 | DMLS | 1040 | ±100, min 827 | 930 | 827 | 720 | 414 | 650 | 414 |
| Hastelloy X | SLM | | | 772 | ±24 | | | 595 | ±28 |
| Inconel 625 | SLM | | | 961 | ±41 | | | 707 | ±41 |
| Inconel 718 | SLM | | | 995 | ±43 | | | 689 | ±67 |
| Inconel 939 | SLM | | | 1009 | ±35 | | | 735 | ±41 |
| Inconel 738 | SLM | | | | | | | | |
| Inconel 939 | SLM | 1140 | | 1190 | | 800 | | 890 | |
| Inconel 939 | SLM | | | 1550 | | | | 1150 | |
| Inconel 939 | Cast | | | 950 | | | | 675 | |
| Cobalt-Chrome | | | | | | | | | |
| EOS CoCr MP1 | DMLS | | | | | | | | |
| CoCr | SLM | | | 1050 | ±20 | | | 835 | ±20 |
| ASTFM F75 | EBM | | | | | | | | |
| ASTFM F75 | EBM | | | 960 | | | | 655 | |
| Others | | | | | | | | | |
| Elektron MAP+43 | DED | 255 | ±6.7 | 246 | ±7.8 | 167 | ±2.9 | 170 | ±6.1 |
| | SLM | | | | | | | | |
| | cast | | | 250 | | | | 180 | |
| Copper | EBM | | | | | | | 76 | |
| | wrought | | | | | | | 69 | |

| Materials | | Mechanical Properties | | | | | | | | | |
|---|---|---|---|---|---|---|---|---|---|---|---|
| Materials | Process | Elongation at Break | | | | Hardness | | | | | |
| | | Hori-zontal [%] | Vari-ation | Verti-cal [%] | Vari-ation | HBW | Vari-ation | HV | HV10 | Vari-ation | HR C |
| Aluminum Alloys | | | | | | | | | | | |
| EOS Aluminum AlSi10Mg | DMLS | | | 1.5% | ±0.5 | 120 | ±5 | | | | |
| EOS Aluminum AlSi10Mg | DMLS | | | 1.2% | ±0.5 | 112 | ±5 | | | | |
| EOS Aluminum AlSi10Mg (200°C) | DMLS | 8 | | 6% | | | | | | | |
| AlSi12 | SLM | | | 5.1% | | | | | 110 | | |
| AlSi10Mg | SLM | 6 | ±1 | 8% | ±1 | | | | 117 | ±1 | |
| AlSi7Mg | SLM | | | 3.3% | | | | | 105 | | |
| AlSi9Cu3 | SLM | | | | | | | | | | |
| AlMg4,5Mn0,4 | SLM | | | | | | | | | | |
| AlSi12 | SLM | | | 2-3% | | | | | | | |
| AlSi10Mg | SLM | | | | | | | 177 (HV0, 3) | | | |
| Scalmalloy | SLM | | | 8% | | | | | | | |
| AlCu7 | EBF³ | | | 19% | | | | | | | |
| AlCu7 | EBF³ | | | 11% | | | | | | | |
| AlCu7 | wrought | | | 18% | | | | | | | |
| AlCu7 | wrought | | | 20% | | | | | | | |
| AlCu7 | wrought | | | 10% | | | | | | | |
| AlCu5Ni1.5CoSbZr | cast | | | 1% | | 90 | | | | | |
| AlSi10Mg | cast | | | 1% | | 90 | | | | | |
| AlSi10Mg | DMLS | | | 11% | | 97 | | | | | |
| Scalmalloy | DMLS | | | 8% | | 168 | | | | | |
| Al + SiC | DMLS | | | 4% | | | | | | | |
| Al + SiC | DMLS | | | 1% | | 20 | | | | | |
| Al + SiC | DMLS | | | 2% | | 23 | | | | | |
| Titanium Alloys | | | | | | | | | | | |
| TiAl6V4 | SLM | 30 | ±10 | 30 | ±10 | | | | 384 | ±5 | |
| TiAl6Nb7 | SLM | | | | | | | | 360 | | |
| Ti | SLM | | | | | | | | 130-210 | | |
| EOS Ti64 | DMLS | | | 11 | ±2 | | | 400-430 | | | 41-44 |
| EOS Ti64 ELI | DMLS | 7 | ±3 | 9 | ±3 | | | | | | |
| EOS Ti64 ELI | DMLS | 13 | ±3, min 10 | 15 | ±4, min 10 | | | | | | |

| | | | | | | | | | | | |
|---|---|---|---|---|---|---|---|---|---|---|---|
| Grade 2 Ti | EBM | 21 | | 55 | | | | | | | |
| Grade 2 Ti | Cast | >20 | | >30 | | | | | | | |
| TIAl6V4 ELI | EBM | 16 | | 50 | | | | | | | 32 |
| TIAl6V4 ELI | Cast | >10 | | >25 | | | | | | | 30-35 |
| TiAl6V4 | EBM | | | | | | | | | | 33 |
| TiAl6V4 | Cast | | | | | | | | | | |
| TiAl6V4 | wrought | | | | | | | | | | |
| TIAl6V4 ELI | EBF³ | | | 9 | | | | | | | |
| TiAl6V4 | | | | 4 | | | | | | | |
| TiAl6V4 | | | | | | | | | | | |
| TiAl6V6 | EBM | | | | | | | | | | |
| TiAl6V6 | wrought | | | | | | | | | | |
| TiAl6V6 | EBM | | | 15 | ±2 | | | | | | |
| Steels | | | | | | | | | | | |
| EOS Stainless Steel GP1 | DMLS | | | 25 | ±5 | | | 230 +-20 (250-400 polished) | | | |
| EOS Stainless Steel PH1 | DMLS | 16 | ±4 ±2, min | 17 | ±4 ±2, min | | | | | | 30-35 min |
| EOS Stainless Steel PH1 | DMLS | 12 | 10 | 12 | 10 | | | | | | 40 |
| EOS Maraging Steel MS1 | DMLS | | | 8 | ±3 | | | | | | 33-37 |
| EOS Maraging Steel MS1 | DMLS | | | 2 | ±1 | | | | | | 50-54 |
| 12.709 | SLM | | | 10 | ±1 | | | | 310 | ±4 | |
| 1.4404 (316L) | SLM | | | 35 | ±4 | | | | 233 | ±2 | |
| 1.2344 (H13) | SLM | | | | | | | | | | |
| 1.4540 (15-5PH) | SLM | | | 16 | ±4 | | | | | | |
| 1.4542 (15-5PH) | SLM | | | | | | | | | | |
| 1.2344 (H13) | MPA | | | | | | | | | | 42-55 |
| 12.367 | MPA | | | | | | | | | | 35-53 |
| 1.4404 (316L) | MPA | | | | | <200 | | | | | |
| 17-4HP | SLM | | | | | | | 300 | | | |
| 17-4HP | DMLS | | | | | | | 250 | | | |
| 17-4HP | wrought | | | | | | | 230 | | | |
| Titanium Aluminide | | | | | | | | | | | |
| | EBM | | | | | | | | | | |

| | | | | | | | | | | | |
|---|---|---|---|---|---|---|---|---|---|---|---|
| Nickel Alloys | | | | | | | | | | | |
| EOS Ni HX | DMLS | 29 | ±8 | 39 | ±8 | | | | | | |
| EOS Ni HX | DMLS | 45 | ±6 | 52 | ±6 | 175 | | | | | |
| EOS Ni IN718 | DMLS | | | 31 | ±3 | 287 | | | | | 30 |
| EOS Ni IN718 | DMLS | | | 15 | ±3, min 12 | 446 | | | | | 47 |
| EOS Ni IN718 | DMLS | | | 18 | 12 | 400 | | | | | 43 |
| EOS Ni IN625 | DMLS | 35 | ±5 | 42 | ±5 | | | | | | |
| EOS Ni IN625 | DMLS | 35 | ±5, min 30 | 44 | ±5, min 30 | 287 | | | | | 30 |
| Hastelloy X | SLM | 20 | ±6 | 21 | ±7 | | | | 284 | ±4 | |
| Inconel 625 | SLM | 33 | ±2 | 51 | ±5 | | | | 285 | ±7 | |
| Inconel 718 | SLM | 29 | ±4 | 47 | ±4 | | | | 306 | ±7 | |
| Inconel 939 | SLM | 30 | ±4 | 45 | ±7 | | | | 302 | ±3 | |
| Inconel 738 | SLM | | | | | | | | | | |
| Inconel 939 | SLM | 24 | | 21 | | | | | | | |
| Inconel 939 | SLM | | | | | | | | | | |
| Inconel 939 | Cast | | | | | | | | | | |
| Cobalt-Chrome | | | | | | | | | | | |
| EOS CoCr MP1 | DMLS | | | | | | | | | | |
| CoCr | SLM | | | | | | | | 345 | | |
| ASTFM F75 | EBM | | | | | | | | | | 47 |
| ASTFM F75 | EBM | | | 20 | | | | | | | 34 |
| Others | | | | | | | | | | | |
| Elektron MAP+43 | DED | 7,9 | ±1.6 | 6,3 | ±1.7 | | | | | | |
| | SLM | | | | | | | | | | |
| | cast | | | 6 | | | | | | | |
| Copper | EBM | | | | | | | | | | |
| | wrought | | | | | | | | | | |

| Materials | | Mechanical Properties | | | | | | |
|---|---|---|---|---|---|---|---|---|
| Materials | Process | young Modulus [Gpa] | | | | Fatigue Strength | | |
| | | Hori-zontal | Vari-ation | Verti-cal | Vari-ation | 30000000 cycles, kt=1, R=0.1 [MPA] | Vertical (50Hz, 5 Mio Cycles, R=-1) | Rotating Beam, 600MPa |
| Aluminum Alloys | | | | | | | | |
| EOS Aluminum AlSi10Mg | DMLS | | | | | | 97+-7 | |
| EOS Aluminum AlSi10Mg | DMLS | | | | | | 93+-3 | |
| EOS Aluminum AlSi10Mg (200°C) | DMLS | 70 | | 70 | | | | |
| AlSi12 | SLM | | | | | | | |
| AlSi10Mg | SLM | | | 64 | ±10 | | | |
| AlSi7Mg | SLM | | | | | | | |
| AlSi9Cu3 | SLM | | | | | | | |
| AlMg4,5Mn0,4 | SLM | | | | | | | |
| AlSi12 | SLM | | | 75 | | | | |
| AlSi10Mg | SLM | | | | | | | |
| Scalmalloy | SLM | | | 65 | | 300 | | |
| AlCu7 | EBF³ | | | | | | | |
| AlCu7 | EBF³ | | | | | | | |
| AlCu7 | wrought | | | | | | | |
| AlCu7 | wrought | | | | | | | |
| AlCu7 | wrought | | | | | | | |
| AlCu5Ni1.5CoSbZr | cast | | | 70 | | | | |
| AlSi10Mg | cast | | | 74 | | 90 | | |
| AlSi10Mg | DMLS | | | 60 | | | | |
| Scalmalloy | DMLS | | | 65 | | 300 | | |
| Al + SiC | DMLS | | | 103 | | | | |
| Al + SiC | DMLS | | | 140 | | 270 | | |
| Al + SiC | DMLS | | | 100 | | 300 | | |
| Titanium Alloys | | | | | | | | |
| TiAl6V4 | SLM | | | 111 | ±4 | | | |
| TiAl6Nb7 | SLM | | | | | | | |
| Ti | SLM | | | 105 | | | | |
| EOS Ti64 | DMLS | | | 110 | ±7 | | | |
| EOS Ti64 ELI | DMLS | 108 | ±20 | 112 | ±13 | | | |
| EOS Ti64 ELI | DMLS | 111 | ±20 | 115 | ±20 | | | |
| Grade 2 Ti | EBM | | | | | | | |
| Grade 2 Ti | Cast | | | | | | | |
| TIAl6V4 ELI | EBM | | | 120 | | | | >1000000 cycles |

| | | | | | | | | |
|---|---|---|---|---|---|---|---|---|
| TIAl6V4 ELI | Cast | | | 114 | | | | |
| TiAl6V4 | EBM | | | 120 | | | | >100000 0 cycles |
| TiAl6V4 | Cast | | | | | | | |
| TiAl6V4 | Wrought | | | | | | | |
| TIAl6V4 ELI | EBF[3] | | | | | | | |
| TiAl6V4 | | | | | | | | |
| TiAl6V4 | | | | | | | | |
| TiAl6V6 | EBM | | | | | | | |
| TiAl6V6 | Wrought | | | | | | | |
| TiAl6V6 | EBM | | | | | | | |
| Steels | | | | | | | | |
| EOS Stainless Steel GP1 | DMLS | | | 195 | | | | |
| EOS Stainless Steel PH1 | DMLS | | | | | | | |
| EOS Stainless Steel PH1 | DMLS | | | | | | | |
| EOS Maraging Steel MS1 | DMLS | | | 180 | ±20 | | | |
| EOS Maraging Steel MS1 | DMLS | | | 180 | ±20 | | | |
| 12.709 | SLM | | | | | | | |
| 1.4404 (316L) | SLM | | | | | | | |
| 1.2344 (H13) | SLM | | | | | | | |
| 1.4540 (15-5PH) | SLM | | | | | | | |
| 1.4542 (15-5PH) | SLM | | | | | | | |
| 1.2344 (H13) | MPA | | | | | | | |
| 12.367 | MPA | | | | | | | |
| 1.4404 (316L) | MPA | | | | | | | |
| 17-4HP | SLM | | | | | | | |
| 17-4HP | DMLS | | | | | | | |
| 17-4HP | wrought | | | | | | | |
| Titanium Aluminide | | | | | | | | |
| | EBM | | | | | | | |
| Nickel Alloys | | | | | | | | |
| EOS Ni HX | DMLS | 195 | ±20 | 175 | ±20 | | | |
| EOS Ni HX | DMLS | 200 | ±20 | 192 | ±20 | | | |
| EOS Ni IN718 | DMLS | | | | | | | |
| EOS Ni IN718 | DMLS | | | 170 | ±20 | | | |
| EOS Ni IN718 | DMLS | | | 170 | ±20 | | | |
| EOS Ni IN625 | DMLS | 170 | ±20 | 140 | ±20 | | | |

| | | | | | | | | |
|---|---|---|---|---|---|---|---|---|
| EOS Ni IN625 | DMLS | 170 | ±20 | 160 | ±20 | | | |
| Hastelloy X | SLM | | | 162 | ±11 | | | |
| Inconel 625 | SLM | | | 182 | ±9 | | | |
| Inconel 718 | SLM | | | 173 | ±17 | | | |
| Inconel 939 | SLM | | | 177 | ±8 | | | |
| Inconel 738 | SLM | | | | | | | |
| Inconel 939 | SLM | 176 | | 181 | ±7 | | | |
| Inconel 939 | SLM | | | 215 | ±10 | | | |
| Inconel 939 | Cast | | | 200 | ±7 | | | |
| Cobald-Chrome | | | | | | | | |
| EOS CoCr MP1 | DMLS | | | | | | | |
| CoCr | SLM | | | | | | | |
| ASTFM F75 | EBM | | | | | | | |
| ASTFM F75 | EBM | | | | | | | >10000000 cycles |
| Others | | | | | | | | |
| Elektron MAP+43 | DED | | | | | | | |
| | SLM | | | | | | | |
| | cast | | | | | | | |
| Copper | EBM | | | | | | | |
| | wrought | | | | | | | |

| Materials | | Mechanical Properties at 649°C | | | | |
|---|---|---|---|---|---|---|
| Materials | Process | Ultimate tensile Strength | Yield Strength | Elongation at Break | Stress rupture | |
| | | [Mpa] | [Mpa] | [Mpa] | 689 MPA | *34,5MPA /8h |
| Aluminum Alloys | | | | | | |
| EOS Aluminum AlSi10Mg | DMLS | | | | | |
| EOS Aluminum AlSi10Mg | DMLS | | | | | |
| EOS Aluminum AlSi10Mg (200°C) | DMLS | | | | | |
| AlSi12 | SLM | | | | | |
| AlSi10Mg | SLM | | | | | |
| AlSi7Mg | SLM | | | | | |
| AlSi9Cu3 | SLM | | | | | |
| AlMg4,5Mn0,4 | SLM | | | | | |
| AlSi12 | SLM | | | | | |
| AlSi10Mg | SLM | | | | | |
| Scalmalloy | SLM | | | | | |

| | | | | | | |
|---|---|---|---|---|---|---|
| AlCu7 | EBF³ | | | | | |
| AlCu7 | EBF³ | | | | | |
| AlCu7 | wrought | | | | | |
| AlCu7 | wrought | | | | | |
| AlCu7 | wrought | | | | | |
| AlCu5Ni1.5CoSbZr | cast | 120 (at 250°C) | 140 (at 250°C) | | | |
| AlSi10Mg | cast | 75 (at 250°C) | 60 (at 250°C) | | | |
| AlSi10Mg | DMLS | 270 (at 250°C) | | | | |
| Scalmalloy | DMLS | 290 (at 250°C) | | | | |
| Al + SiC | DMLS | | | | | |
| Al + SiC | DMLS | 279 (at 250°C) | 230 (at 250°C) | | | |
| Al + SiC | DMLS | 290 (at 250°C) | 250 (at 250°C) | | | |
| | | | | | | |
| Titanium Alloys | | | | | | |
| TiAl6V4 | SLM | | | | | |
| TiAl6Nb7 | SLM | | | | | |
| Ti | SLM | | | | | |
| EOS Ti64 | DMLS | | | | | |
| EOS Ti64 ELI | DMLS | | | | | |
| EOS Ti64 ELI | DMLS | | | | | |
| Grade 2 Ti | EBM | | | | | |
| Grade 2 Ti | Cast | | | | | |
| TIAl6V4 ELI | EBM | | | | | |
| TIAl6V4 ELI | Cast | | | | | |
| TiAl6V4 | EBM | | | | | |
| TiAl6V4 | Cast | | | | | |
| TiAl6V4 | Wrought | | | | | |
| TIAl6V4 ELI | EBF³ | | | | | |
| TiAl6V4 | | | | | | |
| TiAl6V4 | | | | | | |
| TiAl6V6 | EBM | | | | | |
| TiAl6V6 | Wrought | | | | | |
| TiAl6V6 | EBM | | | | | |
| | | | | | | |
| Steels | | | | | | |
| EOS Stainless Steel GP1 | DMLS | | | | | |
| EOS Stainless Steel PH1 | DMLS | | | | | |
| EOS Stainless Steel PH1 | DMLS | | | | | |
| EOS Maraging Steel MS1 | DMLS | | | | | |
| EOS Maraging Steel MS1 | DMLS | | | | | |

| | | | | | | |
|---|---|---|---|---|---|---|
| 12.709 | SLM | | | | | |
| 1.4404 (316L) | SLM | | | | | |
| 1.2344 (H13) | SLM | | | | | |
| 1.4540 (15-5PH) | SLM | | | | | |
| 1.4542 (15-5PH) | SLM | | | | | |
| 1.2344 (H13) | MPA | | | | | |
| 12.367 | MPA | | | | | |
| 1.4404 (316L) | MPA | | | | | |
| 17-4HP | SLM | | | | | |
| 17-4HP | DMLS | | | | | |
| 17-4HP | wrought | | | | | |
| Titanium Aluminide | | | | | | |
| | EBM | | | | | |
| Nickel Alloys | | | | | | |
| EOS Ni HX | DMLS | | | | | |
| EOS Ni HX | DMLS | | | | | |
| EOS Ni IN718 | DMLS | | | | | |
| EOS Ni IN718 | DMLS | 1170+-50, min 965 | 970+-50, min 862 | 16+-3, min 6 | min 23 | 51+-5 |
| EOS Ni IN718 | DMLS | 1210+-50 | 1010+-50 | 20+-3 | | 81+-10 |
| EOS Ni IN625 | DMLS | | | | | |
| EOS Ni IN625 | DMLS | | | | | |
| Hastelloy X | SLM | | | | | |
| Inconel 625 | SLM | | | | | |
| Inconel 718 | SLM | | | | | |
| Inconel 939 | SLM | | | | | |
| Inconel 738 | SLM | | | | | |
| Inconel 939 | SLM | | | | | |
| Inconel 939 | SLM | | | | | |
| Inconel 939 | Cast | | | | | |
| Cobalt-Chrome | | | | | | |
| EOS CoCr MP1 | DMLS | | | | | |
| CoCr | SLM | | | | | |
| ASTFM F75 | EBM | | | | | |
| ASTFM F75 | EBM | | | | | |
| Others | | | | | | |
| Elektron MAP+43 | DED | | | | | |
| | SLM | | | | | |
| | cast | | | | | |

| | | | | | | |
|---|---|---|---|---|---|---|
| Copper | EBM wrought | | | | | |

| Materials | | thermal properties | | | | | | | |
|---|---|---|---|---|---|---|---|---|---|
| Materials | Process | max long term temp [°C] | thermal expansion coef. [m/m°C] | | spez. Heat capacity [J/kg°C] | Thermal Contuctivity [W/m°C] | | | |
| | | [°C] | 20 - 600°C | 20-200°C | | 20°C | 100 | 200 | 300 |
| Aluminum Alloys | | | | | | | | | |
| EOS Aluminum AlSi10Mg | DMLS | | | | | | | | |
| EOS Aluminum AlSi10Mg | DMLS | | | | | | | | |
| EOS Aluminum AlSi10Mg (200°C) | DMLS | | | | | | | | |
| AlSi12 | SLM | | | | | | | | |
| AlSi10Mg | SLM | | | | | | | | |
| AlSi7Mg | SLM | | | | | | | | |
| AlSi9Cu3 | SLM | | | | | | | | |
| AlMg4,5Mn0,4 | SLM | | | | | | | | |
| AlSi12 | SLM | | 20*10^-6 K^-1 | | | 120-180 | | | |
| AlSi10Mg | SLM | | | | | | | | |
| Scalmalloy | SLM | | | | | | | | |
| AlCu7 | EBF³ | | | | | | | | |
| AlCu7 | EBF³ | | | | | | | | |
| AlCu7 | wrought | | | | | | | | |
| AlCu7 | wrought | | | | | | | | |
| AlCu7 | wrought | | | | | | | | |
| AlCu5Ni1.5CoSbZr | cast | | | | | 150 | | | |
| AlSi10Mg | cast | | | | | 160 | | | |
| AlSi10Mg | DMLS | | | | | 170 | | | |
| Scalmalloy | DMLS | | | | | 122 | | | |
| Al + SiC | DMLS | | | | | 150 | | | |
| Al + SiC | DMLS | | | | | 130 | | | |
| Al + SiC | DMLS | | | | | 155 | | | |
| Titanium Alloys | | | | | | | | | |
| TiAl6V4 | SLM | | | | | | | | |
| TiAl6Nb7 | SLM | | | | | | | | |
| Ti | SLM | | | | | | | | |
| EOS Ti64 | DMLS | 350 | | | | | | | |
| EOS Ti64 ELI | DMLS | 350 | | | | | | | |

| | | | | | | | | | |
|---|---|---|---|---|---|---|---|---|---|
| EOS Ti64 ELI | DMLS | 350 | | | | | | | |
| Grade 2 Ti | EBM | | | | | | | | |
| Grade 2 Ti | Cast | | | | | | | | |
| TIAl6V4 ELI | EBM | | | | | | | | |
| TIAl6V4 ELI | Cast | | | | | | | | |
| TiAl6V4 | EBM | | | | | | | | |
| TiAl6V4 | Cast | | | | | | | | |
| TiAl6V4 | wrought | | | | | | | | |
| TIAl6V4 ELI | EBF³ | | | | | | | | |
| TiAl6V4 | | | | | | | | | |
| TiAl6V4 | | | | | | | | | |
| TiAl6V6 | EBM | | | | | | | | |
| TiAl6V6 | wrought | | | | | | | | |
| TiAl6V6 | EBM | | | | | | | | |
| Steels | | | | | | | | | |
| EOS Stainless Steel GP1 | DMLS | 550 | 14*10^-6 | | | 13 | 14 | 15 | 16 |
| EOS Stainless Steel PH1 | DMLS | | | | 460+-20 | 13,8+-0.8 | | | |
| EOS Stainless Steel PH1 | DMLS | | | | 470+-20 | 15.8+-0.8 | | | |
| EOS Maraging Steel MS1 | DMLS | 400 | | | 450+-20 | 15+-0.8 | | | |
| EOS Maraging Steel MS1 | DMLS | 400 | | | 450+-20 | 20+-1 | | | |
| 12.709 | SLM | | | | | | | | |
| 1.4404 (316L) | SLM | | | | | | | | |
| 1.2344 (H13) | SLM | | | | | | | | |
| 1.4540 (15-5PH) | SLM | | | | | | | | |
| 1.4542 (15-5PH) | SLM | | | | | | | | |
| 1.2344 (H13) | MPA | | | | | | | | |
| 12.367 | MPA | | | | | | | | |
| 1.4404 (316L) | MPA | | | | | | | | |
| 17-4HP | SLM | | | | | | | | |
| 17-4HP | DMLS | | | | | | | | |
| 17-4HP | wrought | | | | | | | | |
| Titanium Aluminide | | | | | | | | | |
| | EBM | | | | | | | | |
| Nickel Alloys | | | | | | | | | |
| EOS Ni HX | DMLS | | | | | | | | |
| EOS Ni HX | DMLS | | | | | | | | |

| | | | | | | | | | |
|---|---|---|---|---|---|---|---|---|---|
| EOS Ni IN718 | DMLS | 650 under load, 980 oxidation resictance | 16.6-17.2*10^-6 | 12.5-13.0*10^-6 | | | | | |
| EOS Ni IN718 | DMLS | | | | | | | | |
| EOS Ni IN718 | DMLS | | | | | | | | |
| EOS Ni IN625 | DMLS | 650 under load, 980 oxidation resictance | | | | | | | |
| EOS Ni IN625 | DMLS | | | | | | | | |
| Hastelloy X | SLM | | | | | | | | |
| Inconel 625 | SLM | | | | | | | | |
| Inconel 718 | SLM | | | | | | | | |
| Inconel 939 | SLM | | | | | | | | |
| Inconel 738 | SLM | | | | | | | | |
| Inconel 939 | SLM | | | | | | | | |
| Inconel 939 | SLM | | | | | | | | |
| Inconel 939 | Cast | | | | | | | | |
| Cobalt-Chrome | | | | | | | | | |
| EOS CoCr MP1 | DMLS | | | | | | | | |
| CoCr | SLM | | | | | | | | |
| ASTFM F75 | EBM | | | | | | | | |
| ASTFM F75 | EBM | | | | | | | | |
| Others | | | | | | | | | |
| Elektron MAP+43 | DED | | | | | | | | |
| | SLM | | | | | | | | |
| | cast | | | | | | | | |
| Copper | EBM | | | | | | 390 | | |
| | wrought | | | | | | 391 | | |

| Materials | | Process Data | | | | | | | | | |
|---|---|---|---|---|---|---|---|---|---|---|---|
| Materials | Process | Dens-ity | min layer [µm] | min. wall [mm] | surface as build [µm] | | | surface shot-peening [µm] | | Toler-ances | |
| | | | | | Ra | Rz | Vari-ation | Ra | Rz | small parts | large parts |
| Aluminum Alloys | | | | | | | | | | | |
| EOS Aluminum AlSi10Mg | DMLS | 100% | 30 | 0.3-0.4 | 15-19 | 96-115 | | 7-10 µm | 50-60 | | |

| | | | | | | | | | | | |
|---|---|---|---|---|---|---|---|---|---|---|---|
| EOS Aluminum AlSi10Mg | DMLS | 100% | 30 | 0.3-0.4 | 15-19 | 96-115 | | 7-10 µm | 50-60 | | |
| EOS Aluminum AlSi10Mg (200°C) | DMLS | 100% | | 0.4-1 (Surface) | 4-8 | 20-40 | | 5-9 µm | 28-60 | | |
| AlSi12 | SLM | | | | | 34 | ±4 | | | | |
| AlSi10Mg | SLM | | | | | | | | | | |
| AlSi7Mg | SLM | | | | | 31 | | | | | |
| AlSi9Cu3 | SLM | | | | | | | | | | |
| AlMg4,5Mn0,4 | SLM | | | | | | | | | | |
| AlSi12 | SLM | | | | | | | | | | |
| AlSi10Mg | SLM | | | | | | | | | | |
| Scalmalloy | SLM | | | | | | | | | | |
| AlCu7 | EBF³ | | | | | | | | | | |
| AlCu7 | EBF³ | | | | | | | | | | |
| AlCu7 | wrought | | | | | | | | | | |
| AlCu7 | wrought | | | | | | | | | | |
| AlCu7 | wrought | | | | | | | | | | |
| AlCu5Ni1.5CoSbZr | cast | | | | | | | | | | |
| AlSi10Mg | cast | | | | | | | | | | |
| AlSi10Mg | DMLS | | | | | | | | | | |
| Scalmalloy | DMLS | | | | | | | | | | |
| Al + SiC | DMLS | | | | | | | | | | |
| Al + SiC | DMLS | | | | | | | | | | |
| Al + SiC | DMLS | | | | | | | | | | |
| **Titanium Alloys** | | | | | | | | | | | |
| TiAl6V4 | SLM | | | | | 36 | ±4 | | | | |
| TiAl6Nb7 | SLM | | | | | 36 | ±4 | | | | |
| Ti | SLM | | | | | 36 | ±4 | | | | |
| EOS Ti64 | DMLS | 100% | 30 | 0.3-0.4 | 9-16 µm | 40 -80 | | | | | |
| EOS Ti64 ELI | DMLS | 100% | 50 | 0.3-0.4 | 13-20 µm | 16 - 126 | | 4-9 µm | 22-56 | | |
| EOS Ti64 ELI | DMLS | 100% | 50 | 0.3-0.4 | 13-20 µm | 16 - 126 | | 4-9 µm | 22-56 | | |
| Grade 2 Ti | EBM | | | | | | | | | | |
| Grade 2 Ti | Cast | | | | | | | | | | |
| TIAl6V4 ELI | EBM | | | | | | | | | | |
| TIAl6V4 ELI | Cast | | | | | | | | | | |
| TiAl6V4 | EBM | | | | | | | | | | |
| TiAl6V4 | Cast | | | | | | | | | | |

| | | | | | | | | | | | |
|---|---|---|---|---|---|---|---|---|---|---|---|
| TiAl6V4 | Wrought | | | | | | | | | | |
| TIAl6V4 ELI | EBF[3] | | | | | | | | | | |
| TiAl6V4 | | | | | | | | | | | |
| TiAl6V4 | | | | | | | | | | | |
| TiAl6V6 | EBM | | | | | | | | | | |
| TiAl6V6 | Wrought | | | | | | | | | | |
| TiAl6V6 | EBM | | | | | | | | | | |
| Steels | | | | | | | | | | | |
| EOS Stainless Steel GP1 | DMLS | 100% | 20 | 0.3-0.4 | | | | 2.5-.4.5 | 15-45 (<0.5 polished) | (+-) 20 - 50 µm | 0.2% |
| EOS Stainless Steel PH1 | DMLS | 100% | 20 | 0.3-0.4 | | | | 2.5-.4.5 | 15-45 (<0.5 polished) | (+-) 20 - 50 µm | 0.2% |
| EOS Stainless Steel PH1 | DMLS | 100% | 20 | 0.3-0.4 | | | | 2.5-.4.5 | 15-45 (<0.5 polished) | (+-) 20 - 50 µm | 0.2% |
| EOS Maraging Steel MS1 | DMLS | 100 | 40 | 0.3-0.4 | | | | 4.0-6.5 | 20-50 (<0.5 polished) | | |
| EOS Maraging Steel MS1 | DMLS | 100% | 40 | 0.3-0.4 | | | | 4.0-6.5 | 20-50 (<0.5 polished) | | |
| 12.709 | SLM | | | | 7 | 39 | ±8 | | | | |
| 1.4404 (316L) | SLM | | | | 8 | 40 | ±11 | | | | |
| 1.2344 (H13) | SLM | | | | | 34 | ±4 | | | | |
| 1.4540 (15-5PH) | SLM | | | | | 14 | ±2 | | | | |
| 1.4542 (15-5PH) | SLM | | | | | | | | | | |
| 1.2344 (H13) | MPA | 100 | | | | | | | | | |
| 12.367 | MPA | | | | | | | | | | |
| 1.4404 (316L) | MPA | | | | | | | | | | |
| 17-4HP | SLM | | | | | | | | | | |
| 17-4HP | DMLS | | | | | | | | | | |
| 17-4HP | wrought | | | | | | | | | | |
| Titanium Aluminide | | | | | | | | | | | |
| | EBM | | | | | | | | | | |

| | | | | | | | | | | | |
|---|---|---|---|---|---|---|---|---|---|---|---|
| Nickel Alloys | | | | | | | | | | | |
| EOS Ni HX | DMLS | 100 | | 0.3-0.4 | | | | 3.0-8.0 | 13-40 (<0.5 polished) | 40-60 | 0.2% |
| EOS Ni HX | DMLS | 100 | | 0.3-0.4 | | | | 3.0-8.0 | 13-40 (<0.5 polished) | 40-60 | 0.2% |
| EOS Ni IN718 | DMLS | 100 | 20 | 0.3-0.4 | | | | 4.0-6.5 | 20-50 (<0.5 polished) | 40-60 | 0.2% |
| EOS Ni IN718 | DMLS | 100 | 20 | 0.3-0.4 | | | | 4.0-6.5 | 20-50 (<0.5 polished) | 40-60 | 0.2% |
| EOS Ni IN718 | DMLS | 100 | 20 | 0.3-0.4 | | | | 4.0-6.5 | 20-50 (<0.5 polished) | 40-60 | 0.2% |
| EOS Ni IN625 | DMLS | 100 | | | | | | 4.0-6.5 | 20-50 (<0.5 polished) | 40-60 | 0.2% |
| EOS Ni IN625 | DMLS | 100 | | | | | | 4.0-6.5 | 20-50 (<0.5 polished) | 40-60 | 0.2% |
| Hastelloy X | SLM | | | | 8 | 40 | ±14 | | | | |
| Inconel 625 | SLM | | | | | 28 | | | | | |
| Inconel 718 | SLM | | | | 6 | 34 | ±10 | | | | |
| Inconel 939 | SLM | | | | | | | | | | |
| Inconel 738 | SLM | | | | | | | | | | |
| Inconel 939 | SLM | | | | | | | | | | |
| Inconel 939 | SLM | | | | | | | | | | |
| Inconel 939 | Cast | | | | | | | | | | |
| Cobald-Chrome | | | | | | | | | | | |
| EOS CoCr MP1 | DMLS | | | | | | | | | | |
| CoCr | SLM | | | | | 29 | ±4 | | | | |
| ASTFM F75 | EBM | | | | | | | | | | |
| ASTFM F75 | EBM | | | | | | | | | | |

| | | | | | | | | | | | |
|---|---|---|---|---|---|---|---|---|---|---|---|
| Others | | | | | | | | | | | |
| Elektron MAP+43<br><br><br><br>Copper | DED<br>SLM<br>cast<br>EBM<br>wrought | | | | | | | | | | |

## 10.2 Reports CFD Simulation

### 10.2.1 First Run

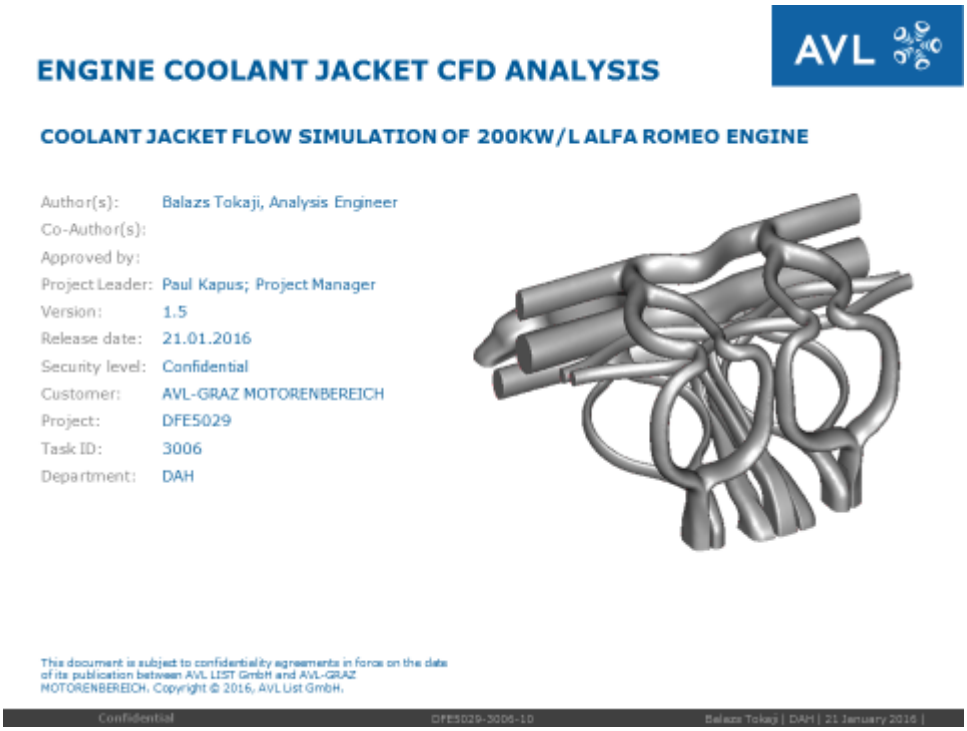

ENGINE COOLANT JACKET CFD ANALYSIS

AVL

COOLANT JACKET FLOW SIMULATION OF 200KW/L ALFA ROMEO ENGINE

Author(s): Balazs Tokaji, Analysis Engineer
Co-Author(s):
Approved by:
Project Leader: Paul Kapus; Project Manager
Version: 1.5
Release date: 21.01.2016
Security level: Confidential
Customer: AVL-GRAZ MOTORENBEREICH
Project: DFE5029
Task ID: 3006
Department: DAH

## TABLE OF CONTENT





## ANALYSIS MODEL

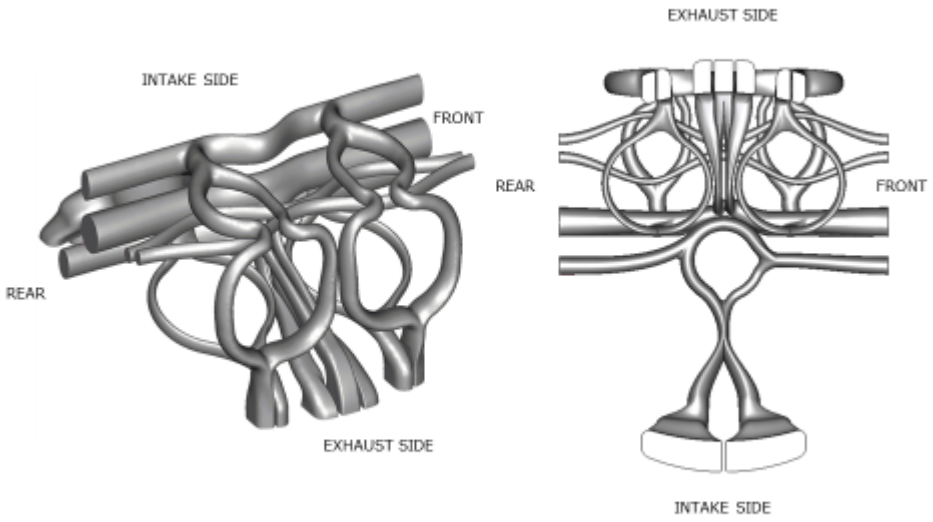

## ANALYSIS MODEL TARGET LEVEL

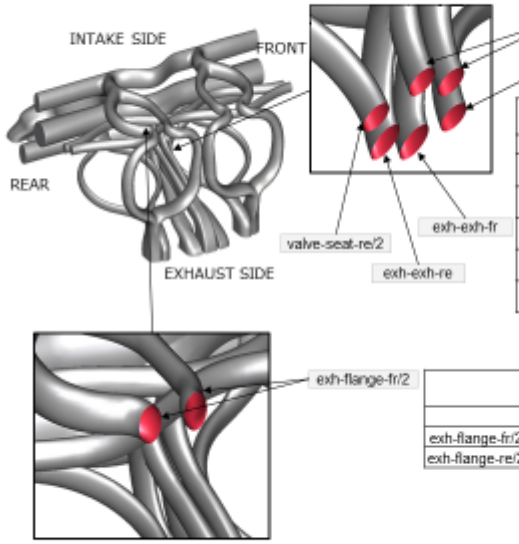


| | Cross-section | Velocity | Volume Flow | Volume Flow |
|---|---|---|---|---|
| | mm2 | m/s | m3/s | l/m |
| exh-exh-mid/2 | 6.24 | 7 | 4.37E-05 | 2.62 |
| valve-seat-fr/2 | 6.24 | 7 | 4.37E-05 | 2.62 |
| valve-seat-re/2 | 6.24 | 7 | 4.37E-05 | 2.62 |
| exh-exh-re | 7.79 | 7 | 5.45E-05 | 3.27 |
| exh-exh-fr | 7.79 | 7 | 5.45E-05 | 3.27 |




| | Cross-section | Velocity | Volume Flow | Volume Flow |
|---|---|---|---|---|
| | mm2 | m/s | m3/s | l/m |
| exh-flange-fr/2 | 11.73 | 7 | 8.21E-05 | 4.93 |
| exh-flange-re/2 | 11.73 | 7 | 8.21E-05 | 4.93 |

Confidential DFE5029-3006-10 Belaza Tokaj | DAH | 21 January 2016 | 9

## ANALYSIS MODEL TARGET LEVEL

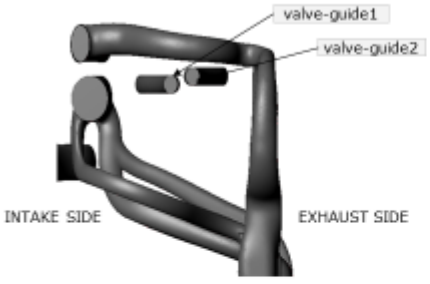


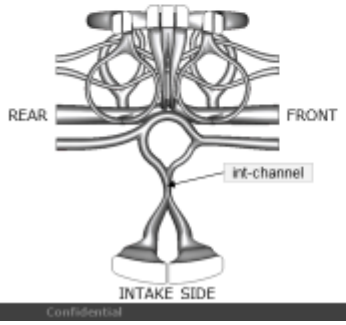


| | Cross-section | Velocity | Volume Flow | Volume Flow |
|---|---|---|---|---|
| | mm2 | m/s | m3/s | l/m |
| valve-guide1 | 8.84 | 5 | 4.42E-05 | 2.65 |
| valve-guide2 | 8.77 | 5 | 4.39E-05 | 2.63 |

| | Cross-section | Velocity | Volume Flow | Volume Flow |
|---|---|---|---|---|
| | mm2 | m/s | m3/s | l/m |
| int-channel | 19.24 | 5 | 9.62E-05 | 5.77 |

| TOTAL FLOW RATE Per Cylinder | | |
|---|---|---|
| valve-guide1 | 2.65 | l/m |
| valve-guide2 | 2.63 | l/m |
| exh-exh-mid | 5.24 | l/m |
| valve-seat-fr | 5.24 | l/m |
| valve-seat-re | 5.24 | l/m |
| exh-exh-re | 3.27 | l/m |
| exh-exh-fr | 3.27 | l/m |
| int-channel | 5.77 | l/m |
| exh-flange-fr | 9.85 | l/m |
| exh-flange-re | 9.85 | l/m |
| SUM | 53.03 | l/m |

Confidential DFE5029-3006-10 Belaza Tokaj | DAH | 21 January 2016 | 10

## ANALYSIS MODEL
## ESTIMATION BASED ON V52 RESULTS CYL1

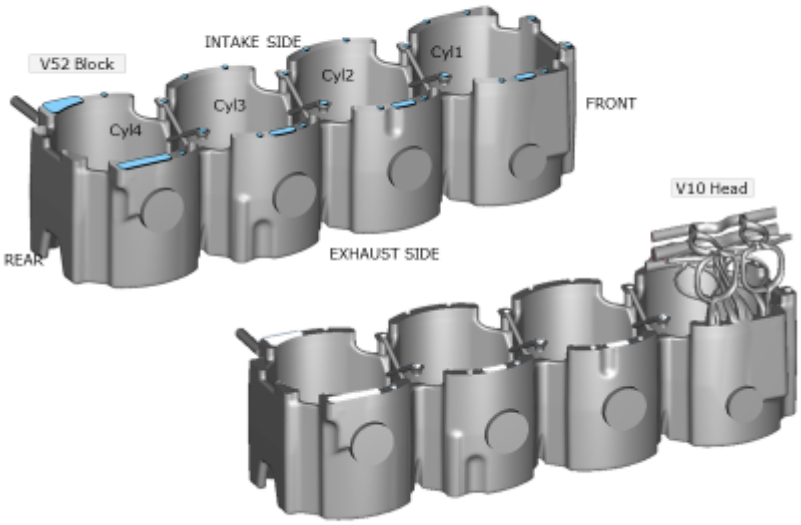




## ANALYSIS MODEL
## ESTIMATION BASED ON V52 RESULTS CYL1

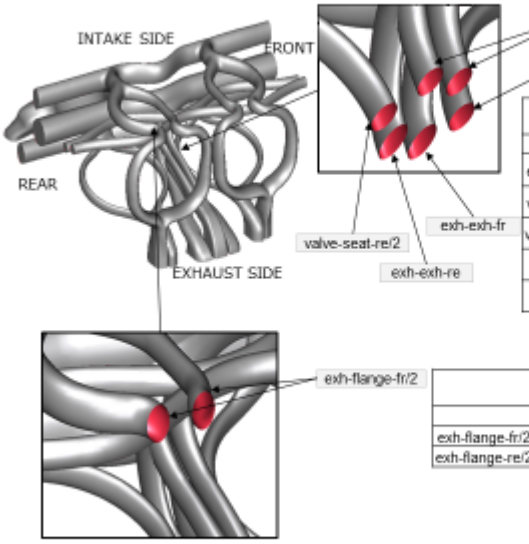


| | Cross-section | Velocity | Volume Flow |
|---|---|---|---|
| | mm2 | m/s | l/m |
| exh-exh-mid/2 | 6.24 | 13.29 | 4.98 |
| valve-seat-fr/2 | 6.24 | 3.95 | 1.48 |
| valve-seat-re/2 | 6.24 | 3.41 | 1.28 |
| exh-exh-re | 7.79 | 20.7 | 9.67 |
| exh-exh-fr | 7.79 | 20.7 | 9.67 |




| | Cross-section | Velocity | Volume Flow |
|---|---|---|---|
| | mm2 | m/s | l/m |
| exh-flange-fr/2 | 11.73 | 2.1 | 1.48 |
| exh-flange-re/2 | 11.73 | 1.78 | 1.25 |

## ANALYSIS MODEL
## ESTIMATION BASED ON V52 RESULTS CYL1

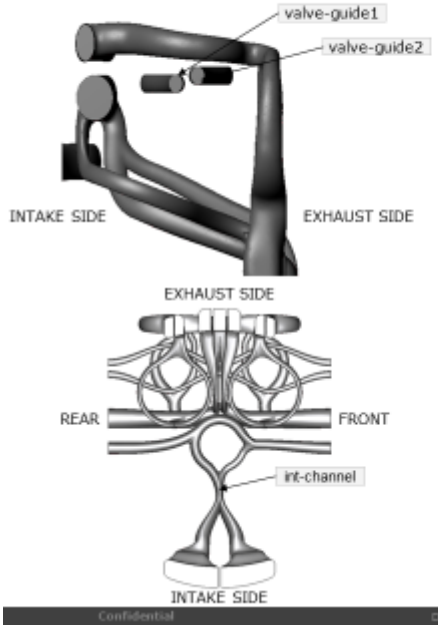


| | Cross-section | Velocity | Volume Flow |
|---|---|---|---|
| | mm2 | m/s | l/m |
| valve-guide1 | 8.84 | 9.9 | 5.8 |
| valve-guide2 | 8.77 | 9.98 | 4.7 |

| | Cross-section | Velocity | Volume Flow |
|---|---|---|---|
| | mm2 | m/s | l/m |
| int-channel | 19.24 | 9.81 | 11.3 |

| TOTAL FLOW RATE Per Cylinder | | |
|---|---|---|
| valve-guide1 | 5.8 | l/m |
| valve-guide2 | 4.7 | l/m |
| exh-exh-mid | 9.96 | l/m |
| valve-seat-fr | 2.96 | l/m |
| valve-seat-re | 2.56 | l/m |
| exh-exh-re | 9.67 | l/m |
| exh-exh-fr | 9.67 | l/m |
| int-channel | 11.3 | l/m |
| exh-flange-fr | 2.56 | l/m |
| exh-flange-re | 2.5 | l/m |
| SUM | 61.68 | l/m |

Confidential DFE5029-3006-10 Balazs Tokaji | DAH | 21 January 2016 | 13

## MATERIALS AND PROPERTIES

Coolant: Water / Glycol 50/50 [vol%]

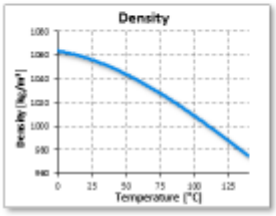


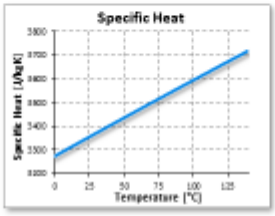


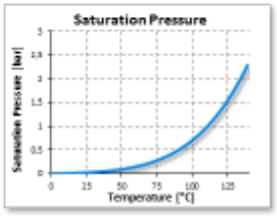


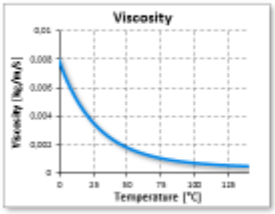


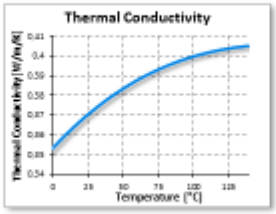


Validity range for absolute pressure:
0.5 - 6.0 bar (50 - 600 kPa)

Confidential DFE5029-3006-10 Balazs Tokaji | DAH | 21 January 2016 | 15

## LOADS AND CONSTRAINTS

| ID | Name | Type | Value | Unit | Value from | Value to | Source (doc,version) | Owner | Date |
|---|---|---|---|---|---|---|---|---|---|
| 1 | Volume flow rate of coolant pump | | 216 | l/min | | | DFE2106_7001-Input_data_summary.pptm | Susanna Neuhold | 12.05.2015 |
| 2 | Inlet coolant temperature to Head | | 92.7 | °C | | | Assumption | Balazs Tokaji | 20.01.2016 |
| 3 | Absolute pressure level at head out | | 2300 | mbar | | | Assumption | Balazs Tokaji | 20.01.2016 |
| 4 | Assumed wall temperature around valve seat rings | | 132.7 | °C | | | Assumption | Balazs Tokaji | 20.01.2016 |
| 5 | Assumed wall temperature on rest of the head | | 112.7 | °C | | | Assumption | Balazs Tokaji | 20.01.2016 |
| 6 | | | | | | | | | |
| 7 | | | | | | | | | |
| 8 | | | | | | | | | |
| 9 | | | | | | | | | |
| 10 | | | | | | | | | |
| 11 | | | | | | | | | |
| 12 | | | | | | | | | |
| 13 | | | | | | | | | |
| 14 | | | | | | | | | |
| 15 | | | | | | | | | |
| 16 | | | | | | | | | |
| 17 | | | | | | | | | |
| 18 | | | | | | | | | |
| 19 | | | | | | | | | |
| 20 | | | | | | | | | |
| 21 | Load | | | | | | | | |
| 22 | Boundary condition | | | | | | | | |
| 23 | Initial condition | | | | | | | | |
| 24 | | | | | | | | | |



## FLOW RATES IN HEAD TROUGH COLLECTOR RAILS

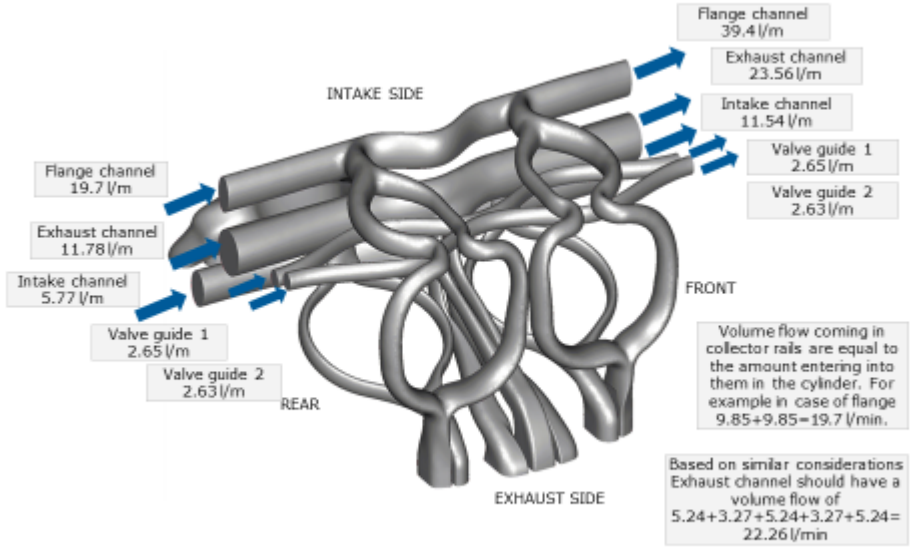


Volume flow coming in collector rails are equal to the amount entering into them in the cylinder. For example in case of flange 9.85+9.85=19.7 l/min.

Based on similar considerations Exhaust channel should have a volume flow of 5.24+3.27+5.24+3.27+5.24= 22.26 l/min

## FLOW RATES IN HEAD TROUGH GASKETS

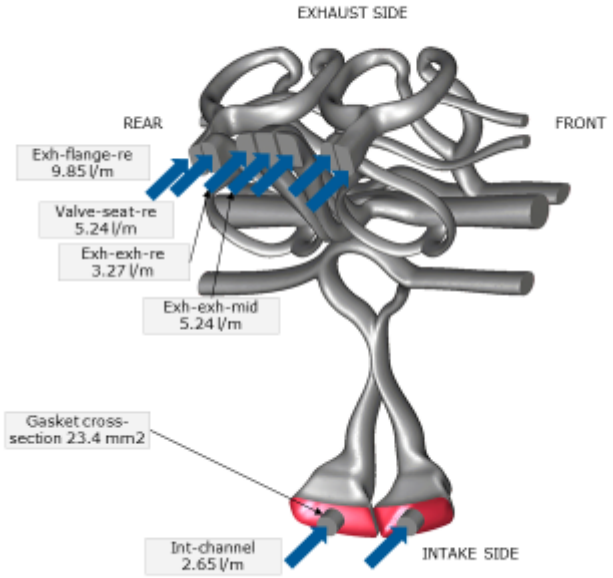


| Flow rates in head trough gasket openings | | |
|---|---|---|
| exh-exh-mid | 5.24 | l/m |
| valve-seat-fr | 5.24 | l/m |
| valve-seat-re | 5.24 | l/m |
| exh-exh-re | 3.27 | l/m |
| exh-exh-fr | 3.27 | l/m |
| int-channel | 5.77 | l/m |
| exh-flange-fr | 9.85 | l/m |
| exh-flange-re | 9.85 | l/m |



## TOTAL PRESSURE

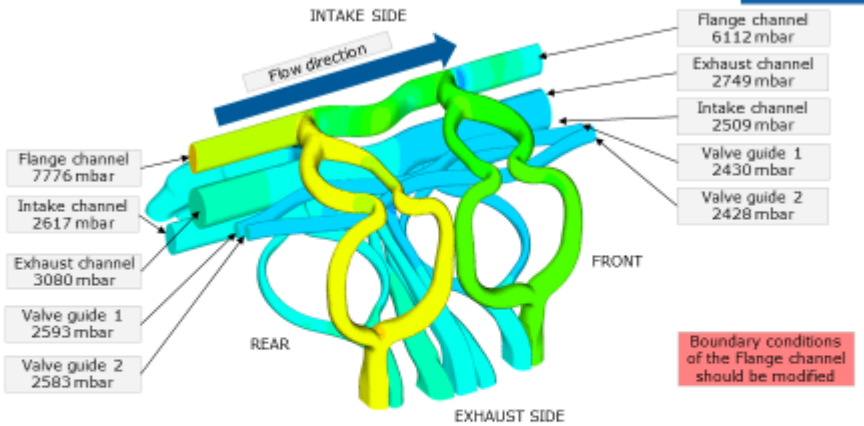


Boundary conditions of the Flange channel should be modified

| TOTAL Pressure loss Per Cylinder | | | | | | |
|---|---|---|---|---|---|---|
| name | Inlet | | Outlet | | Loss | |
| exh-exh-ch | 3080 | mbar | 2749 | mbar | 331 | mbar |
| int-ch | 2617 | mbar | 2509 | mbar | 108 | mbar |
| flange-ch | 7776 | mbar | 6112 | mbar | 1664 | mbar |
| valve-guide1 | 2593 | mbar | 2430 | mbar | 163 | mbar |
| valve-guide2 | 2583 | mbar | 2428 | mbar | 155 | mbar |

## HEAT TRANSFER COEFFICIENT

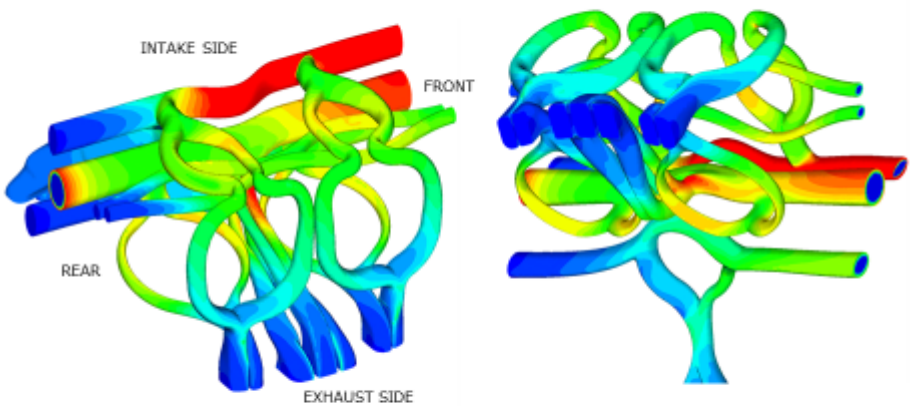


Good overall HTC level on the critical areas




## VELOCITY CONTOUR

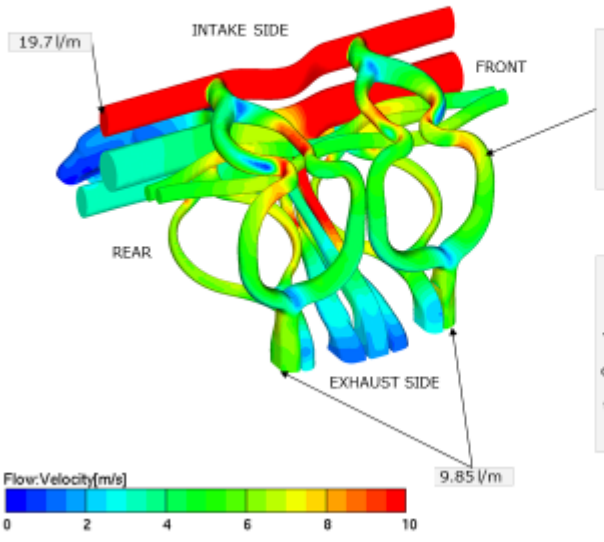


Velocities in the flange region can be decreased, therefore the overall volume flow in the flange channel would decrease. Alternatievely the cross section of the flange collector rail can be increased.

Exhaust channel has an inlet volume flow of 11.78 l/m instead of 22.26 l/min, but it still results high >10 m/s velocities towards the outlet of the channel. Volume flow cannot be decreased too much, therefore the cross-section of the collector channel should be increased, or bypass channel should be applied.

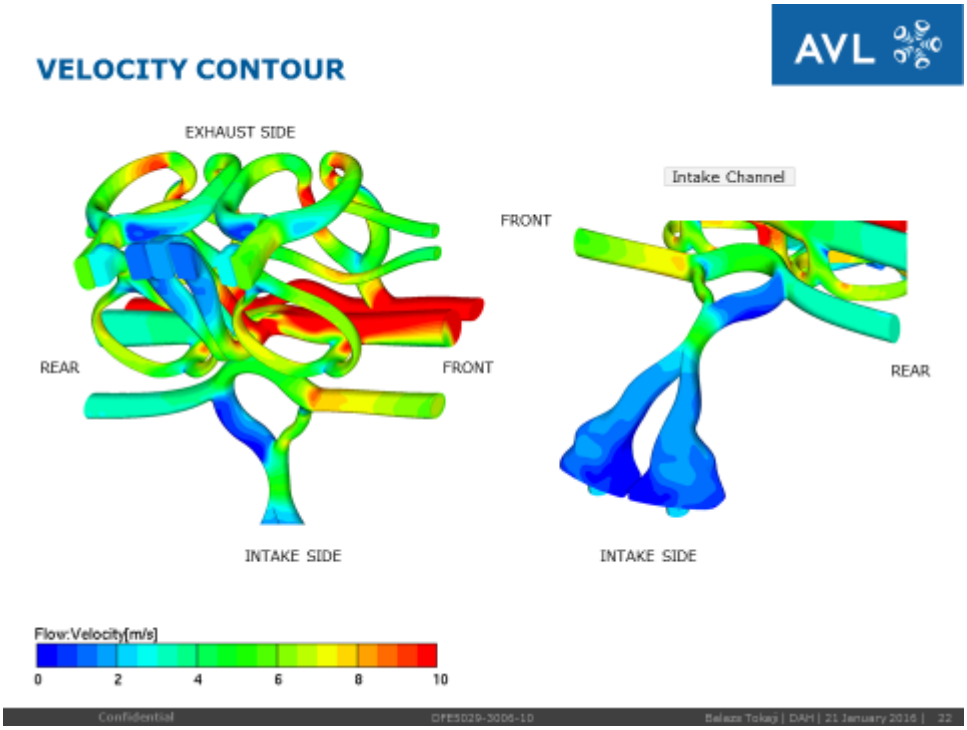


### 10.2.2 Second Run

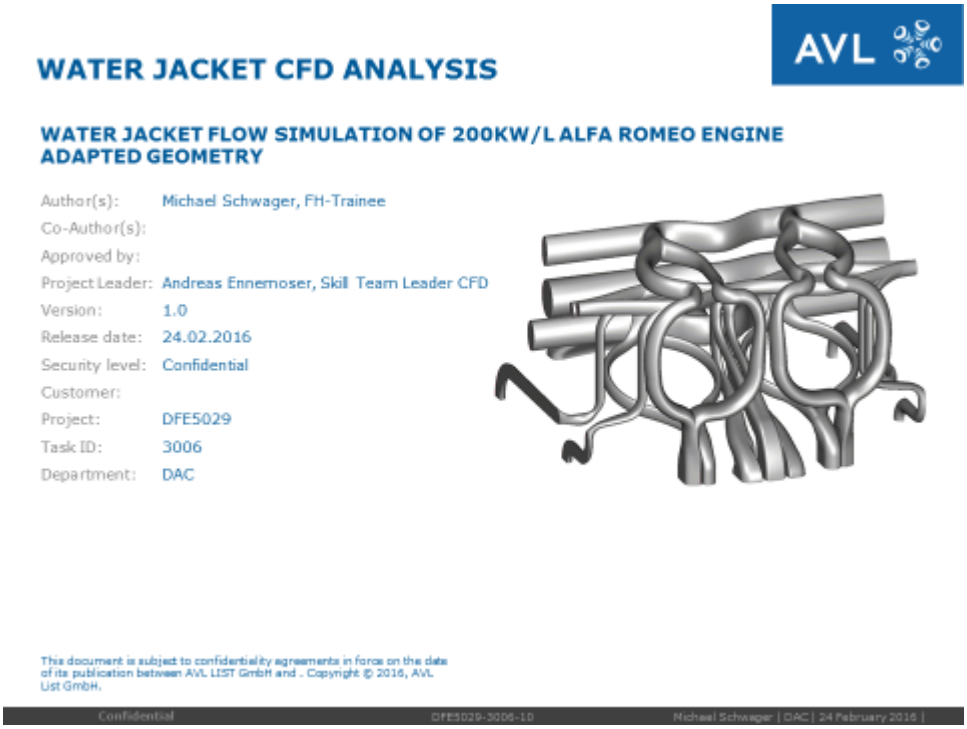

## TABLE OF CONTENT





## INTRODUCTION

- Description
  - This document summarizes information about the 3D-CFD analysis of a water cooling jacket. There is already an existing CFD analysis of the mentioned water jacket, where the Polymesher was used for mesh generation. But the geometry of the water jacket was adapted afterwards. Therefore, another CFD model was build, using the FIRE FAME Hexa mesher.
  - The calculation case got set up according to Workflow 3006. While evaluating the calculation results, particular attention is paid to pressure loss characteristics, velocity characteristics and HTC.
- Analysis objectives
  - Analysis of the existing model and its results
  - Mesh-generation in FIRE FAME Hexa
  - Set-up of the calculation case according to Workflow 3006
  - Evaluation of the results

## SYSTEM DESCRIPTION

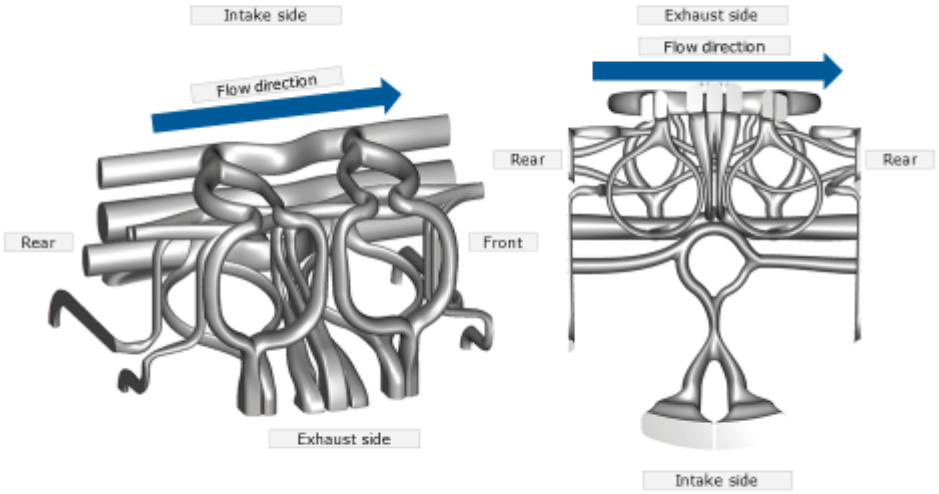


Confidential OFE5029-3006-10 Michael Schwager | OAC | 24 February 2016 | 3

## SUMMARY

- During the analysis work the following jobs were performed:
  - Analysis of the existing polymesh and its results
  - Mesh generation in FIRE FAME Hexa
  - Set up and perform a calculation case
    - according to workflow 3006
    - wall temperatures according to the existing calculation
    - adapted flow rates
  - Post-processing of simulation case
    - Pressure loss characteristics
    - Velocity characteristics
    - HTC
- Next steps
  - Mapping of the case (FE shells)

Confidential OFE5029-3006-10 Michael Schwager | OAC | 24 February 2016 | 4

## CONCLUSIONS RECOMMENDATIONS

| # | Conclusions | Recommended actions |
|---|---|---|
| 1 | The existing calculation shows a pressure loss of about 1,7 bar and high velocity in the collector of the flange channel | Modification of boundary conditions in the flange channel -> 50% reduced volume flow in flange channel |
| 2 | Collector passages do not yet consider flow accumulation along engine | Graduate cross section for flow accumulation, especially in exhaust flange collector channel |
| 3 | | |
| 4 | | Compensation of parallel flow passages (upper exhaust valve bridges) => throttling of front side passage |
| 5 | | Re-distribute flow rates among passages:<br>• increase exhaust flange passages<br>• reduce lower exh-exh passages |

Achieved | Borderline | Not Achieved



## ANALYSIS MODEL MATERIALS AND PROPERTIES

Coolant: Water / Glycol 50/50 [vol%]

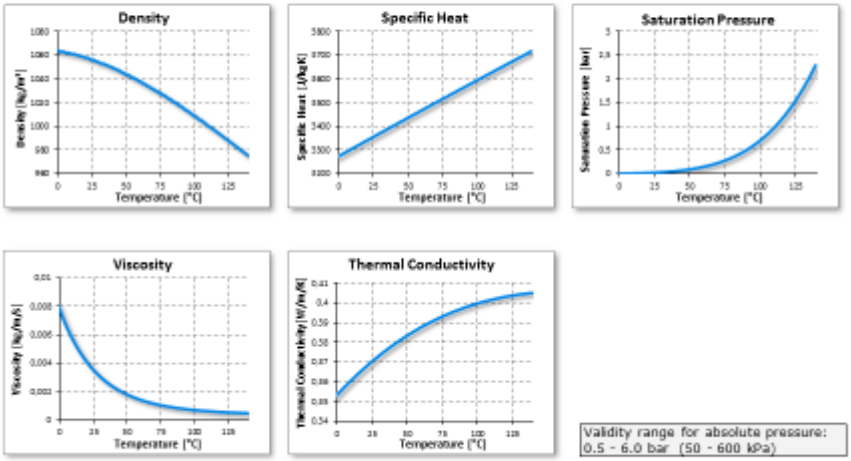

## ANALYSIS MODEL
## LOADS AND CONSTRAINTS

| ID | Name | Type | Value | Unit | Value from | Value to | Source (doc,version) | Owner | Date |
|---|---|---|---|---|---|---|---|---|---|
| 1 | Volume flow rate of coolant pump | | **216** | l/min | | | DFE2106_7001-Input_data_summary.pptm | Susanna Neuhold | 12.05.2015 |
| 2 | Inlet coolant temperature to Head | | 92.7 | °C | | | Assumption | Balazs Tokaji | 20.01.2016 |
| 3 | Absolute pressure level at head out | | 2300 | mbar | | | Assumption | Balazs Tokaji | 20.01.2016 |
| 4 | Assumed wall temperature around valve seat rings | | 132.7 | °C | | | Assumption | Balazs Tokaji | 20.01.2016 |
| 5 | Assumed wall temperature on rest of the head | | 112.7 | °C | | | Assumption | Balazs Tokaji | 20.01.2016 |
| 6 | Volume flow rate (one cylinder) | | 75.88 | l/min | | | Assumption | Michael Schwager | 22.02.2016 |
| 7 | | | | | | | | | |
| 8 | | | | | | | | | |
| 9 | | | | | | | | | |
| 10 | | | | | | | | | |
| 11 | | | | | | | | | |
| 12 | | | | | | | | | |
| 13 | | | | | | | | | |
| 14 | | | | | | | | | |
| 15 | | | | | | | | | |

Calculation case: 00-WaterJacket-WFR_75c88lpmin-TWI_92c7degC-0c5WG-ass_ST

L .. Load
B .. Boundary condition
I .. Initial condition



## ANALYSIS MODEL
## SUMMARY FLOW RATES – NEW GEOMETRY

| | | Volume Flow | Mass Flow | Cross Section | Velocity |
|---|---|---|---|---|---|
| **Valve guides (1&2)** | | l/min | kg/s | mm² | m/s |
| | **Inlet 1** | 2.65 | 0.04461 | 9.24 | 4.78 |
| | **Inlet 2** | 1.325 | 0.022305 | 6.05 | 3.65 |
| | **Inlet 3** | 1.325 | 0.022305 | 6.05 | 3.65 |
| | **Outlet** | 5.3 | | | |
| | | | | | |
| **Intake channel** | | l/min | kg/s | mm² | m/s |
| | **Inlet 1** | 5.77 | 0.09713 | 31.24 | 3.08 |
| | **Inlet 2** | 2.885 | 0.048565 | 23.4 | 2.05 |
| | **Inlet 3** | 2.885 | 0.048565 | 23.4 | 2.05 |
| | **Outlet** | 11.54 | | | |
| | | | | | |
| **Flange channel** | | l/min | kg/s | mm² | m/s |
| | **Inlet 1** | 9.85 | 0.16581 | 24.98 | 6.57 |
| | **Inlet 2** | 4.925 | 0.082905 | 29.27 | 2.80 |
| | **Inlet 3** | 4.925 | 0.082905 | 29.27 | 2.80 |
| | **Outlet** | 19.7 | | | |

## ANALYSIS MODEL
## SUMMARY FLOW RATES – NEW GEOMETRY

| Exhaust channel | Volume Flow | Mass Flow | Cross Section | Velocity |
|---|---|---|---|---|
| | l/min | kg/s | mm² | m/s |
| Inlet 1 | 11.78 | 0.19830 | 62.64 | 3.13 |
| Inlet 2 | 5.24 | 0.088207 | 29.05 | 3.01 |
| Inlet 3 | 3.27 | 0.055045 | 42.39 | 1.29 |
| Inlet 4 | 5.24 | 0.088207 | 43.35 | 2.02 |
| Inlet 5 | 3.27 | 0.055045 | 42.39 | 1.29 |
| Inlet 6 | 5.24 | 0.088207 | 29.05 | 3.01 |
| Outlet | 34.04 | | | |

| Volume Flow Distribution | | |
|---|---|---|
| | l/min | % |
| Valve guide 1 | 5.3 | 6.985 |
| Valve guide 2 | 5.3 | 6.985 |
| Intake channel | 11.54 | 15.21 |
| Flange channel | 19.7 | 25.96 |
| Exhaust channel | 34.04 | 44.86 |
| Total of cylinder | 75.88 | 100 |

Confidential DFE5029-3006-10 Michael Schwaiger | DAC | 24 February 2016 | 10

## ANALYSIS MODEL
## ESTIMATION BASED ON V52 RESULTS CYL1

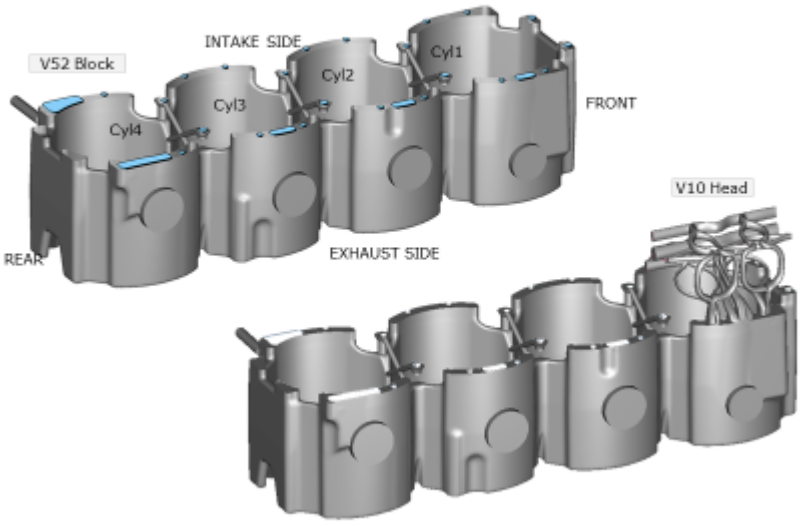


Confidential DFE5029-3006-10 Michael Schwaiger | DAC | 24 February 2016 | 11

## ANALYSIS MODEL
## ADAPTED GEOMETRY

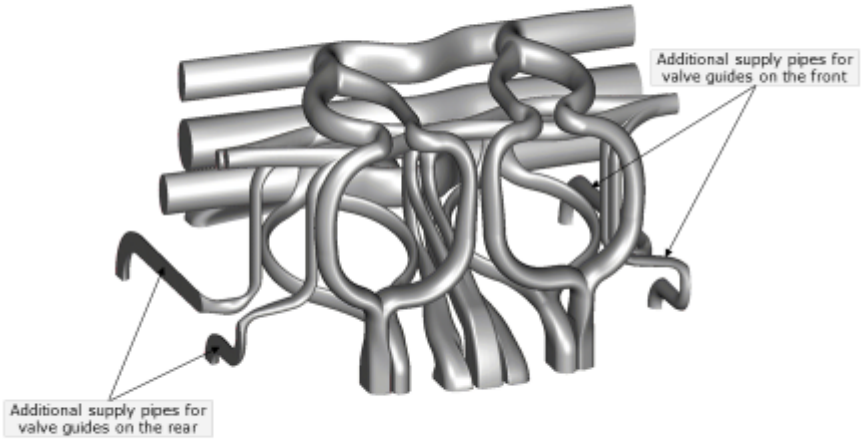


Confidential DFE5029-3006-10 Michael Schwaiger | OAC | 24 February 2016 | 12

## ANALYSIS MODEL
## FLOW RATES – ADAPTED GEOMETRY

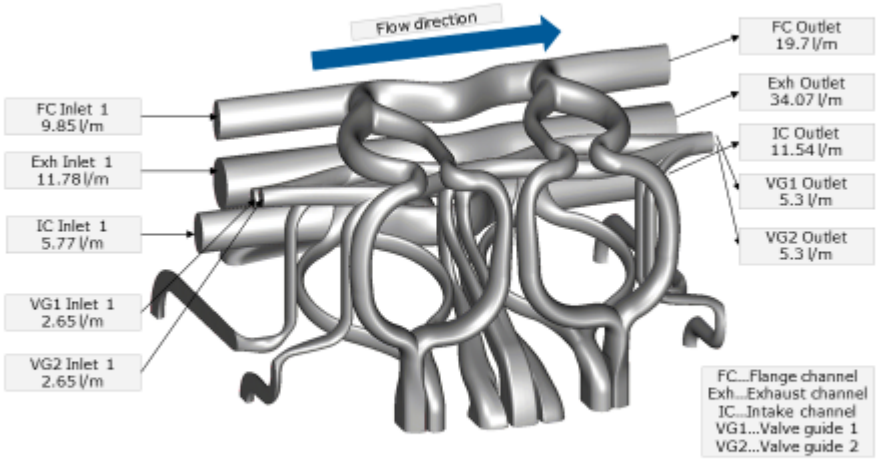


Confidential DFE5029-3006-10 Michael Schwaiger | OAC | 24 February 2016 | 13

## ANALYSIS MODEL
## FLOW RATES – ADAPTED GEOMETRY

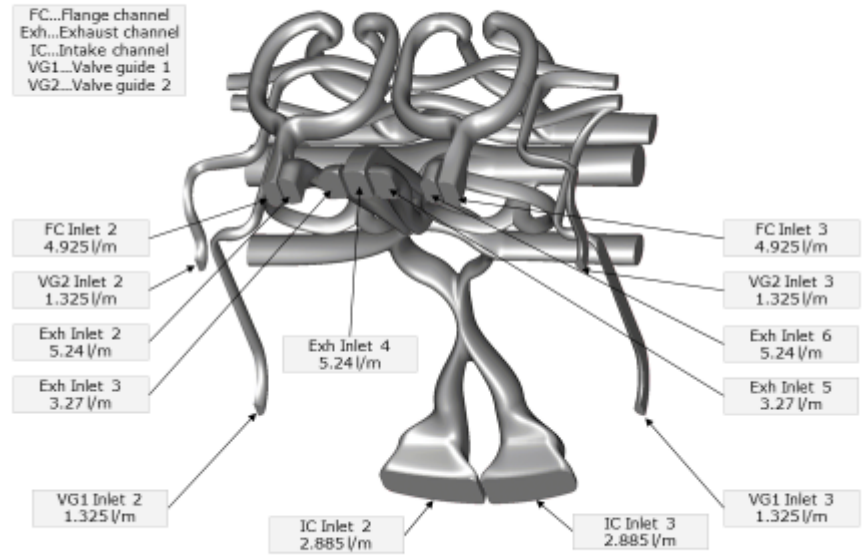


Confidential DFE5029-3006-10 Michael Schwager | OAC | 24 February 2016 | 14

## ANALYSIS RESULTS
## ABSOLUTE PRESSURE

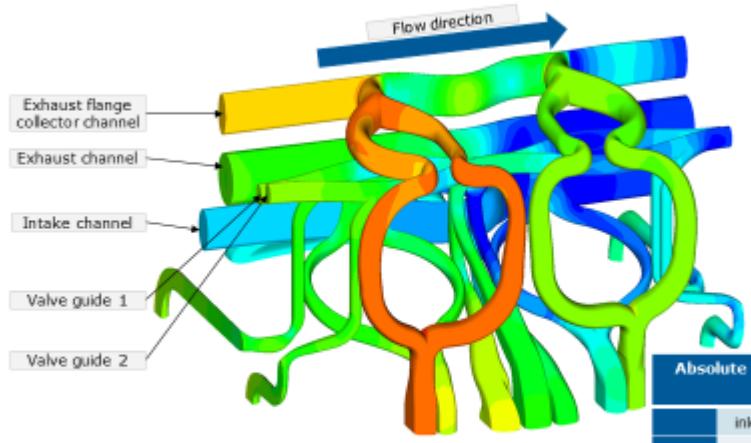


**Absolute Pressure Loss in mbar**

| | inlet | outlet | loss |
|---|---|---|---|
| VG1 | 3052 | 2316 | 736 |
| VG2 | 3085 | 2305 | 780 |
| IC | 2545 | 2301 | 244 |
| FC | 3313 | 2340 | 973 |
| EC | 2970 | 2302 | 668 |

Confidential DFE5029-3006-10 Michael Schwager | OAC | 24 February 2016 | 15

## ANALYSIS RESULTS ABSOLUTE PRESSURE

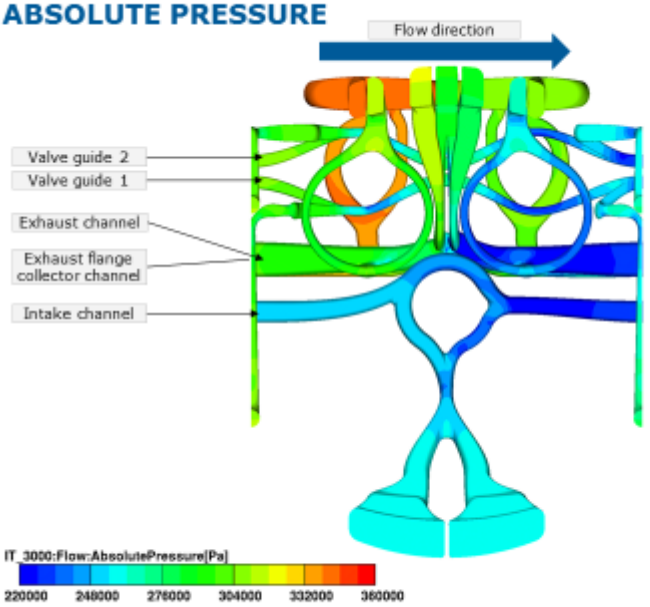


| Absolute Pressure Loss in mbar | | | |
|---|---|---|---|
| | inlet | outlet | loss |
| VG1 | 3052 | 2316 | 736 |
| VG2 | 3085 | 2305 | 780 |
| IC | 2545 | 2301 | 244 |
| FC | 3313 | 2340 | 973 |
| EC | 2970 | 2302 | 668 |



## ANALYSIS RESULTS VELOCITY

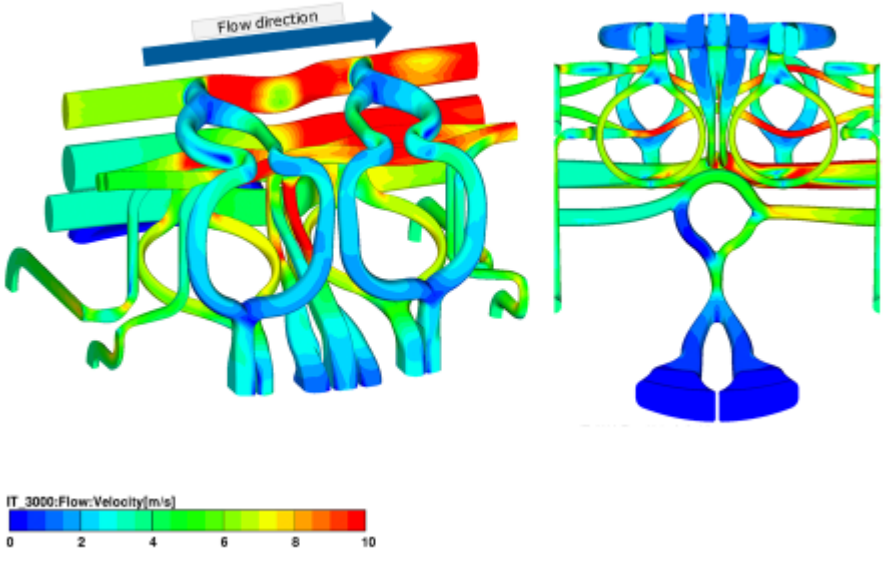

## ANALYSIS RESULTS VELOCITY

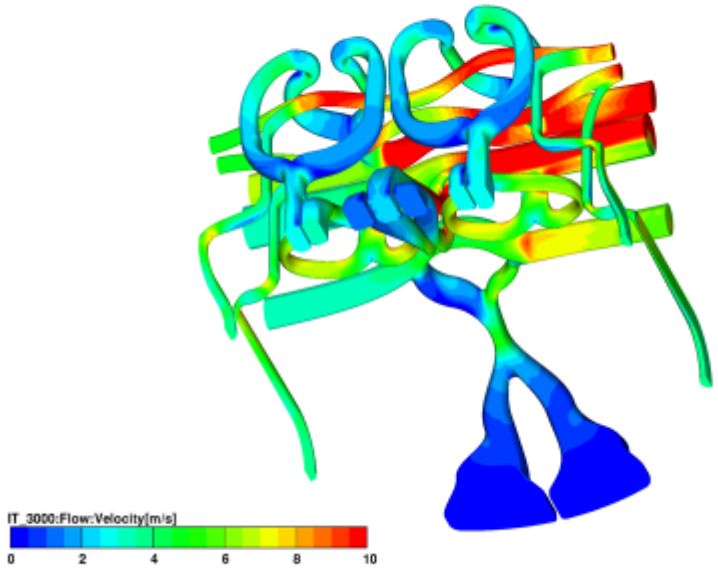




## ANALYSIS RESULTS VELOCITY

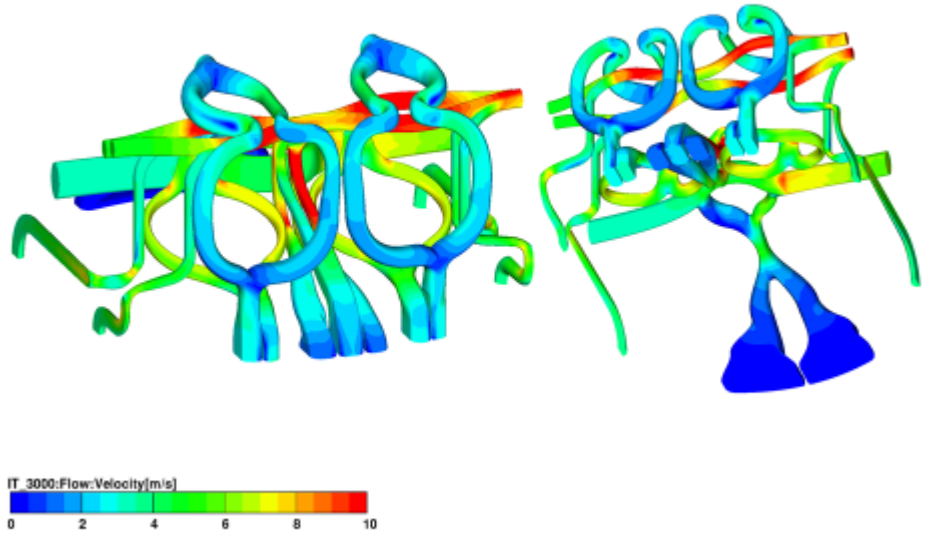

## ANALYSIS RESULTS
## HEAT TRANSFER COEFFICIENT

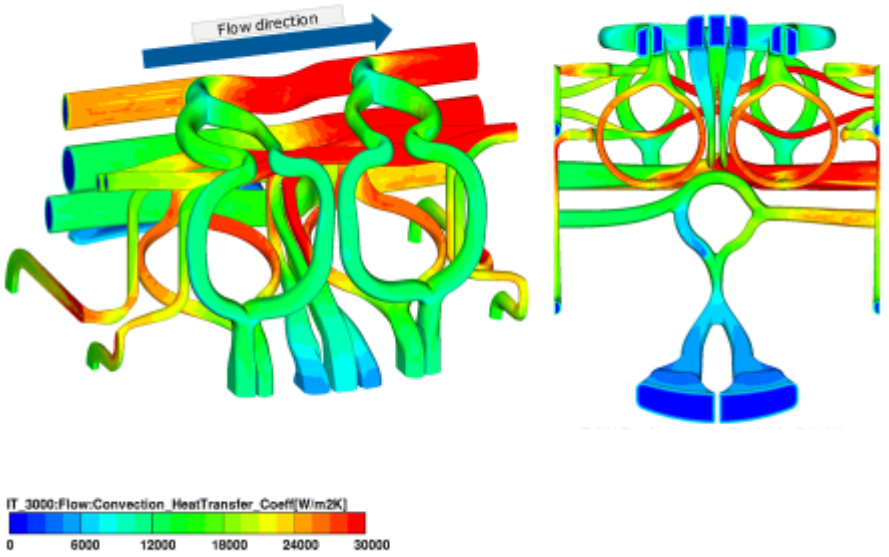




## ANALYSIS RESULTS
## HEAT TRANSFER COEFFICIENT

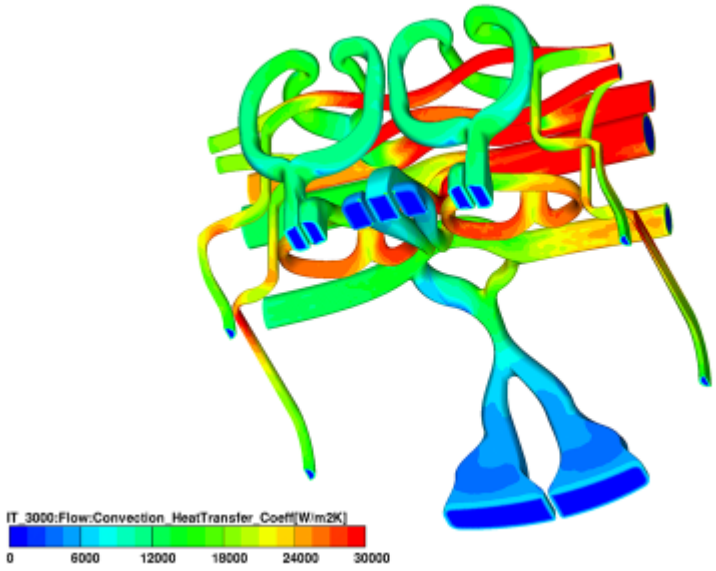

## ANALYSIS RESULTS
## HEAT TRANSFER COEFFICIENT

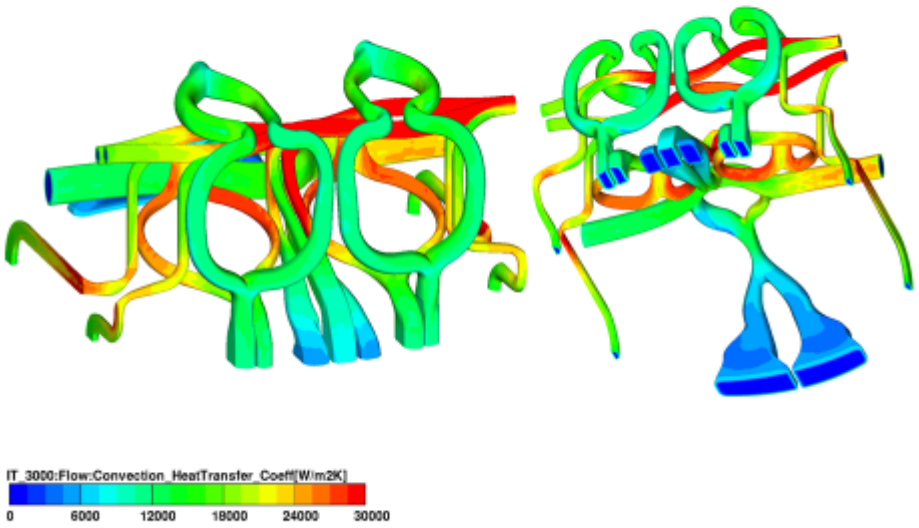




## APPENDIX
## COMPARISON POLYMESH VS. HEXA MESH

Polymesh
Number of cells: 198.525

Hexa mesh
Number of cells: 2.002.776

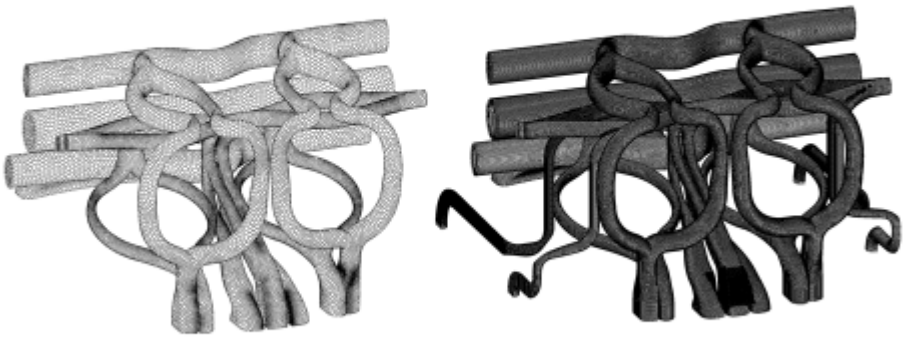

# 11 Register

## 11.1 Sources

[1] Design Guidelines for Cylinder Head, Christof Knollmayr, 2008, AVL

[2] Scriptum Industrielle Fertigung und Präzisionsfertigung, Rapid Prototyping, TU Graz

[3] Scriptum Pulvermetallurgie, TU Graz

[4] SLM Solutions: http://stage.slm-solutions.com/index.php?index_de

[5] ACRAM: http://www.arcam.com/

[6] HERMLE Maschinenbau GmbH: http://www.hermle-generativ-fertigen.de/cms/en/technology/

[7] EOS: http://www.eos.info/systems_solutions/metal

[8] LASER CONCEPT: http://www.concept-laser.de/

[9] Tool Craft: http://www.toolcraft.de/

EURO PM 2015:

[10] 3D Laser Clading of gradient Structures in Ti-Ni-Al System, Heinrich Kestler, Plansee SE. I. Shishkovsky, F. Missemer, Ecole Nationale d'Ingenieurs de Saint-Etienne, Lebedev Physics Institute of Russian Academy of Sciences,

[11] Additive Manufacturing of Elektron ® 43 Alloy using Laser Powder Bed and Direct Energy Deposition, Claus Aumund-Kopp, Fraunhofer IFAM, Racjiv Tandon, Magnesium Elektron Powders, Timothy Wilks, Magnesium Elektron, Matthias Gieseke, Christian Noelke, Stefan KaierleLaser Zentrum Hannover e.V., Todd Palmer, The Pennsylvania State University

[12] EBSD Observation of Grains Microstructures Produced by Selective Laser Melting, Dov Chaiat, Tungsten Powder Technology, F. Royer, Y Bienvenu, F Gaslain, MINES ParisTech, PSL, MAT

[13] Effect of Microstructure on the Tensile Strength of Ti6Al4V Specimens Manufactured using Additive Manufacturing Electron Beam Process, Ralf Carlström, Höganäs AB, Thays Machry, David Eatock, Jonathan Meyer, Airbus Group, Alphons Antonysamy, GKN Aerospace, Alister Ho, Phil Pragnell, The Manchester University

[14] Progress of Precision Ink Jet Printing on Powder Bed, Heinrich Kestler, Plansee SE, Robert Frykholm, Bo-göran Andersson, Ralf Carlström, Höganäs AB

[15] Research about the Influence of Process Parameters of Selective Laser Melting on material EN AW 2918, Adeline Riou, Erasteel SAS, Ondrej Koukal, Daniel Koutny, David Palousek, Radek Vrana, Tomas Zikmund, Libor Pantelejev, Brno University of Technology

[16] The Impact of Recycling AM Powders, Christoph Laumen, Linde Gas, D.J. Novotnak, L.W. Lherbier, Carpenter Powder Products

[17] Effects of Powder Characteristics on the DMLS of 17-4PH Stainless Steel, Christoph Laumen, Linde AG, Harish Irrinki, Sundar V. Atre, University of Louisville, Brenton Barmore, Michael Dexter, Oregon State University, Jason Stitzel, Metal Technologies, Sunil Badwe, Somayeh Pasebani, North American Hoganas

[18] Effect of Processing Parameters and Chemical Composition of Tool Steels on Integrity and Proerpties of Low-Thickness Part Produced by Selective Laser Melting, Dov Chaiat, TPT Tungsten Powder Technology, J. Lemke, R. Casati, A.G. Demir, B. Previtali, M. Vedani, Politcnico di Milano, C. Andrianopoli, M. Massazza, Cogne Acciai Speciali SpA

[19] Heat Treatment and Mechanical Testing of Selective Melted Superalloy, Inigo Iturriza, Hakan Brodin, Siemens Industrial Turbomachinery AB

[20] Heat treatment Optimization of Hastelloy X Superalloy Produced by Direct Metal Laser Sintering, Keitch Murray, Sandvik Osprey Ltd, Giulio Marchese, Sara Biamino, Matteo Pavese, Daniele Ugues, Mariangela Lombardi, Paolo Fino, Politecnico di Torino, Gianfranco Vallillo, GE Avio s.r.l.

[21] Impact Resistance of Lattice Structure made by Selective Laser Melting Technology, Christoph Laumen, Linde AG, Radek Vrana, David Palousek, Daniel Koutny, Ondrej Koukal, Tomas Zikmund, Petr Krejci, Brno University of Technology

[22] Mechanical Properties of Ti-6Al-4V Additively Manufactured by Electron Beam Melting, Marco Actis Grande, Politecnico di Torino, A. Krichner, B. Klöden, T. Weißgärber, B. Kieback, Frauenhofer Institute IFAM, A. Schoberth, S. Bagehorn, D. Greitemeier, Airbus Group Innovations

[23] Mesoscale Modelling of Short Crack Initiation in Metallic Selective Laser Melting Microstructures, Christoph Laumen, Linde Gas, Tom Anderesson, Anssi Laukkanen, Tatu Pinomaa, Antero Jokinen, Antti Vaaajoki, Tarja Laitinen, VTT Technical Research Center of Finnland Ltd

[24] Microstructural and Mechanical Characterization of Al Si10Mg – TiB2 Composites Produced by Direct Metal Laser Sintering Technique, Alexander Kirchner, IFAM, A. Aversa, M. Pavese, S. Biamino, P. Fino, Politecnico di Torino, D. Manfredi, F. Calignano, E. Ambrosio, Instituto intaliano di tecnologia

[25] Modification of H13 (AISI) Tool Stell Powders to Manufacture Inserts and Cooling Systems for Moulds by SLM, Alexander Kirchner, IFAM, A. R. Farinha, C. Batista, L. F. Dias, E. W. Sequeiros, M. T. Vieira, CEMUC, Department of Mechanical Engineering

[26] Multi-Physical Simulation of Selective Laser Melting of Molybdenum, Adeline Riou, Erasteel SAS, K.-H. Leitz, P. Singer, A. Plankensteiner, B. Tabernig, H. Kestler, L. S. Sigl, Plansee SE

[27] Mew Materials and Applications by 3D Printing for Innovative Approaches, Heinrich Kestler, Plansee SE, Juan Isaza, Claus Aumund-Kopp, Sandra Wieland, Frank Petzoldt, Mathis Bauschulte, Dirk Godlinski, Frauenhofer IFAM

[28] Process Development and Material Properties of Gears Manufactured by Laser Metal Deposition, Claus Aumund Kopp, Frauenhofer IFAM, Marleen Rombouts, Gert Maes, Vito – Vlaamse Instelling voor Technologisch Onderzoek, Freddy Vansringel, VCST, Scott Wilson, Oerlikon Metco

[29] Progress of Precision Ink Jet Printing on Powder Bed, Heinrich Kestler, Plansee SE, Robert Frykholm, Bo-Göran Andersson and Ralf Carlström, Höganäs AB

[30] Selective Laser Sintering in Cu-Al-Ni System and some of their Properties, Adeline Riou, Erasteel SAS, I. Shishkovsky, I. Yadroitsev, Yu. Morozov, Russian Academy of Science

[31] Ti6Al4V Alloy Selective Laser Melted: Microstructure Evolution Trough Post-Heating Treatment, Erich Neubauer, RHp Technology GmbH, M. Regniere, B. Desplanques, S. Saunier, C. Desrayaud, Ecole des Mines de Saint Etienne, C. Reynaud, Centre Technique des Industires Mecaniques, P. Bertrand, Ecole Nationale d'Ingenieur de Saint Etienne

[32] Titanium Aluminides for Automotive Applications Processed by Electron Beam Melting, giorgia Baudana, Sara Biamino, Paolo Fino, Claudio Badini, Plotecnico di Torino, Burghardt Klöden, Frauenhofer Institute IFAM, Anita Buxton, TWI Ltd

[33] Towards Improved Quality and Production Capcity for Ni based Powders for Additive Manufacturing, Inigo Iturriza, CEIT, P. Vikner, R. Giraud, C. Mayer, Erasteel, M. Sarasola, Metallied Powder Solutions

[34] Poom group: http://www.pomgroup.com/

[35] 3D systems: http://www.3dsystems.com/

[36] Z-Cooperation: www.zcorp.com/

Wikipedia

[37] Additive Manufacturing: https://en.wikipedia.org/wiki/3D_printing

[38] Inkjet 3D Printing: https://en.wikipedia.org/wiki/Powder_bed_and_inkjet_head_3D_printing

[39] EBM: https://en.wikipedia.org/wiki/Electron_beam_additive_manufacturing

[40] SLM: https://en.wikipedia.org/wiki/Selective_laser_melting

[41] SLS: https://en.wikipedia.org/wiki/Selective_laser_sintering

[42] DMLS: https://en.wikipedia.org/wiki/Direct_metal_laser_sintering

[43] EBF3: https://en.wikipedia.org/wiki/Electron_beam_freeform_fabrication

[44] Yield Strength: https://en.wikipedia.org/wiki/Ultimate_tensile_strength

[45] sciaky: http://sciaky.com

[46] Appliation of SLM during Cylinder Head Development, M. Hartweg, R. Dittrich, H.-P. Kollmeier, J. Stammler, Frauenhofer Projektgruppe NAS

[47] NASA EBF3: http://www.techbriefs.com/component/content/article/ntb/tech-briefs/manufacturing-and-prototyping/478

[48] Electron Beam Freeform Fabrication for Cost Effective Near-Net Shape Manufacturing, Karen M. Taminger, Robert A. Hafley, NASA Langley Research Center

[49] Fabrication Copper Components with Electron Beam Melting, P. Frigola, RadiaBeam Technologies LLC, O.A. Harrysson, T.J. Horn, H.A. West, R.L. Aman, J.M. Rigsbee, North Carolina State University, D.A. Ramirez, L.E. Murr, F. Medina, R.B. Wicker, E. Rodriguez, University of Texas

[50] http://www.sciaky.com/additive-manufacturing/electron-beam-additive-manufacturing-technology

[51] http://www.sciaky.com/additive-manufacturing/wire-am-vs-powder-am

[52] Micro Laser Sintering by 3D Micco Print GmbH – Industrial Production of Micro Metal Part, 2015

[53] Microbauteile durch Lasersintern im Vakuum, P. Regenfuß, R. Ebert, S, Klötzer, L. Hartwig, H. Exner, Laserinstitut Mittelsachsen e.V. Hochschule Mittweida; T. Petsch, §D – Micromac AG

[54] Projekt PoSt – Einstellung definierter Eigenschaftsprofile poröser mediendurchgängiger Strukturen, M. Eng Robert Kahlenberg, Günther Köhler Institut, IFW Jena, 2016

[55]ALFA – 200KW/L – Main Bolt Connections _ Status Report, Matthias Neubauer, AVL Graz, 2015

[56] www.focus.de
[57] custompart.net
[58] claim.engin.umich.edu
[59] www.trumpf-laser.com

## 11.2 Image Register

## 11.3 Table Register



## 11.4 Chart Register

# 12 Acknowledgement

I would like to take this opportunity to express my gratitude to all those people who contributed to this work, helped me out, gave me input and shared their knowledge and experience. Thanks to following people in alphabetical order:

**David Binder**

for further mathematical Simulia and Tosca Support

**Aldo Bregnant,**

for making the mesh and refining it several times

**Reinhard Glanz,**

for the idea of this thesis and proposing it to me. Furthermore, the immanent interest in its progress and support where possible.

**Robert Grundner,**

for assembling the solid model in NX and help with CAD issues

**Hannes Hick,**

for a supportive and patient supervision from TU Graz

**Bernhard Kaltenegger,**

for supervision from AVL and managing to get the right support when and where needed

**Christian Krahser,**

for solving most of my face-to-face troubles with CREO

**Michael Lutze,**

for checking the feasibility of the AM water jacket

**Kathrin Maier,**

Further support on material topics, especially plastics

**Kambiz Mehrabi,**

background knowledge on material science and a large paper pile of journals about AM

**Robert Pöschl,**

for input on the AM water jacket

**Eloy Rama,**

for official Simulia support

**Michael Schwager,**

For the second CFD simulation

**Tomasz Siczek,**

for helpling with my day-to-day Abaqus issues and set up

**Hartwig Siegfried,**

for helpful input on Tosca issues

**Matej Smolnikar**

For support, ideas and motivation whenever it was needed

**Balazs Tokaji,**

For the first CFD simulation

**Monika Veresuk,**

for helping out with all bureaucratic issues a company has to offer